STRUCTURAL EFFECTIVENESS OF EXTERNALLY BONDED CFRPs IN STRENGTHENING RC BEAMS

A dissertation submitted
in partial fulfillment of the requirements for
the award of degree of

MASTER OF ENGINEERING

IN

STRUCTURAL ENGINEERING

Submitted by

MANDEEP SINGH

(Roll No. 801422018)

UNDER THE SUPERVISION OF

DR. PREM PAL BANSAL

Associate Professor

Department of Civil Engineering

DEPARTMENT OF CIVIL ENGINEERING

THAPAR UNIVERSITY, PATIALA 147004

JULY 2016

DECLARATION

I, Mandeep Singh, hereby declare that this thesis entitled **"Structural Effectiveness of Externally Bonded CFRPs in Strengthening RC Beams"** is an authentic record of my study carried out as requirements for the award of degree of **Master of Engineering** in **Structural Engineering** in the Civil Engineering Department, Thapar University, Patiala under the supervision of **Dr. Prem Pal Bansal, Associate Professor,** Department of civil engineering, Thapar University, Patiala during July 2015 to July 2016. This matter embodied in this reporthas not been submitted in part or full to any other university or institute for the award of any degree.

Mandeep Singh

Date: JULY 14, 2016

(Mandeep Singh)
Roll No. 801422018

CERTIFICATE

This is to certify that above statement made by the student concerned is correct and true to the best of my knowledge and belief.

Dr. Prem Pal Bansal
Associate Professor
Department of Civil Engineering
Thapar University, Patiala

Countersigned by

Dr. Naveen Kwatra
Professor & Head
Department of Civil Engineering
Thapar University, Patiala

Dr. S.S. Bhatia
Dean of Academic Affairs
Thapar University, Patiala

ACKNOWLEDGEMENT

A dissertation cannot be completed without the help of many people who contribute directly or indirectly through there constructive criticism in the evolution and preparation of this work. It would not be fair on my part, if I don't say a word of thanks to all those whose sincere advice made this period a real educative, enlightening, pleasurable and memorable one.

First of all, a special debt of gratitude is owned to my supervisor **Dr. Prem Pal Bansal** for his gracious efforts and keen pursuits, which has remained as a valuable asset for the successful completion of research work.

I also like to offer my sincere thanks to all faculty members, teaching and non-teaching staff of Civil Engineering Department (CED), and staff of central library, TU, Patiala for their assistance. I am extremely thankful to my friends, Mr. Varun Garg, Mr. Harshsav Sethi and all other manpower for helping me carry out experimental work.

Mandeep Singh
M.E. (Structures)
Roll no. 801422018

ABSTRACT

The desirable characteristics of carbon fibre reinforced polymer (CFRP) composites such as their high stiffness-to-weight ratio, high environmental durability, high tensile strength, and ease of application have led to their use as an alternative to conventional materials used for shear and flexural strengthening of reinforced concrete (RC) members. Over the past two decades, many studies have been conducted in order to investigate the performance of FRP composites in civil engineering and structural applications. A primary concern of FRP structural strengthening systems is that FRP sheets may de-bond from the concrete surface at a force significantly lower than the strength of the FRP material. Debonding failures are often brittle and occur with little warning, therefore making them an undesirable failure mode. ACI 440.2R-08 mentions the use of transversely placed FRP sheets, or U-wraps, to delay debonding. There is, however, scarcity of research pertaining to strengthening beams in shear with FRP strips or continuous wraps.

The research work presented here focus on the strengthening efficiency of reinforced concrete beams with externally bonded CFRPs. A detailed experimental program provides evaluations of structural behaviour of the combined flexural and shear strengthening of RC beams by using CFRP sheets prebonded on the tension face of the beam for flexural strengthening, and then reinforced in shear by the CFRP sheets in various schemes. The variables investigated in this research study included CFRP amount and distribution (i.e., continuous wrap versus strips), bonded surface (i.e., lateral sides versus U-wrap) orientation of fibres (i.e., 90°/45°) and laminate width. During the experiments, the following aspects were evaluated regarding the response of the tested beams: load-deflection analysis, crack patterns, deformation behaviour, failure modes and ductility index of beams.

In order to attain these goals, fifteen beams were tested, out of which two beams were considered as controlled/ unstrengthened beams, whereas all other thirteen beams were strengthened with externally bonded CFRP sheets in various schemes. Research output shows that the flexural–shear strengthening arrangement is much more effective than the flexural one in enhancing the stiffness, the ultimate strength of the beam. In addition theoretical calculations on estimating the shear capacities of the strengthened beams based on debonding failure mode are presented and compared with the corresponding experimental results in a reasonably good agreement.

CONTENTS

LIST OF FIGURES

LIST OF TABLES

CHAPTER-1 INTRODUCTION

1.1 GENERAL

The repair of deteriorated, damaged and substandard civil infrastructure has become one of the important issues for the civil engineer worldwide. The rehabilitation of existing structures is fast growing, especially in developed countries, which completed most of their infrastructure in the middle period of the last century.

Within the scope of rehabilitation of concrete structures, it is essential to differentiate between the terms *repair*, *strengthening* and *retrofitting*; these terms are often erroneously interchanged, but they do refer to three different structural conditions. In 'repairing' a structure, the composite material is used to improve a structural or functional deficiency such as crack or a severely damaged structural component. In contrast 'strengthening' of a structure is specific to those cases where the addition or application of the composite would enhance the existing desired performance level. The term 'retrofit' is specifically used to relate the seismic upgrade of facilities, such as in case of the use of composite jackets for the confinement of columns.

Strengthening/rehabilitating/retrofitting existing structures, manufactured from the more conventional materials, by utilizing advanced fibre reinforced polymer (FRP) composites is a powerful and viable alternative to the use of steel. Since the 1980s, the realization amongst civil/structural engineers of the importance of the specific weight and stiffness, the resistance to corrosion, durability, tailorability, and ease of installation is encouraging the use of FRP composites in the rehabilitation of structures throughout the world.

Externally bonded FRP composite strengthening is particularly attractive where there are severe access restraints or high cost associated with installation time. In addition, the capacity of FRP composites strengthening to extend the life of historical structures with minimum disruption to users makes for genuinely sustainable engineering solutions. Furthermore, the fabrication technologies for the production of FRP composites have been revolutionized by sophisticated manufacturing techniques. These methods have enabled polymer composite materials to produce good-quality laminates with minimal voids and accurate fibre alignment. This work is a study of the behaviour of reinforced concrete beams strengthened with CFRPs.

1.2 DESCRIPTION OF THE COMPOSITE MATERIALS

The FRP composites comprise fibres of high tensile strength within a polymer matrix. The fibres are generally carbon or glass, in a matrix such as vinylester or epoxy. These materials are preformed to form plates under factory conditions, generally by the pultrusion process. For experimentation, plates may be manufactured in smaller quantities from pre-impregnated fibre mats.

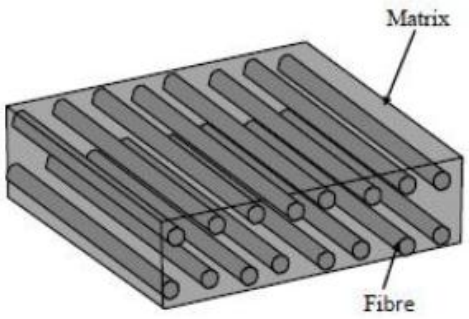

Figure 1.1 - Schematic Representation of a Unidirectional FRP Plate

Fibre reinforced polymer (FRP) composites consist of high strength fibres embedded in a matrix of polymer resin as shown in Figure 1.1. Fibres typically used in FRP are glass, carbon and aramid. Typical values for properties of the fibres are given in Table 1.1. These fibres are all linear elastic up to failure, with no significant yielding compared to steel. Fibres generally consist of a number of long filaments, which have exceptionally high specific stiffness and strength. Their diameters are of the order of 10μm with an aspect ratio, of length to diameter, between 1000 and infinity for continuous fibres.

Table 1.1 - Typical Proprieties of Fibres (Feldman 1989, Kim 1995)

Material	Elastic modulus (GPa)	Tensile strength (MPa)	Ultimate tensile strain (%)
Carbon			
High strength	215-235	3500-4800	1.4-2.0
Ultra high strength	215-235	3500-6000	1.5-2.3
High modulus	350-700	2100-2400	0.5-0.9
Ultra high modulus	500-700	2100-2400	0.2-0.4
Glass			
E	70	1900-3000	3.0-4.5
S	85-90	3500-4800	4.5-5.5
Aramid			
Low modulus	70-80	3500-4100	4.3-5.0
High modulus	115-130	3500-4000	2.5-3.5

The primary functions of the matrix in a composite are to transfer stress between the fibres, to provide a barrier against the environment and to protect the surface of the fibres from mechanical abrasion.

The mechanical properties of composites are dependent on the fibre properties, matrix properties, fibre-matrix bond properties, fibre amount and fibre orientation. A composite with all fibres in one direction is designated as unidirectional. If the fibres are woven, or oriented in many directions, the composite is bi- or multidirectional. Since it is mainly the fibres that provide stiffness and strength composites are often anisotropic with high stiffness in the fibre direction(s). In strengthening applications, unidirectional composites are predominantly used. The approximate stiffness and strength of a unidirectional CFRP with a 65% volume fraction of carbon fibre is given in Table 1.2. As a comparison the corresponding properties for steel are also given.

Table 1.2 - Typical Properties of Prefabricated FRP strips (fib 2001)

Material	**Elastic modulus (GPa)**	**Tensile strength (MPa)**	**Ultimate tensile strain (%)**
	E_f	f_f	ε_{fu}
Prefabricated strips			
Low modulus CFRP strips	170	2800	1.6
High modulus CFRP strips	300	1300	0.5
Mild steel	200	400	25 (yield strain = 0.2%)

The FRP essentially acts as additional reinforcement. The major differences, as compared to traditional reinforcing bars, are: (i) the strength of FRP is much higher; (ii) the behaviour of most FRP is linearly elastic up to failure; (iii) the load transfer from FRP to concrete is by adhesion of epoxy as opposed to mechanical bond between bars and concrete; and (iv) the structural elements are under stress (load) when FRP is applied and these stresses and corresponding strains should be taken into account in the design.

Two major components of a composite are high-strength fibres and a matrix that binds these fibres to form a composite-structural component. The fibres provide strength and stiffness, and the matrix (resin) provides the transfer of stresses and strains between the fibres. To obtain full composite action, the fibre surfaces should be completely coated (wetted) with matrix. Two or more fibre types can be combined to obtain specific composite property that is not possible to obtain using a single fibre type. For example, the modulus, strength, and fatigue performance of glass-reinforced polymers (GRP) can be enhanced by adding carbon fibres. Similarly, the impact energy of carbon fibre reinforced polymers (CFRP) can be increased by the addition of glass or aramid fibres.

The optimized performance that hybrid composite materials offer has led to their widespread growth throughout the world (Hancox, 1981; Shan and Liao, 2002). In recent years, hybrid composites have found uses in a number of applications such as abrasive resistant coatings, contact lens, sensors, optically active films, membranes, and absorbents (Cornelius and Marand, 2002).

Carbon fibres offer the highest modulus of all reinforcing fibres. Among the advantages of carbon fibres are their exceptionally high tensile-strength-to-weight ratios as well as high tensile-modulus-to-weight ratios. In addition, carbon fibres have high fatigue strengths and a very low coefficient of linear thermal expansion and, in some cases, even negative thermal expansion. This feature provides dimensional stability, which allows the composite to achieve near zero expansion to temperatures as high as 300 °C in critical structures such as spacecraft antennae. If protected from oxidation, carbon fibres can withstand temperatures as high as 2000 °C. Above this temperature, they will thermally decompose. Carbon fibres are chemically inert and not susceptible to corrosion or oxidation at temperatures below 400°C.

Carbon fibres possess high electrical conductivity, which is quite advantageous to the aircraft designer who must be concerned with the ability of an aircraft to tolerate lightning strikes. However, this characteristic poses a severe challenge to the carbon textile manufacturer since carbon fibre debris generated during weaving may cause "shorting" or electric shocks in unprotected electrical machinery. Other key disadvantages are their low impact resistance and high cost (Amateau, 2003; Mallick, 1993).

Adhesives are used to attach the composites to other surfaces such as concrete. The most common adhesives are acrylics, epoxies and urethanes. Epoxies provide high bond strength with high temperature resistance, whereas acrylics provide moderate temperature resistance with good strength and rapid curing. Several considerations are involved in applying adhesives effectively. Careful surface preparation such as removing the cement paste, grinding the surface by using a disc sander, removing the dust generated by surface grinding using an air blower and carful curing are critical to bond performance.

Epoxy resins are a broad family of materials that provide better performance as compared to other organic resins. Aerospace applications use epoxy resins almost

exclusively, except when high temperature performance is a key factor. Epoxies generally outperform most other resin types in terms of mechanical properties and resistance to environmental degradation.

The primary advantages of epoxy resins include:

- wide range of material properties;
- minimum or no volatile emissions and low shrinkage during cure;
- excellent resistance to chemical degradation;
- very good adhesion to a wide range of fibres and fillers.

The high cost of epoxies, long cure time, and handling difficulties are the principal disadvantages (Mallick, 1993).

Composites for structural strengthening are available today in the form of precured strips or uncured sheets. Precured strips are typically 0.5–1.5 mm thick and 50–200 mm wide, and made of unidirectional fibres (carbon, glass, aramid) in an epoxy matrix.

Uncured sheets typically have a nominal thickness of less than 1 mm, are made of unidirectional or bidirectional fibres, often called fabrics, (in the latter case) that are either pre-impregnated or in situ-impregnated with resin, and are highly conformable to the surface onto which they are bonded. Bonding is typically achieved with high-performance epoxy adhesives.

Historically, composites were first applied as flexural strengthening materials for RC bridges – Meier 1987; Rostasy 1987 and as confining reinforcement of RC columns – Fardis and Khalili 1981; Katsumata et al. 1987. The number of applications involving composites as strengthening/repair or retrofit materials worldwide has grown from just a few 10-15 years ago to several thousand today. Developments since the first research efforts in the mid-1980s have been tremendous. The range of applications has expanded to include masonry structures, timber, and even metals.

Various types of structural elements have been strengthened, including beams, slabs, columns, shear walls, joints, chimneys, vaults, domes, and trusses.

1.3 COMPARISON OF FIBRE PROPERTIES

For comparison with steel, typical stress-strain diagrams for unidirectional composites short-term monitoring loading are given in Figure 1.2.

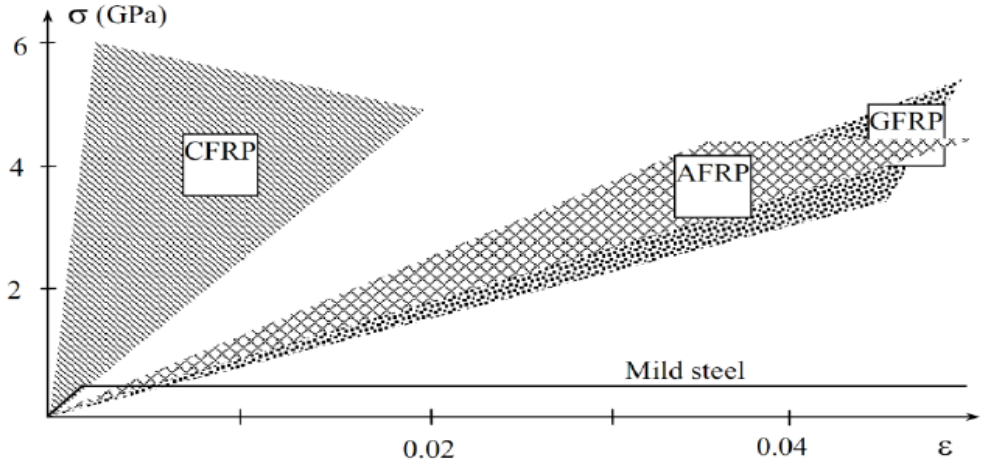

Figure 1.2 - Uniaxial tension stress-strain diagrams for different unidirectional FRPs and steel CFRP = carbon FRP, AFRP = aramid FRP, GFRP = glass FRP (Source: fib 2001)

Figure 1.3 compares the tensile modulus (stiffness) of typical fibres with that of traditional metals used in engineering applications. The bar chart shows that ultra-high-modulus (UHM) carbon fibre has a modulus three times that of steel and standard modulus carbon fibre has a modulus twice to that of aluminum.

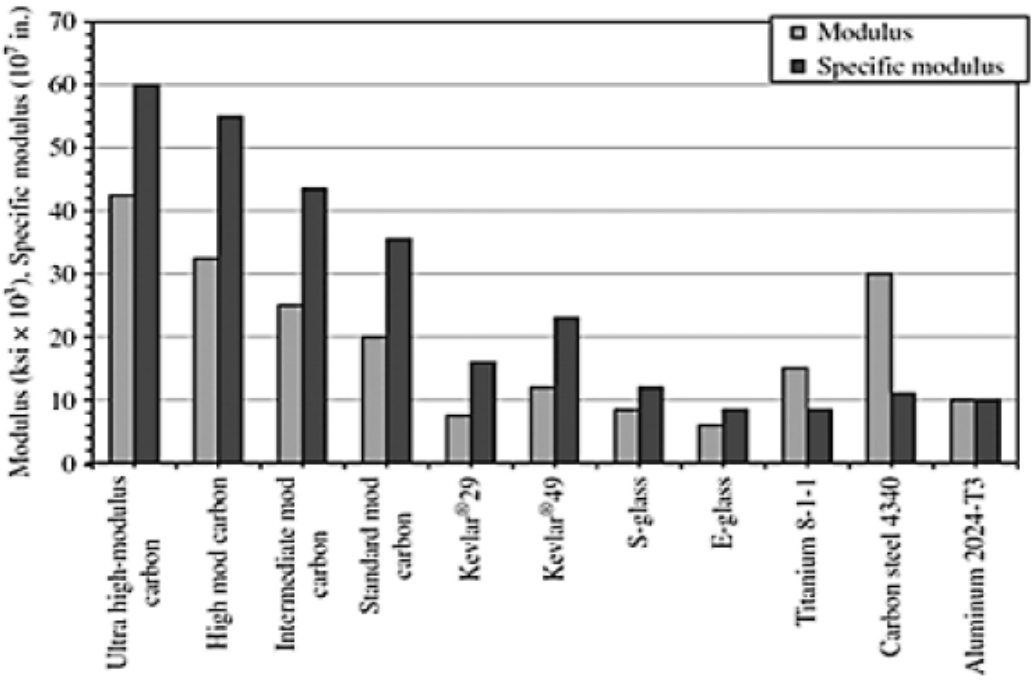

Figure 1.3 - Tensile modulus (stiffness) of typical fibres and metals (Source: Composite Tek, 2003)

Consider the tensile strength of common fibre reinforcements when compared to that of titanium, steel, and aluminum. The tensile strength of the fibres considered here far exceed that of aluminum by as much as 400%. For the most part, carbon, Kevlar®, and fibre glass also exceed the strength of steel by as much as two times. The specific strength of all of the fibres surpasses that of the metals by as much as ten times. Carbon, Kevlar®, and fibre glass fibres offer superior strength at a lower weight when compared to metals.

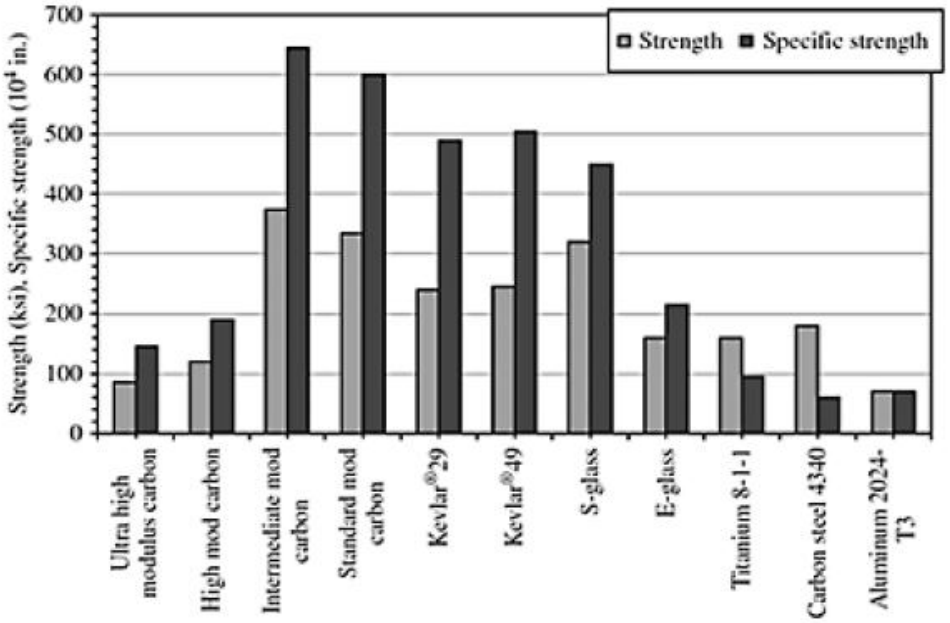

Figure 1.4 - Tensile strength of typical fibres and metals (Source: Composite Tek, 2003)

Most of the FRP systems used nowadays consist of carbon fibres embedded in epoxy matrix. According to Meier (2005), the question regarding which type of fibre is most suitable for this usage is still the subject of lengthy discussions. The author emphasizes that, for bridge repair, carbon fibre is the material best suited in most cases, because the fibre is alkaline resistant and does not suffer stress corrosion, two very important arguments for such applications.

Actually, there are many reasons that make carbon fibres one of the most attractive alternatives for post-strengthening concrete structures. Considering all reinforcing fibre materials used to produce FRPs, the carbon fibres have the highest specific modulus and specific strength that provide a great stiffness to the system, being an ideal choice to be applied in structures sensitive to weight and deflection. Compared with steel, carbon fibres can be five times lighter and present a tensile strength eight to 10 times higher.

Table 1.3 - Comparison of characteristics of FRP sheet made from different fibres (Meier, 1995)

Characteristics	Carbon	Aramid	E-glass
Tensile strength	Very good	Very good	Very good
Compressive strength	Very good	Inadequate	Good
Stiffness	Very good	Good	Adequate
Long term behaviour	Very good	Good	Adequate
Fatigue behaviour	Excellent	Good	Adequate
Bulk density	Good	Excellent	Adequate
Alkaline resistance	Very good	Good	Inadequate
Cost	Adequate	Adequate	Very good

Nonetheless, experimental data have indicated that, in many cases, the failure of the strengthening layer is premature, which means that it is not possible to use all the considerable load capacity offered by these high performance fibres. Several studies are being developed to understand and prevent the mechanisms of premature failure. Despite this eventual shortcoming, the effectiveness of FRP systems is still quite high, given the low specific weight, ease of application, and good mechanical behaviour. Therefore, the main barrier to a wider use of this technique is the relatively high cost of the carbon fibre-reinforced polymer CFRP systems. This is inhibiting their dissemination, especially in third world countries, which have, in most cases, to import all the components of the system.

To overcome this problem, some researchers have suggested the use of alternative fibre-matrix combinations, incorporating less costly but still high performance fibres. This might become an attractive proposition for situations where strength and durability requirements are not so strict. However, it is important to ensure that these new fibre-matrix combinations have an appropriate mechanical behaviour and good coMPatibility with other building materials.

Glass fibres were chosen due to their good strength and lower cost, compared with carbon and aramid fibres, which make them potentially feasible, both technically and economically, for applications demanding a moderate increase in load capacity. In general, glass fibres are white in appearance and are characterized by a high strength

(1,500–3,500 MPa), moderate modulus of elasticity (65–75 GPa), and density = 2.5–2.6, and low thermal conductivity (1 w/mk for E-glass).

Given the reduced stiffness, they might not present an adequate rigidity for some post-strengthening applications, such as the reinforcement of structural members of airplanes and bridges. Another problem is that low cost glass fibres, such as E-glass, are not alkaline resistant and might suffer premature creep failures when subjected to high sustained stress levels. Due to this problem, the document *ACI 440.2R-02*, of the American Concrete Institute, suggests that design loads for glass fibre-reinforced polymers (GFRPs) are limited to 30% of their ultimate strength. According to Wallenberger et al. 2005, despite these limitations, glass fibres are among the most versatile industrial materials known today and are used in the manufacture of several structural composites and in a wide range of special-purpose products.

Aramid fibres, on the other hand, are usually yellow in appearance, have low density (1.4 -1.5 g/cm$^{\wedge 3}$) and are nonconductive. Mechanically, they present higher longitudinal tensile strength (3,400–4,100 MPa) when compared to other materials, such as glass fibres, and are known for their toughness, impact, and abrasion resistance. Moreover, aramid fibres have good resistance to chemical degradation and are relatively inert when exposed to most solvents, although strong acids and bases may degrade them (Callister 2004). Aramid fibres, however, are sensitive to degradation from exposure to ultraviolet radiation and are sensitive to creep. Overall, the economical and mechanical performance of aramid fibre-reinforced polymers (AFRPs) can be positioned between those of glass and carbon fibres.

The selection of the most adequate fibre to create an FRP system for a specific application must be based on considerations regarding cost, stiffness, strength, and long-term behaviour. Depending on the fibre utilized, different performances may be achieved.

1.4 ADVANTAGES AND DISADVANTAGES OF FRP COMPOSITE PLATE BONDING

All structural problems have more than one technical solution, and final selection will ultimately rest upon an economic evaluation of the alternatives. The most obvious technical solution with which to compare FRP composite plate bonding is steel plate bonding, as many of the aspects are common to both. Such a comparison is made

below. However, FRP composite plate bonding should not be thought of as simply an improved form of steel plate bonding. The new material offers such versatility that new solutions will become practicable, particularly those arising from pre-stressing of the plates. The potential advantages of FRP composite plate bonding are as follows:

- *Strength of plates*: FRP composite plates may be designed with components to meet a particular purpose and may comprise varying proportions of different fibres. The ultimate strength of the plates can thus be varied, but for strengthening schemes the ultimate strength of the plates is likely to be at least three times the ultimate strength of steel for the same cross-sectional area.

- *Weight of plates*: the density of FRP composite plates is only 20% of the density of steel. Thus composite plates may be less than 10% of the weight of steel of the same ultimate strength. Apart from transport costs, the biggest saving arising from this is during installation. Composite plates do not require extensive jacking and support systems to move and hold in place. The adhesives alone will support the plate until curing has taken place. In contrast, fixing of steel plates constitutes a significant proportion of the works costs.

- *Transport of plates*: the weight of plates is so low that a 20m long composite plate may be carried on site by a single man. Some plates may also be bent into a coil as small as 1.5 m diameter, and thus may be transported in a car or van without the need for lorries or subsequent cranage facilities. The flexibility of plates enables strengthening schemes to be completed within confined spaces.

- *Versatile design of systems*: steel plates are limited in length by their weight and handling difficulties. Welding *in situ* is not possible, because of damage to adhesives, and expensive fixing of lap plates is therefore required. In contrast, composite plates are of unlimited length, may be fixed in layers to suit strengthening requirements, and are so thin that fixing in two directions may be accommodated by varying the adhesive thickness.

- *Easy and reliable surface preparation*: steel plates require preparation by grit blasting, followed by careful protection until shortly before installation. In

contrast, the ROBUST project has demonstrated that composite plates may be produced with a peel-ply protective layer that may be easily stripped off just before the adhesive is applied.

- *Reduced mechanical fixing*: composite plates are much thinner than steel plates of equivalent capacity. This reduces peeling effects at the ends of the plates and thus reduces the likelihood of a need for end fixing. The overall depth of the strengthening scheme is reduced, increasing headroom and improving appearance.

- *Durability of strengthening system*: there is the possibility of corrosion on the bonded face of steel plates, particularly if the concrete to which they are fixed is cracked or chloride contaminated. This could reduce the long term bond. Composite plates do not suffer from such deterioration.

- *Improved fire resistance*: composite plates are a low conductor of heat when compared with steel, thus reducing the effect fire has on the underlying adhesives. The composite itself chars rather than burns and the system thus remains effective for a much longer period than steel plate bonding.

- *Reduced risk of freeze/thaw damage*: there is theoretical risk of water becoming trapped behind plate systems, although this should not occur if they are properly installed. In practice, this has not been found to be a problem. However, if water did become trapped in this way, the insulating properties of the composite materials would reduce the risk of disruption of the concrete due to freeze/thaw. Loss of bond would also be evident by tapping the composite, but would be more difficult to detect with steel.

- *Reduced construction period*: many of the practical advantages described above combine to enable composite plates to be installed in greatly reduced time periods when compared with steel plates. As well as lower contract costs, the traffic delay costs are minimized. Installation from mobile platforms becomes possible and it may become practicable to confine work within such restraints as limited railway possessions or night-time working.

- *Ability to prestress*: the ability to prestress composites opens up a whole new range of applications for plate bonding. The plate bonding may be used to replace lost prestress and the shear capacity of sections will be increased by the longitudinal stresses induced. Formation of cracks will be inhibited and the serviceability of the structure enhanced.

- *Maintenance of strengthening system*: steel plates will require maintenance painting and may incur traffic disruption and access costs as well as the works costs. Composite plates will not require such maintenance, reducing the whole life cost of this system.

The potential disadvantages of FRP composite plate bonding are as follows:

- *Cost of plates*: fibre reinforced composite plates are more expensive than steel plates of the equivalent load capacity. However, the difference between the two materials is likely to be reduced as production volumes and competition between manufacturers increases. Comparison of total contract costs for alternative methods of strengthening will be based on labor and access costs as well as material costs. Open competition has already shown that FRP composite plate bonding is the most economical solution in virtually all tested cases, without taking into account additional advantages such as durability.

- *Mechanical damage*: FRP composite plates are more susceptible to damage than steel plates and could be damaged by a determined attack, such as with an axe. In vulnerable areas with public access, the risk may be removed by covering the plate bonding with a render coat. Fortunately, if damage should occur to exposed FRP composite plate, such as by a high load, repairs can be undertaken much more easily than with a steel plate. A steel plate may be dislodged, or bond broken over a large area, which would damage bolt fixings and necessitate complete removal and replacement. However, with FRP composite plate bonding the damage is more likely to be localized, as the plate is thinner and more flexible. With FRP composite, the plate may be cut out over the damaged length, and a new plate bonded over the top with an appropriate lap.

1.5 STRENGTHENING CONCRETE STRUCTURES USING FRP COMPOSITES

1.5.1 Flexural Strengthening

Beams

The first application of FRP strengthening was to beams, using wet lay-up sheets or pre-cured plates bonded to the tension face of the beam with the fibre direction aligned to the beam axis. The effectiveness of flexural strengthening of RC beams with FRP is evident from the large data base of experiments reported by Smith and Teng (2002) among others. Bond between FRP and concrete has a pronounced impact on the failure mode and, consequently, on the ductility and failure modes of the strengthened member.

Slabs

The effectiveness of strengthening slabs using FRP has been demonstrated by numerous experimental investigations. A significant of FRP strengthening is around new openings in slabs. Strengthening with FRP strips of one-way and two-way slabs with an opening in the positive moment region can be used to effectively recover the strength of slab prior to making the cut-out and to increase the stiffness (Casadei et al., 2003a).

Columns

Columns may need flexural strengthening, especially for seismic upgrade of structures originally designed for gravity loads. In this case, the maximum bending moments are usually attained at the upper and lower cross-sections of the column, and hence the strengthening system requires anchorage to the adjacent beams. This anchorage may be implemented (for example) with the 'U-anchor system' (Khalifa et al., 1999).

1.5.2 Shear Strengthening

To strengthen RC beams or columns in shear, FRP laminates are bonded to the sides of the member. Efficient design requires the principle fibre direction to be parallel to that of the maximum principal tensile stresses, i.e. (in the most cases) at approximately 45° to the member axis. However, for practical reasons it is usually preferred to attach the external FRP reinforcement with the principal fibre direction perpendicular to the member axis.

NSM reinforcement can also be used effectively to enhance the shear capacity of RC beams. In this case, the bars are embedded in grooves cut on the sides of the member at the desired angle to the axis of beam.

1.6 FAILURE MODES OF STRUCTURES STRENGTHENED WITH FRP MATERIALS

This section discusses common failure modes of FRP strengthened structural members. Reinforced concrete elements strengthened with FRP systems have several additional failure modes compared with reinforced concrete elements that are not strengthened with FRP systems. It is essential that the engineer accounts for all relevant failure modes, as they can have very different failure loads, and behaviours. Since carbon fibers have very high strength in tension relative to the concrete and to the adhesive that binds them to the concrete, the common failure mode of bonded FRP sheets is debonding, not rupture of the sheets. Debonding failures are typically sudden and brittle, and occur before the full strength of the FRP sheet has been reached, so require increased attention by structural engineers. For this reason, it is important to understand and be able to accurately predict the behaviour of bonded FRP sheets.

The most heavily researched FRP application is flexural strengthening of reinforced concrete beams. Through extensive laboratory testing, researchers have defined several distinct failure modes for flexural strengthened beams. It is worth noting that the terminology used to describe the various failure modes varies within the literature. (Smith and Teng, 2001) lists six failure modes, which are shown in Figure 1.5: FRP rupture, concrete cover separation, crushing of compressive concrete, plate end interfacial debonding, shear failure, and intermediate crack induced interfacial debonding.

The three failure modes on the right side of Figure 1.5 are generally termed debonding failures, and involve the beam failing before the strength of the FRP sheet is reached. Debonding failures are the most common type of failures, and are particularly troublesome because they are generally non ductile failures, that occur with little warning. Debonding failures can be further grouped into two categories; plate end interfacial debonding (plate end debonding) and intermediate crack induced debonding (IC debonding). In IC debonding, debonding initiates at the location of an intermediate flexural or flexural-shear crack and then propagates away from the crack towards one of the ends of the beam. In plate end debonding, failure initiates near the end of the beam, often at the termination of the FRP sheet, and then propagates towards the middle of the beam. The failure can either travel up to the tensile reinforcement and then along the reinforcement, so that the concrete cover debonds, which is termed concrete cover separation, or it can propagate near the FRP-concrete interface, which

is termed plate end interfacial debonding. What is common among the debonding failures is that they initiate at stress concentrations; at the termination of the FRP in plate end failures, and at a cracks in interfacial debonding failures. Once failure initiates, it usually progresses very quickly, with little or any increase in load capacity of the member (S.T. Smith and J.G. Teng, 2001). IC debonding and plate end debonding are the most common failure modes of beams flexurally strengthened with FRP.

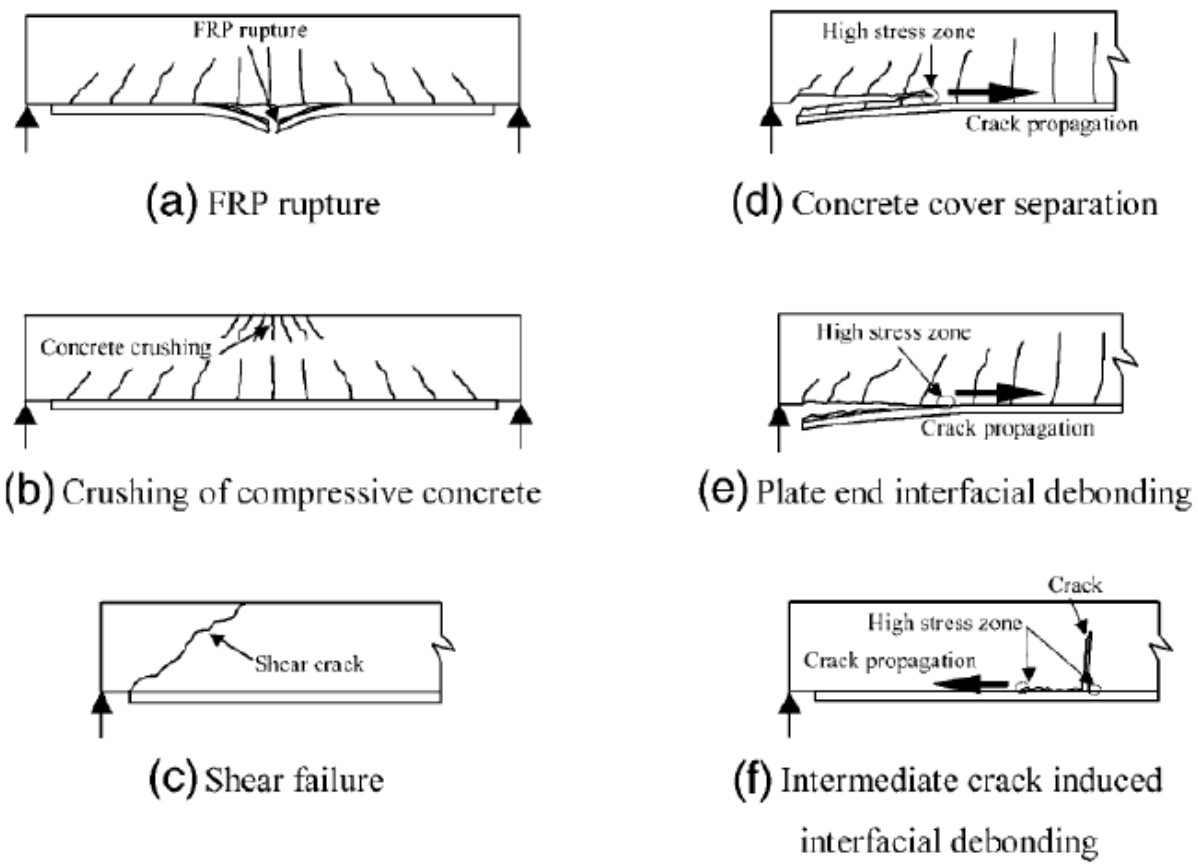

Figure 1.5 – Failure modes of FRP-strengthened RC beams
(S.T. Smith and J.G. Teng, 2001)

The use of FRP for shear strengthening is less researched than for flexural strengthening; however there are common failure modes for both strengthening applications. In shear strengthening applications, interfacial debonding and FRP rupture are the most common failure modes. Interfacial debonding can be difficult to design against in shear strengthening systems, since the space on the side of a beam where the FRP sheet is applied often limits the length of the sheet that can be applied; this is in contrast to FRP that is applied along the length of a flexurally strengthened beam, in which there is usually enough space to develop the strength of the bonded sheet.

1.7 OBJECTIVES OF THESIS

The main objectives of the present work are:

- To study the structural effectiveness of externally bonded CFRPs in strengthening RC beams in combined flexure and shear.

- To examine the effect of different variables such as CFRP amount and distribution, bonded surface, fibre orientation and laminate width on the response of beams in terms of failure modes, increase in load carrying capacity, stiffness and ductility.

- To investigate the effect of transversely placed FRP sheets, or U-wraps, to delay debonding.

1.8 ORIENTATION OF THESIS

The Thesis report is divided into five chapters.

Chapter-1 *Introduction* presents the description of the composite materials, advantages and disadvantages of FRP composite plate bonding, strengthening concrete structures using FRP composites and their failure modes along with objectives of the thesis.

Chapter-2 *Literature Review* presents a brief review of the existing literature in the area of reinforced concrete (RC) beams strengthened with externally bonded FRP laminates.

Chapter-3 *Experimental Program* comprises of description of the experimental work that has been done in the laboratory and description of the characteristics of the composite materials used in strengthening the beams.

Chapter-4 *Results and Discussions* reflects the response behaviours of the tested beams taking into account different variables. The discussions are based on the load-deflection analysis, crack patterns, deformation behaviour and failure modes.

Chapter-5 *Conclusions* gives the specific findings of the study. Recommendation for future study is also discussed.

References

Appendix-A deals with the design approach for computing the shear capacity of strengthened beams based on debonding failure mode.

CHAPTER-2 LITERATURE REVIEW

2.1 INTRODUCTION

The flexural strength of reinforced concrete beams can be significantly increased by bonding a fibre-reinforced polymer (FRP) sheet/plate to their tension face. The shear resistance of reinforced concrete beams can be enhanced by externally bonding fiber-reinforced polymer sheets around the entire section (complete wrapping), to the two sides as well as the soffit of the beam (U-jacketing), and to the two sides of the beam only (side bonding). A large literature exists on fiber-reinforced polymers (FRP) flexure or shear strengthening of reinforced concrete elements. This chapter presents a brief review of the existing literature in the area of reinforced concrete (RC) beams strengthened with externally bonded FRPs. The major achievements and results reported in the literature are highlighted.

2.2 RESEARCH FINDINGS

Three series of 1.3 m long RC beams shear strengthened with CFRP strips were tested by **Chaallal et al. (1998)**. The beams in one series were fully reinforced in shear with steel stirrups (FS), while beams in the second series were under reinforced in shear (US). In the third series the beams were fabricated in the same manner as in the second series and then bonded in the shear span with 50 mm wide side strips either perpendicularly (RS90) or diagonally (RS135) to the axis of the beam (Fig. 2.1). The RS series was designed to achieve the same shear capacity as the series FS. The beams in the US series failed in shear whereas, the beams in FS series and RS series achieved the yielding load of the tensile reinforcement. For the RS series, the CFRP strips reduced extend and severity of the shear cracks and thereby increasing the shear strength and stiffness of the beams. The vertical strips in series RS90 forced the diagonal cracks to bend less than in conventional RC beams, while the diagonal strips in RS135 series limited the propagation of the shear cracks. Most of the beams in RS series failed due to peeling of laminate initiated longitudinal and transverse cracking towards the bottom of the beams. These cracks were attributed to high peeling (normal tensile) stresses developed at ends of the CFRP strips near the bottom of the beams, especially at higher load levels. The authors concluded that although strips oriented at 135 degrees to the beam axis outperformed the perpendicular strips, U-strips and U-jackets should be utilized to minimize the peeling stresses at the ends of the strips leading to premature failure.

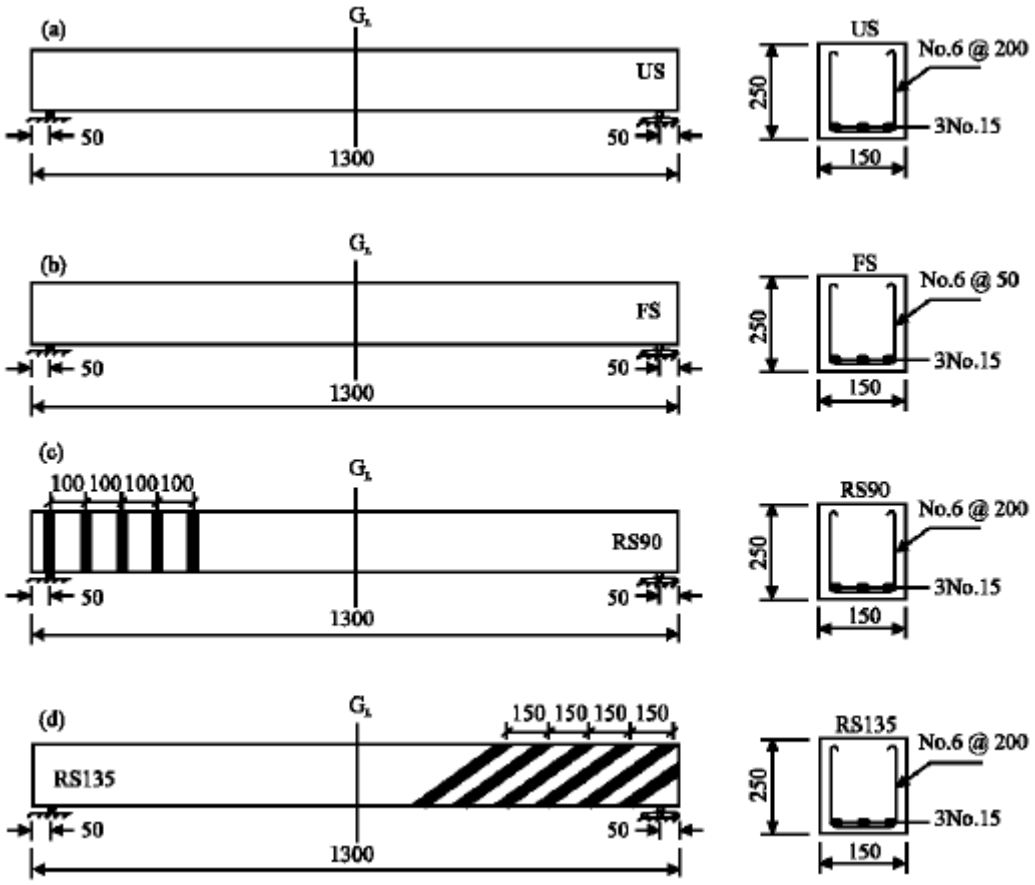

Figure 2.1 – Test specimens (a) US, (b) FS, (c) RS90, and (d) RS 135 Chaallal et al. (1998)

Khalifa and Nanni (2000) investigated the performance of T-beam strengthened in shear with CFRP sheets. They found that by using various configurations such as side strips and continuous wraps of CFRP sheets, the shear capacity of the beams could be increased by 35 to 135%. It was found that an optimum quantity of FRP exists, beyond which strengthening effectiveness is uncertain. Strips of FRP applied only to the beam sides provide less strength enhancement than those bonded in U-shaped configuration Although strips proved to be as effective as continuous sheets, researchers recommended that sheet be utilized in field applications. Since damage to an individual strips is more detrimental to its behaviour.

Ramana et al. (2000) experimentally investigated the flexural strengthening of reinforced concrete beams by the external bonding of high-strength, light-weight carbon fibre reinforced polymer composite (CFRPC) laminates to the tension face of the beam. Four sets of beams, three with different amounts of CFRPC reinforcement by changing the width of CFRPC laminate, and one without CFRPC were tested in four-point bending over a span of 900 mm. The tests were carried out under displacement control. One beam in a set was extensively

instrumented to monitor strains and deflections over the entire range of loading till the failure of the beam. The increase in strength and stiffness provided by the bonded laminate was assessed by varying the width of laminate. The results indicate that the flexural strength of beams was significantly increased as the width of laminate increased.

Deniaud and Cheng (2001) tested 3700 mm long concrete T-beams strengthened externally using FRP sheets to study the interaction between FRP sheets and steel stirrups in carrying shear. The beams were designed to provide a flexural capacity 2.0 to 3.5 times greater than shear capacity without the FRP contribution Three types of FRP were applied externally to strengthen the web of the T-beams: uniaxial glass fibre, uniaxial carbon fibre and triaxial glass fibre. The test setup consisted of a four-point loading system Test results showed that FRP reinforcement increased the shear strengths from 77 to 117% above that of the beams without strengthening. The magnitude of the increase in shear capacity depends not only on the type of FRP but also on the amount of internal shear reinforcement. The FRP strains were found to be uniformly distributed for the fibres crossing the crack at the shear crack.

Toutanji and Ortiz (2001) investigated the influence of surface preparation before attaching CFRP sheets on the bonding strength and load carrying capacity of RC beams strengthened through the EBR method. The main purpose of surface preparation was to remove the weak external layer as well as the impurities concealed in the concrete surface pores which prevent proper attachment of CFRP sheets. Results revealed that surface preparation not only enhanced the ultimate load capacity but also postponed the debonding of CFRP sheets off the concrete surface to a limited extent through providing a sufficient bond interface between the CFRP sheets and the concrete substrate.

Neto et al. (2001) investigated the shear strength of eight-T reinforced concrete simply supported beams. Six of the beams were strengthened with unidirectional layers of CFRP. The main variables investigated were the direction of the CFRP layer (vertical and inclined at 45°) and the number and width of the layers (Figure 2.2). Four beams were preloaded to service load before being strengthened. The beams were 4400 mm in total length, 400 mm of overall height and had a 150 mm web width. The clear span was 4000 mm. The beams had identical flexural reinforcement. Beams 1 to m did not have stirrups in the shears span while beams 4 to 8 had steel stirrups. The results showed that ultimate loads of the strengthened beam were from 7 to 35% higher than the control beams. All the strengthened beams failed

due to peeling of the CFRP laminates at the ends close to the flange with a thin layer of concrete attached to the laminate.

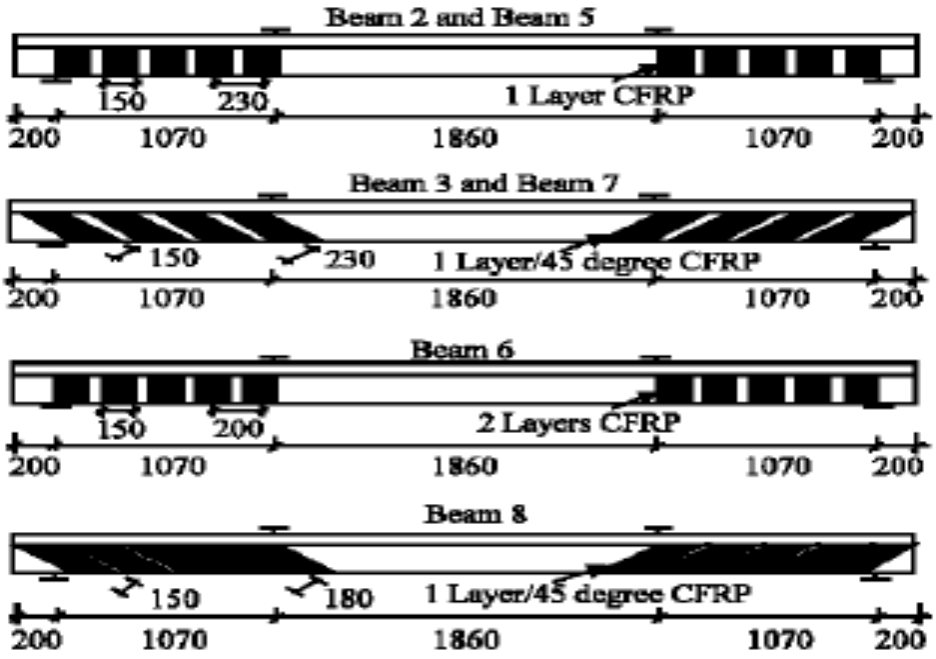

Figure 2.2 – Test specimens of Neto et al. (2001)

Lee and Al-Mahaidi (2003) tested four large scale T-beams with identical reinforcement details (Figure 2.3). The beams were 6000 mm long, 490 mm deep, the web was 225 mm wide and flange was 720 mm wide. All the beams were designed to exhibit shear failure. The first beam was used as the control beam with no strengthening carried out. The second and third and fourth beams were strengthened with L shaped laminate strips spaced at 0.75D, 0.6D and 0.5D where D is the overall depth of the beam. The nominal width of the plates was 40 mm with thickness of 1.2 mm. The beams were subjected to four-point loading with a shear span to depth ratio of 3.0. The test results showed that the stiffness of all beams tested were similar to each other in the early stage of loading. The presence of the external shear reinforcement did not affect significantly the initial stiffness of the strengthened beams compared to the control beam at first loading. The control beam failed in a gradual manner whereas the strengthened beams failed in an abrupt manner with a significant drop in load almost after reaching the peak load. From the results, an increase in shear capacity of 54 to 81% was achieved in the T-beams strengthened with the external CFRP reinforcement with all beams failing in shear. The presence of CFRP external shear reinforcement did not delay the initial formation of shear cracks but impeded their propagation and growth.

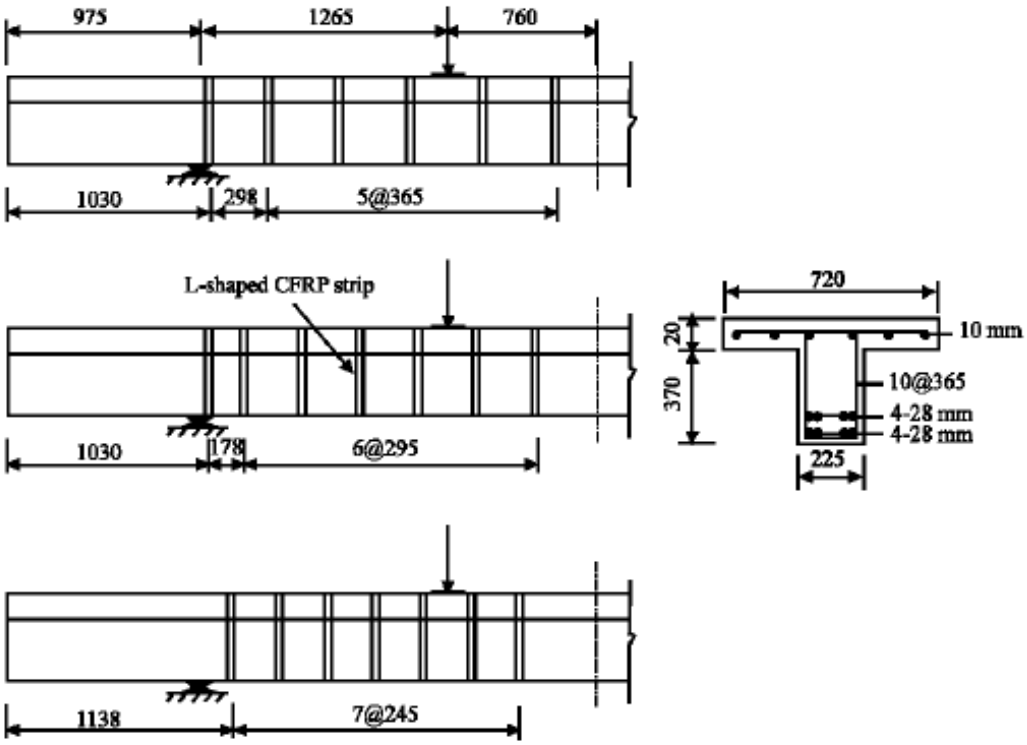

Figure 2.3 – Details of Lee and Al-Mahaidi (2003) T-beams

Rita and Vecchio (2003) used the EBR method for shear strengthening of RC beams with CFRP composites in their experimental study. The mechanism increased the shear resistance of the beam by both providing better interlock between aggregates and restricting the shear crack propagation. They found that as a result of these processes, the failure mechanism changed from a brittle shear mode to a ductile shear-flexural one and the ultimate load capacity and mid-span deflection were also increased by up to 50% and 350% respectively, relative to their control beam which lacked any external strengthening. However, premature debonding was observed in specimens strengthened by the EBR method.

Adhikary and Mutsuyoshi (2004) tested eight 150 mm wide, 200 mm deep by 2600 mm long concrete beams strengthened in shear. The beams had no internal shear reinforcement in the desired shear failure region to ensure shear failure even after the application of carbon fibre sheets. The effects of various CFRP sheets configuration and layouts were studied. The test variables were the number of layers of the CFRP sheet, sheet depth, direction of fibre (vertical or horizontal) and side application or U-wrap. All the beams failed in shear. The ultimate loads for the shear strengthened beams were 29 to 119% higher than the control beam. The greatest shear strength was obtained for the beam with full U-wrapped sheets having vertically aligned fibres. Researchers concluded that the results confirm the

effectiveness of the U-wrap configuration in strengthening beams in shear. They recommended that the shear strengthened beam should be reinforced with CFRP up to the maximum possible section depth to achieve the best strengthening effects.

Islam et al. (2005) investigated shear strengthening of RC deep beams using externally bonded FRP systems. In this study, six identical beams were fabricated and tested to failure for this purpose. One of these beams was tested in its virgin condition to serve as reference, while the remaining five beams were tested after being strengthened using carbon fibre wrap, strip or grids. The test results have shown that the use of a bonded FRP system leads to a much slower growth of the critical diagonal cracks and enhances the load-carrying capacity of the beam to a level quite sufficient to meet most of the practical upgrading requirements. Although FRP grids placed in normal orientation demonstrated to be the most effective system as far as the amount of material used in strengthening is concerned, other systems were found to be almost equally effective. An enhancement of shear strength in the order of about 40%, was achieved in this study.

Saafan (2006) studied the shear strengthening of reinforced concrete (RC) beams using GFRP wraps. The objective of the experimental work was to investigate the efficiency of GFRP composites in strengthening simply supported reinforced concrete beams designed with insufficient shear capacity. Using the hand lay-up technique, successive layers of a woven fibre glass fabric were bonded along the shear span to increase the shear capacity and to avoid catastrophic premature failure modes. The strengthened beams were fabricated with no web reinforcement to explore the efficiency of the proposed strengthening technique using the results of control beams with closed stirrups as web reinforcement. The test results of 18 number of beams were reported, addressing the influence of different shear strengthening schemes and variable longitudinal reinforcement ratios on the structural behaviour. The results indicated that significant increase in the shear strength and improvements in the overall structural behaviour of beams with insufficient shear capacity could be achieved by proper application of GFRP wraps.

Mosallam and Banerjee (2007) studied experimentally on shear strength enhancement of reinforced concrete beams externally reinforced with fibre-reinforced polymer (FRP) composites. A total of nine full-scale beam specimens of three different classes, as-built

(unstrengthened), repaired and retrofitted were tested. Three composite systems namely carbon/epoxy wet layup, E-glass/epoxy wet layup and carbon/epoxy procured strips were used for retrofit and repair evaluation. Experimental results indicated that the composite systems provided substantial increase in ultimate strength of repaired and strengthened beams as compared to the pre-cracked and as-built beam specimens. A comparative study of the experimental results with published analytical models, including the ACI 440 model, was also conducted in order to evaluate the different analytical models and identify the influencing factors on the shear behaviour of FRP strengthened reinforced concrete beams. Comparison indicates that the shear span-to-depth ratio (*a/d*) is an important factor that actively controls the shear failure mode of beam and consequently influences on the shear strength enhancement.

Nadeem A. Siddiqui et al. (2009) studied the efficiency and effectiveness of different FRP schemes for flexure and shear strengthening of RC beams. For this purpose, 6 RC beams were cast in two groups, each group containing 3 beams. The specimens of first group were designed to be weak in flexure and strong in shear, whereas specimens of second group were designed just in an opposite manner. In each group, out of the three beams, one beam was taken as a control specimen and the remaining two beams were strengthened using two different Carbon FRP (CFRP) strengthening schemes. All the beams of two groups were tested under similar loading. The response of control and strengthened beams were compared and efficiency and effectiveness of different schemes were evaluated. It was observed that tension side bonding of CFRP sheets with U-shaped end anchorages is very efficient in flexural strengthening; whereas bonding the inclined CFRP strips to the side faces of reinforced concrete beams are very effective in improving the shear capacity of beams.

Sundarraja and Rajamohan (2009) studied on strengthening of reinforced concrete (RC) beams which are deficient in shear using glass fibre reinforced polymer(GFRP) inclined strips experimentally. Included in the study are effectiveness in terms of width and spacing of inclined GFRP strips, spacing of internal steel stirrups, and longitudinal steel rebar section on shear capacity of the RC beam. The study also aims to understand the shear contribution of concrete, shear strength due to steel bars and steel stirrups and the additional shear capacity due to GFRP strips in a RC beam. And also the failure modes, shear strengthening effect on ultimate force and load deflection behaviour of RC beams bonded externally with GFRP inclined strips on the shear region of the beam. The use of GFRP strips had effect in delaying

the growth of crack formation, which is, evident from the load causing the initial cracks. When both the wrapping schemes were considered, it was found that the retrofitted beams with inclined U-wrap GFRP strips had a better load-deflection behaviour compared to the side strips, which is very important for shear strengthening of the RC beams. Finally, the use of inclined GFRP strips was able to avoid the brittle failure of the beams.

Bukhari et al. (2010) investigated on the shear strengthening of reinforced concrete (RC) beams with carbon fibre reinforced polymer (CFRP). The paper reviews existing design guidelines for strengthening beams in shear with CFRP sheets and proposes a modification to Concrete Society Technical Report TR55. It goes on to present the results of an experimental program which evaluated the contribution of CFRP sheets towards the shear strength of continuous reinforced concrete (RC) beams. A total of seven, two-span concrete continuous beams with rectangular cross-sections were tested. The control beam was not strengthened, and the remaining six were strengthened with different arrangements of CFRP sheets. The experimental results showed that the shear strength of the beams was significantly increased by the CFRP sheet and that it was beneficial to orient the FRP at 45º to the axis of the beam.

Habibur Rahman Sobuz et al. (2011) experimentally investigated the flexural behaviour of reinforced concrete beams strengthened with CFRP laminates attached to the bottom of the beams by epoxy adhesive subjected to transverse loading. A total of five beams having different CFRP laminates configurations were tested to failure in four-point bending over a clear span 1900mm. Four beams were strengthened by changing the levels of CFRP laminates whereas the last one was not strengthened with FRP and considered as a control beam. Test results showed that the addition of CFRP sheets to the tension surface of the beams demonstrated significantly improvement in stiffness and ultimate capacity of beams. The response of control and strengthened beams were compared and efficiency and effectiveness of different CFRP configurations were evaluated. It was observed that tension side bonding of CFRP sheets with U-shaped end anchorages is very efficient in flexural strengthening.

Kaushal Parikh et al. (2012) carried out experimental and analytical investigation on preloaded retrofitted beam with GFRP for enhancement in flexural strength. They took seventeen beam for experimental study, out of that two were control beams and fifteen were preloaded at 0%, 40% and 90% of control beam. Author used new arrangement of FRP for

strengthening the beam in which they were apply full length of single layer, they reduced length and width in second and third layer. Author also carried out analytical investigation using ATENA 3D software which are based on finite element method. Author concluded from the analytical and experimental results, new arrangement so effective that was shift the flexural crack away from the flexural region and also come out from the debonding failure. They observed load vs. deflection not more than 5% varied in experimental and analytical results, failure mode are also remarkable compared.

Sherif H. Al-Tersawy et al. (2013) examined the performance of reinforced concrete (RC) beams strengthened in shear. Experimental investigation was carried out on nine RC beams of three different sets, as-built beams (un-strengthened), beams strengthened with vertical carbon fibre-reinforced polymer (CFRP) wraps, and beams strengthened with inclined CFRP wraps. The main parameters investigated were concrete strength, CFRP thickness and wraps orientations (90°, 45°). The results of the experimental work indicated that externally bonded CFRP wraps enhanced the shear strength of beams significantly and that inclined CFRP configuration is more effective than vertical ones.

Mostofinejad and Tabatabaei (2013) developed an alternative technique called the ‘‘Externally Bonded Reinforcement on Grooves (EBROG)” to prevent the debonding of FRP sheets used for shear strengthening in the conventional EBR and NSM methods, Their results showed that the shear failure mode changed to the flexural when vertical grooves were cut prior to shear strengthening of beams by CFRP sheets through the EBROG technique as a substitute for the conventional surface preparation, and that it increased the load carrying capacity of the beams by about 17–23% relative to the non-strengthened control beams.

Mostofinejad and Shameli (2013) utilized the technique of Externally Bonded Reinforcement in Grooves (EBRIG) for the flexural strengthening of RC beams by combining the EBROG and NSM methods using a wet lay-up procedure. In this technique, groove surfaces are in direct contact with CFRP sheets. Results showed that, compared to the case with the EBROG method, not only did the ultimate load capacities of the test RC beams subjected to the EBRIG method increase by about 3%, 38%, and 56% with one, two, and three FRP layers, respectively, as a result of the enhanced contact area between the CFRP sheets and groove surfaces, but the premature debonding of FRP sheets was completely eliminated as well.

CHAPTER-3 EXPERIMENTAL PROGRAM

3.1 INTRODUCTION

The aim of the experimental program is to study the effect of externally bonded (EB) fibre reinforced polymer (FRP) sheets on the performance of reinforced concrete beams under static loading condition. The brief description of all materials and equipment required to perform tests is discussed in this chapter. Furthermore strengthening procedure, experimental setup and description of specimens is discussed in the end.

3.2 MATERIALS AND EQUIPMENT

For the entire experimental program, the following materials and equipment were used:

3.2.1 Cement

Cement is a fine, grey powder. It is mixed with water and materials such as sand, gravel, and crushed stone to make concrete. The cement and water form a paste that binds the other materials together as the concrete hardens. Grade 43 Ordinary Portland cement was used for casting the beams. The cement was of uniform colour i.e. grey and was free from any hard lumps. The various tests were conducted on the cement before its use and the results are shown in Table 3.1.

Table 3.1 - Properties of Cement (OPC-43)

Sr. no.	Characteristics	Experimental values obtained	IS 8112: 2013 Specified values	Test method referred to
1	Specific gravity	3.04	-	IS: 4031 (11)
2	Standard Consistency (%)	33	-	IS: 4031 (4)
3	Setting time (min.)			IS: 4031 (5)
	Initial	40	30 (min.)	
	Final	320	600 (max.)	
4	Compressive strength (MPa)			IS: 4031 (6)
	3 days	24.5	23	
	7 days	33.5	33	
	28 days	44.5	43	

3.2.2 Coarse Aggregates

The crushed stone is generally used as a coarse aggregate. The nature of work decides the maximum size of the coarse aggregate. The natural crushed stone aggregates of sizes 10mm and 20mm were used in this experimental program. The aggregates were washed to remove the dust and dirt and then dried to obtain surface dry condition. The aggregates were tested as per IS: 383-1970. The sieve analysis results are shown in Table 3.2 and 3.3. The results of various tests conducted on coarse aggregate are given in Table 3.4.

Table 3.2 - Sieve Analysis of Coarse Aggregates (10mm)

Total weight of sample taken = 3000gm

Sr.no.	Sieve size	Mass retained (g)	Percentage retained (%)	Cumulative percentage retained, C	Percent passing, (100 - C)
1	20 mm	0	0	0	100
2	10 mm	1246	41.53	41.53	58.47
3	4.75 mm	1634	54.47	96	4
4	Pan	120	4	Sum = 137.53	0

FM of 10 mm Coarse Aggregate = (137.53+500)/100 = 6.37

Table 3.3 - Sieve Analysis of Coarse Aggregates (20mm)

Total weight of sample taken = 3000gm

Sr.no.	Sieve size	Mass retained (g)	Percentage retained (%)	Cumulative percentage retained, C	Percent passing, (100 - C)
1	40 mm	0	0	0	100
2	20 mm	0	0	0	100
3	10 mm	2656	88.53	88.53	11.47
4	4.75 mm	326	10.87	99.4	0.6
5	Pan	18	0.6	Sum = 187.93	0

FM of 10 mm Coarse Aggregate = (187.93+500)/100 = 6.87

Table 3.4 - Physical Properties of Coarse Aggregates

Sr. no.	Properties	Nominal size (10 mm)	Nominal size (20 mm)
1	Specific gravity	2.68	2.61
2	Total water absorption (%)	1.63	1.66
3	Fineness modulus	6.37	6.87

3.2.3 Fine Aggregates

Fine aggregate/sand is an accumulation of grains of mineral matter derived from disintegration of rocks. It is distinguished from gravel only by the size of the grains or particles, but is distinct from clays which contain organic material. The sand used for the experimental program was locally procured and confirmed to IS: 383-1970. The sand was first sieved through 4.75mm sieve to remove any particles greater than 4.75mm and then was washed to remove the dust. The aggregates were sieved through a set of sieves to obtain sieve analysis and the same is presented in Table 3.5. The properties of the fine aggregate/sand used in the experimental work are given in Table 3.6.

Table 3.5 - Sieve Analysis of Fine aggregate/sand

Total weight of sample taken = 1000gm

Sr.no.	Sieve size	Mass retained (g)	Percentage retained (%)	Cumulative percentage retained, C	Percent passing, (100 - C)
1	4.75 mm	7.5	0.75	0.75	99.25
2	2.36 mm	84	8.4	9.15	90.85
3	1.18 mm	167	16.7	25.85	74.15
4	600µm	218	21.8	47.65	52.35
5	300µm	288	28.8	76.45	23.55
6	150µm	199.5	19.95	96.4	3.6
7	Pan	36	3.6	Σ=256.25	

Fineness Modulus of Sand = 2.56

Table 3.6 - Physical Properties of Fine aggregate/sand

Sr. no.	Properties	Value
1	Specific gravity	2.46
2	Total water absorption (%)	0.83
3	Fineness modulus	2.56

3.2.4 Water

Generally, water that is suitable for drinking is satisfactory for use in concrete. Water from lakes and streams that contain marine life also usually is suitable. When water is obtained from sources mentioned above, no sampling is necessary. In the present experimental program, potable tap water is used for casting of beam specimens.

3.2.5 Reinforcing Steel

HYSD bars confirming to IS: 1786-1985 of grade Fe-500 Tata Tiscon steel of 8mm and 6mm diameters are used as main longitudinal steel. 8mm dia. bars are used as tension reinforcement and 6mm dia. bars are used as compression steel as well as for shear reinforcement.

3.2.6 CFRP Material

Unidirectional CFRP sheets 500mm wide and 0.167mm thickness as shown in Figure 3.1 were used for the strengthening of the beams. The sheets were manufactured by Toray industries. Under stress, fibre utilizes the plastic flow of matrix to transfer the load to the fibre which results in high strength and high modulus composite. The main function of matrix is to combine and to protect the fibre against external environment in which the composite will be placed. The properties of the fibre used are given in Table 3.7.

3.2.7 Epoxy Resin

The success of the strengthening technique primarily depends on the performance of the epoxy resin used for bonding of FRP to concrete surface. Various types of epoxy resins with a wide range of mechanical properties are commercially available in the market. These epoxy resins are generally available in two parts, a resin and a hardener. The epoxy resin used in this study was Dr. Fixit 211 epoxy bonding agent. The properties of the epoxy resin used in the experimental work are given in Table 3.8.

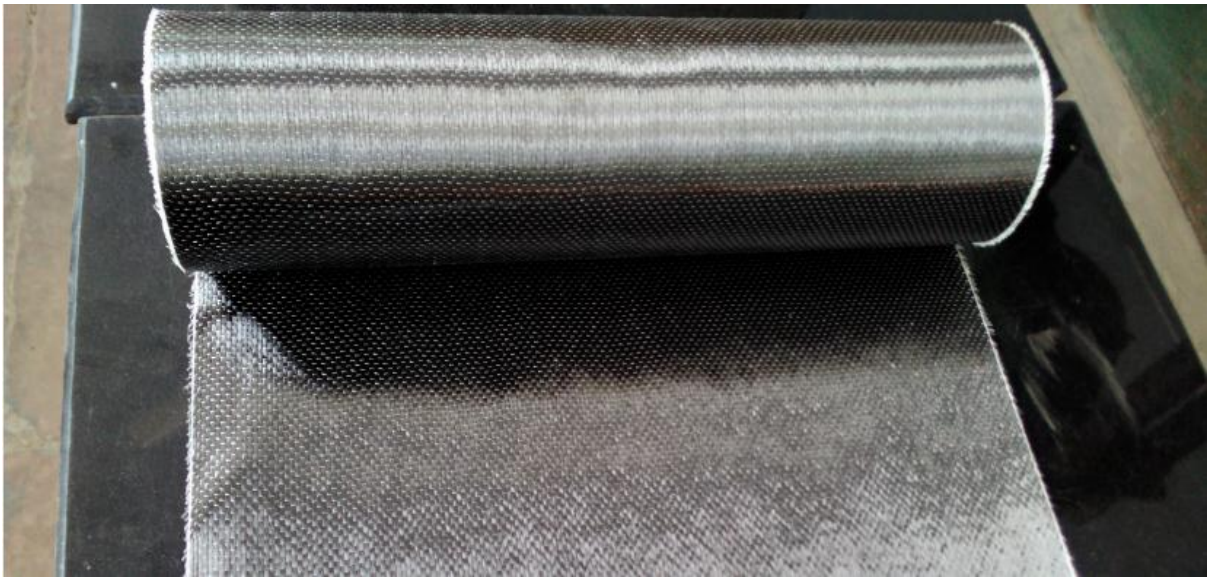

Figure 3.1 – CFRP sheet used for strengthening of beams

Table 3.7 - Properties of Fibre (provided by manufacturer)

Sr. no.	Physical properties	Value
1	Tensile strength	4216 MPa
2	Modulus of Elasticity	2.52 x $10^{\wedge 5}$ MPa
3	Density	1.76 g/cm^3
4	Thickness	0.167 mm
5	Ultimate strain	1.76 %

Table 3.8 - Properties of Epoxy resin (provided by manufacturer)

Sr. no.	Physical properties	Value
1	Mix Density	1120 kg/m^3
2	Colour	Grey
3	Pot Life @ 30° C	± 30-40 mins.
4	Cure time	7 days
5	Tensile strength, 7 days	10.4 N/mm^2
6	Compressive strength, 7 days	60 N/mm^2
7	Flexural Strength	28.1 N/mm^2

3.2.8 Roller

A special type of roller was used for impregnating the adhesive substance to the fibre.

3.2.9 Dial gauge

The dial gauge (digital) was used to measure the deflection at the centre of the beam. The least count of the dial gauge was 0.001mm.

Figure 3.2 – Dial gauge used for measuring the deflection

3.3 DESIGN OF CONCRETE MIX

M25 concrete mix was designed by using the properties of cement, fine aggregate/sand and crushed stone coarse aggregates as per IS 10262: 2009 guidelines. The water/cement ratio was taken as 0.46. The details of mix proportions are given in Table 3.9. The cubes were prepared with this mix proportions and were tested at the age of 7days and 28 days. The compressive strength test results of cubes prepared with trial mixes are given in Table 3.10.

Table 3.9 - Mix Proportions for M25 grade concrete

Water	Cement	Fine Aggregate/sand	Coarse Aggregates
192 kg	417.39 kg	544.38 kg	1190 kg
0.46	1	1.30	2.85

Table 3.10 – Compressive strength test results of trial mixes

Sr. no.	Particulars	Compressive strength (MPa) 7 days	Compressive strength (MPa) 28 days
1	Average value of 3 cubes	20.9	34.0

3.4 DESIGN OF BEAM

The beam was designed to behave as under-reinforced section with M25 grade concrete and Fe- 500 steel of cross dimensions 150*150*700 mm. The reinforcement to be provided was two bars of 8mm dia. in the tension zone and two bars of 6mm dia. in the compression zone. Stirrups were also provided as two-legged of 6mm dia. with 75mm c/c spacing. The structural detailing of the beam is shown in Figure 3.3.

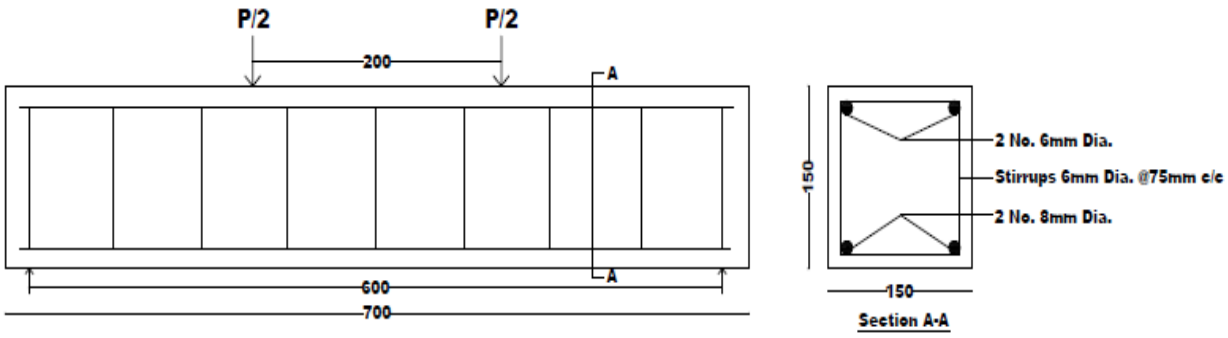

Figure 3.3 – Structural Detailing of the beam

3.5 CASTING OF BEAMS

As per the design, the beams were casted. The shuttering steel plates were joined together through nut bolts to form the formwork to the required dimensions. Proper oiling of the plates was done, to ensure the finished surface of the beams after the removal of formwork. The steel mesh so formed was kept inside the formwork with proper cover blocks of 25mm below the mesh. The vibrator was also used to ensure proper coMPaction of the concrete. After the removal of formwork, the curing was done with the jute bags for 7 days.

Figure 3.4 – Beam specimens at the time of casting

3.6 STRENGTHENING PROCEDURE

Before bonding the laminates on the beam specimens, the surfaces were ground to remove all the contaminations and weak surface layers and to expose the aggregates which provides better adhesion of beam surface with the fibre. After this the dust and debris were removed by air blast. The resultant concrete surface was characterized by a uniformly abraded surface with exposed small to medium sized pieces of aggregates (Figure 3.5).

Figure 3.5 – Surface of beam after grinding

The CFRP sheets were cut to the required length, prior to the preparation of the epoxy resin. The next step was applying an epoxy resin to the beam surface over which the laminate was attached. The epoxy that comes in two components was mixed thoroughly until a smooth and homogenous mix was obtained. The mix was applied evenly with brush ensuring that on the beam surfaces all gaps were covered. The epoxy adhesive thickness was maintained constant throughout the length, for all the beams. Then the CFRP sheet was placed on top of epoxy resin coating and the resin was squeezed through the roving of the fabric with the roller. Air bubbles entrapped at the epoxy/concrete or epoxy/fabric interface were eliminated.

During hardening of the epoxy, a constant uniform pressure was applied on the composite fabric surface in order to extrude the excess epoxy resin and to ensure good contact between the epoxy, the concrete and the fabric. This operation was carried out at room temperature. Concrete beams strengthened with carbon fibre fabric were cured for minimum of one week at room temperature before testing.

3.7 EXPERIMENTAL SETUP

The beams were tested after 28 days from the date of casting. All the beam specimens were tested as simply supported beams subject to two-point loading with loads applied at L/3 distance from the each end; where L is the effective span i.e. 600 mm. The shear span to effective depth ratio (*a/d*) was equal to 1.6. This load case was chosen because it gives constant moment and zero shear in the section between the loads, and constant maximum shear force between support and load. The moment was linearly varying between supports and load. The testing procedure for the entire beam specimens was same. The tests were performed using the setup as shown in the Figure 4.6.

Figure 3.6 – Experimental setup used for testing

The testing of beams was carried out in Universal testing machine (UTM) of 1000 kN load capacity. The tests were carried out using displacement control, and the applied loads were monitored through a high accuracy load cell with a load sensitivity of 0.001 kN. The load was applied at the rate of 4 kN/min. One dial gauge was placed just below the center of the beam, i.e. at L/2 distance to measure the deflection. The reading was taken at regular intervals of load. During loading, the specimen was visually inspected and cracks were marked. For the clear visibility of cracks, the surfaces were painted with white distemper prior to testing.

3.8 DESCRIPTION OF STRENGTHENING SCHEMES:

The experimental program consists of fifteen (15) simply supported RC beams having same dimensions of 150*150*700 mm. The same reinforcement is provided in all the beams. The longitudinal reinforcement consists of two bars of 8mm dia. in the tension zone and two bars of 6mm dia. in the compression zone. Stirrups are also provided as two-legged of 6mm dia. with 75mm centre-to-centre spacing. The description of beams strengthened with various schemes is given in Table 3.11. A more detailed description of beams strengthened with CFRP in various schemes along with their cross-sections is given in 3.8.1 to 3.8.8.

Table 3.11 – Description of Strengthening Schemes

Beam Label	Description of Strengthening Schemes	External CFRP Reinforcement	
		Flexural	Shear
CB-01	Control/ Un-strengthened Beams	-	-
CB-02			
SB-01	Beams strengthened with Scheme I	150 mm wide laminate at bottom	-
SB-02			
SB-03	Beams strengthened with Scheme II	150 mm wide laminate at bottom	50 mm wide U-strips in shear spans
SB-04			
SB-05	Beams strengthened with Scheme III	150 mm wide laminate at bottom	150 mm wide U-wrap in shear spans
SB-06			
SB-07	Beams strengthened with Scheme IV	150 mm wide laminate at bottom	40 mm wide inclined strips in shear spans
SB-08			
SB-09	Beams strengthened with Scheme V	150 mm wide laminate at bottom	40 mm wide inclined strips (with grooves)
SB-10			
SB-11	Beams strengthened with Scheme VI	150 mm wide laminate at bottom	125 mm wide side - wrap (with grooves)
SB-12			
SB-13	Beam strengthened with Scheme VII	100 mm wide laminate at bottom	60 mm wide U-strip at ends of the beam

3.8.1 Control/ Un-strengthened Beams: The two beams named CB-01 and CB-02 are served as the controlled beams which are not strengthened with CFRP laminates. The internal shear reinforcement is provided in the beam according to the maximum load carrying capacity of the beam to avoid shear failure.

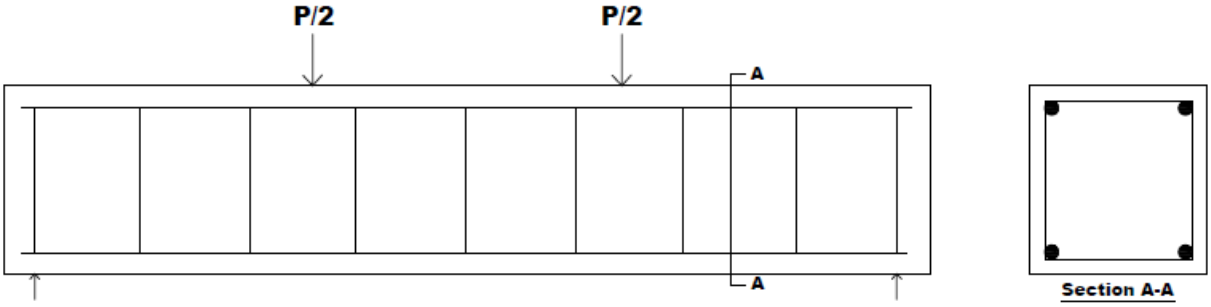

Figure 3.7 – Description of control beams

As the beam is designed as an under-reinforced section, the yielding of tension steel was expected followed by crushing of concrete in compression zone and the same failure mode was obtained in test results. (discussed in section 4.2.1 and 4.2.2)

3.8.2 Beams strengthened with Scheme I: As controlled beams failed in flexure, so the primary requirement is to strengthen beams in flexure to enhance the load capacity of the beams. The two beams named SB-01 and SB-02 are strengthened with single layer of CFRP sheet at the bottom face. The sheet is provided with a width of 150 mm and length of 500 mm.

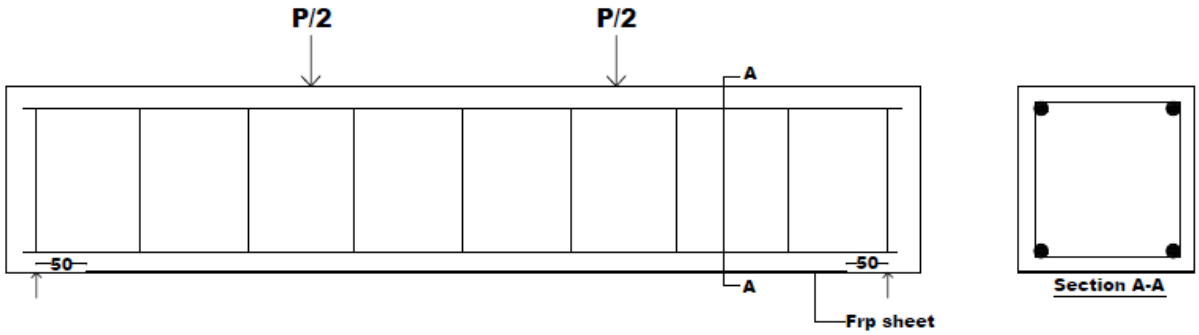

Figure 3.8 – Description of strengthened beams (Scheme I)

The load carrying capacity of the beams was increased due to strengthening in flexure with CFRP laminate. Due to increase in load, the shear force also increases and the failure occurred due to critical diagonal shear crack formed at the end of the laminate. Therefore in the next strengthening schemes, the beams are strengthened in shear with CFRP laminates.

3.8.3 Beams strengthened with Scheme II: The two beams named SB-03 and SB-04 are strengthened with single layer of CFRP sheet at the bottom face. In addition, the U-strips of 50 mm width and 450 mm length are provided in shear spans of the beams to enhance the shear capacity of the beams. The centre-to-centre spacing of strips is 85mm.

3.8.4 Beams strengthened with Scheme III: The two beams named SB-05 and SB-06 are strengthened with single layer of CFRP sheet at the bottom face. In contrast to Type II, the beams are strengthened with 150 mm full U-wrap in shear spans of the beams.

3.8.5 Beams strengthened with Scheme IV: The two beams named SB-07 and SB-8 are strengthened with single layer of CFRP sheet at the bottom face. In shear spans, two-strips (L-shape) of 40 mm width, with an inclination of 45° to the longitudinal axis of the beam, are provided. The centre-to-centre spacing of strips is 60 mm.

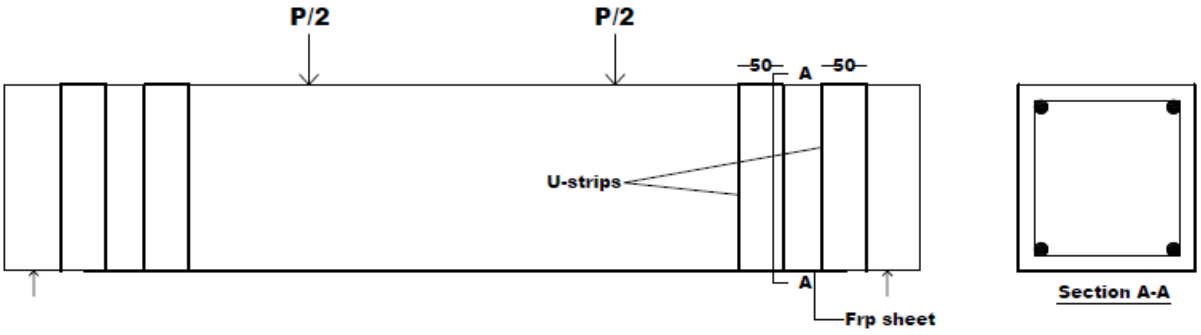

Figure 3.9 – Description of strengthened beams (Scheme II)

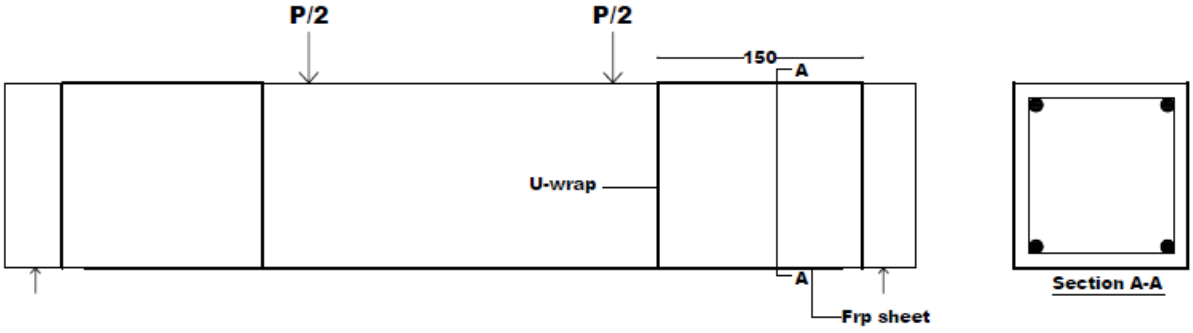

Figure 3.10 – Description of strengthened beams (Scheme III)

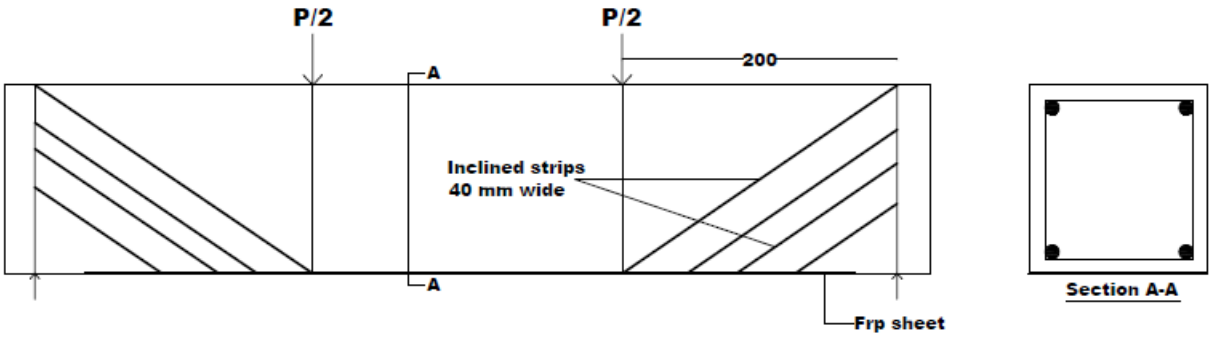

Figure 3.11 – Description of strengthened beams (Scheme IV)

In strengthening schemes II and III, the increase in load carrying capacity was achieved as compared to beams strengthened only in flexure (SB-01 and SB-02) but the sudden failure occurred due to debonding of CFRP strips and U-wraps which reduces the effectiveness of strengthening. Therefore in the next strengthening schemes (V and VI) the grooving method is used to increase the interface area or to delay debonding of CFRP side strips and U-wraps.

3.8.6 Beams strengthened with Scheme V: The two beams named SB-09 and SB-10 are strengthened with single layer of CFRP sheet at the bottom face. In contrast to Type IV, the grooves of 6 mm width and 10 mm depth are cut, at the location where strips are to be bonded, and then filled with epoxy to increase the interface area.

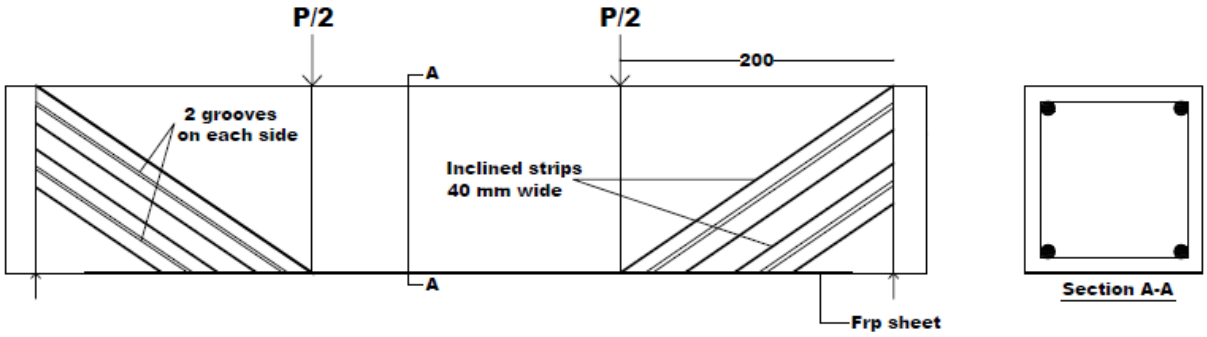

Figure 3.12 – Description of strengthened beams (Scheme V)

3.8.7 Beams strengthened with Scheme VI: The two beams named SB-11 and SB-12 are strengthened with single layer of CFRP sheet at the bottom face. In addition, 125mm wide side strips (L-shape) are provided in the shear spans of the beams. The grooves of 6 mm width and 10 mm depth are cut, at the location where strips are to be bonded, and then filled with epoxy to increase the interface area.

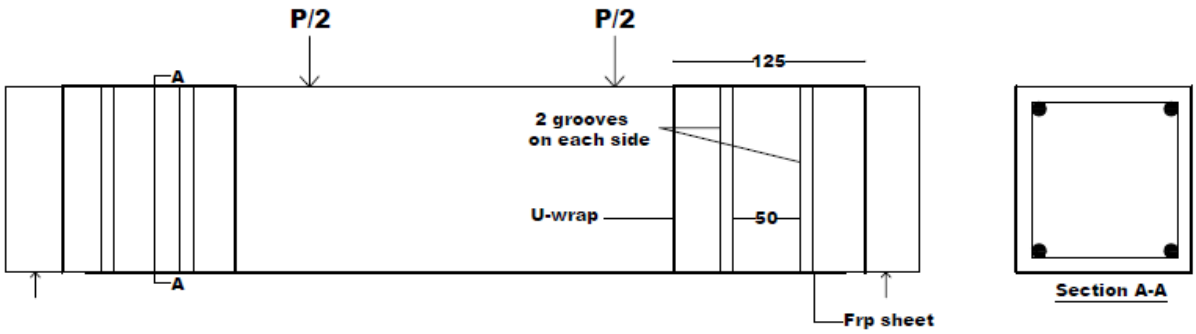

Figure 3.13 – Description of strengthened beams (Scheme VI)

3.8.8 Beams strengthened with Scheme VII: The beam named SB-13 is provided with a single layer of 100 mm wide CFRP sheet at the bottom face. In shear span, 65 mm wide U-strip is provided. The arrangement is chosen to compare the effect of laminate width, because in all the strengthened beams (from Type I to Type VI) 150 mm wide CFRP sheet was used.

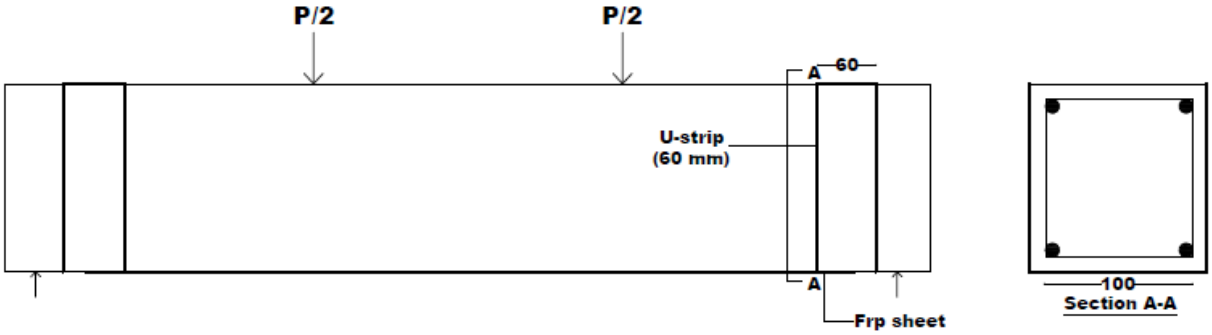

Figure 3.14 – Description of strengthened beam (Scheme VII)

CHAPTER -4 RESULTS AND DISCUSSIONS

4.1 INTRODUCTION

In the present work the strengthening of beams is done by Externally Bonded CFRP sheets. Fifteen numbers of reinforced concrete beams were casted and then tested up to failure by applying symmetrical two-point loading. Out of fifteen beams, two beams were not strengthened by FRP and were considered as controlled beams, whereas all other thirteen beams were strengthened with externally bonded CFRP sheets with different schemes in flexure as well as in shear.

This chapter includes presentation of each of the beam results, effect of strengthening on load capacity, stiffness and ductility of beams. In the end, an overall comparative view of the tested beams is made in order to compare and contrast them. In this way, we can point out some valuable aspects about the behaviour of tested beams.

4.2 EXPERIMENTAL RESULTS

The experimental results of all the beams are presented in this section. The discussions are based on the following topics: load-deflection analysis, crack patterns, deformation behaviour and failure modes.

4.2.1 Result of Controlled Beam (CB-01)

First control beam CB-01 was tested. As expected the beam failed in the flexural conventional mode, after extensive yielding of tension steel followed by crushing of concrete in the compression zone. The load-deflection data is given in Table 4.1 and corresponding to it the load-deflection curve is shown in Fig 4.1.

The maximum load carrying capacity of the beam was 75.10 kN and at this load, the deflection at centre was 5.782 mm. The load at the time, steel reinforcement started to yield was 60 kN and corresponding to this the deflection at centre was 2.536 mm.

The first crack was visible exactly at the centre of the beam at 16 kN of load. As the load enhanced, more flexural cracks developed in the region between the two point loads. The first diagonal crack was observed at a load of 70 kN in the shear span of the beam and propagated towards the point load. The failure of beam along with cracks pattern is shown in Figure 4.2.

Table 4.1 - Load v/s Deflection data of control beam CB-01

Load (KN)	Deflection at L/2 (mm)	Load (KN)	Deflection at L/2 (mm)
2	0.006	45	1.766
4	0.034	50	2.006
6	0.081	60	2.536
11.5	0.169	70	4.236
15	0.256	75.10	5.782
20	0.431	70.68	6.767
25	0.696	63.835	7.427
30	0.957	59.005	7.647
35	1.249	56.25	7.897
40	1.514	50.65	8.127

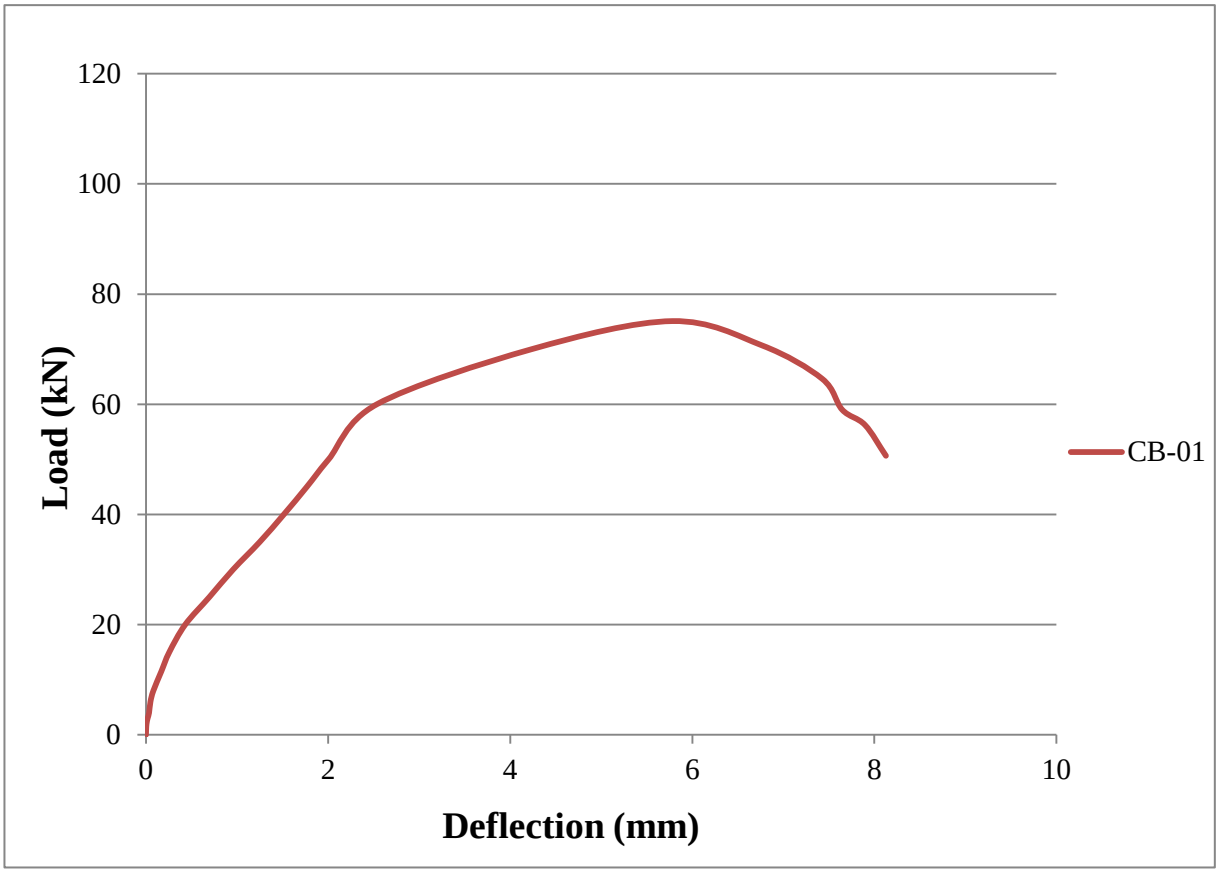

Figure 4.1 - Load v/s Deflection curve of control beam CB-01

Figure 4.2 – Crack patterns in control beam CB-01at failure

4.2.2 Result of Controlled Beam (CB-02)

Another control specimen (CB-02) was tested on the same grounds as CB-01 was tested, to compare the results. The load-deflection data is given in Table 4.2 and corresponding to it the load-deflection curve is shown in Fig 4.3.

The maximum load carrying capacity of the beam was 77.8 kN and at this load, the deflection at centre was 5.49 mm. As seen from the curve, after 62 kN of load, the yielding of tension steel had started and at that point, the deflection at centre was 2.541 mm.

Table 4.2 - Load v/s Deflection data of control beam CB-02

Load (KN)	Deflection at L/2 (mm)	Load (KN)	Deflection at L/2 (mm)
2	0.008	45	1.7
4	0.032	50	1.942
6	0.092	60	2.472
11.5	0.182	70	4.157
15	0.271	77.08	5.845
20	0.449	72.66	6.835
25	0.669	65.518	7.498
30	0.942	60.985	7.721
35	1.212	58.23	7.974
40	1.454	52.63	8.203

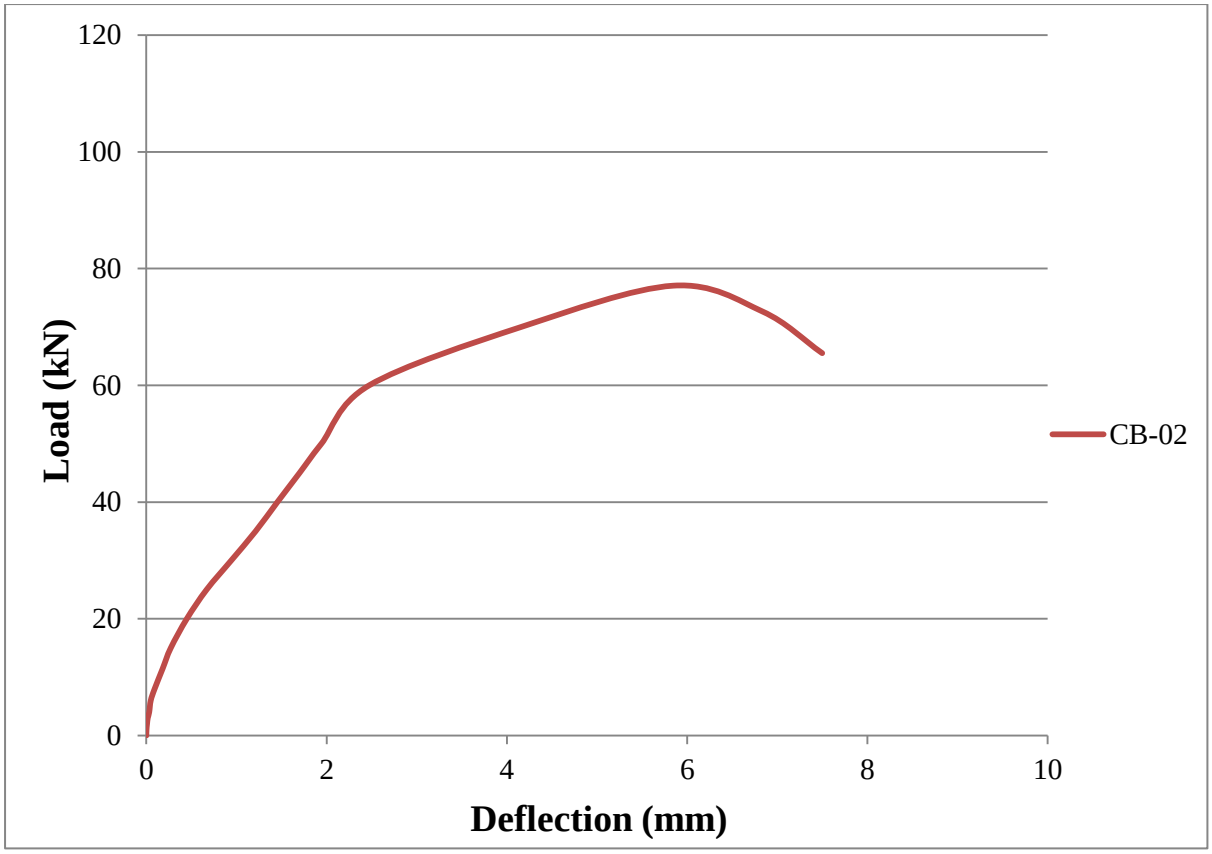

Figure 4.3 - Load v/s Deflection curve of control beam CB-02

The damage in the beam started with bending cracks in the central region of the beam. The first appearance of crack was noted at 17 kN. As the load enhanced more flexural cracks were observed near to first crack, which formed at the centre of the beam (shown in Figure 4.4). After yielding of tension steel, the flexural cracks start to grow in length and width. As load reaches at 70 kN, diagonal cracks were also observed in the shear spans of the beam. Finally, the beam failed due to crushing of concrete in compression zone with large deformations. The first crack became the critical crack for the ultimate failure of the beam.

Figure 4.4 – Failure of control beam CB-02

4.2.3 Reference Control Beam (RCB)

From the results of deflection of the control beams (CB-01 and CB-02), their average values have taken and corresponding to it the load-deflection curve is plotted as shown in Figure 4.5. This is done because this average graph would be chosen as reference control beam (RCB) to compare the results of strengthened beams.

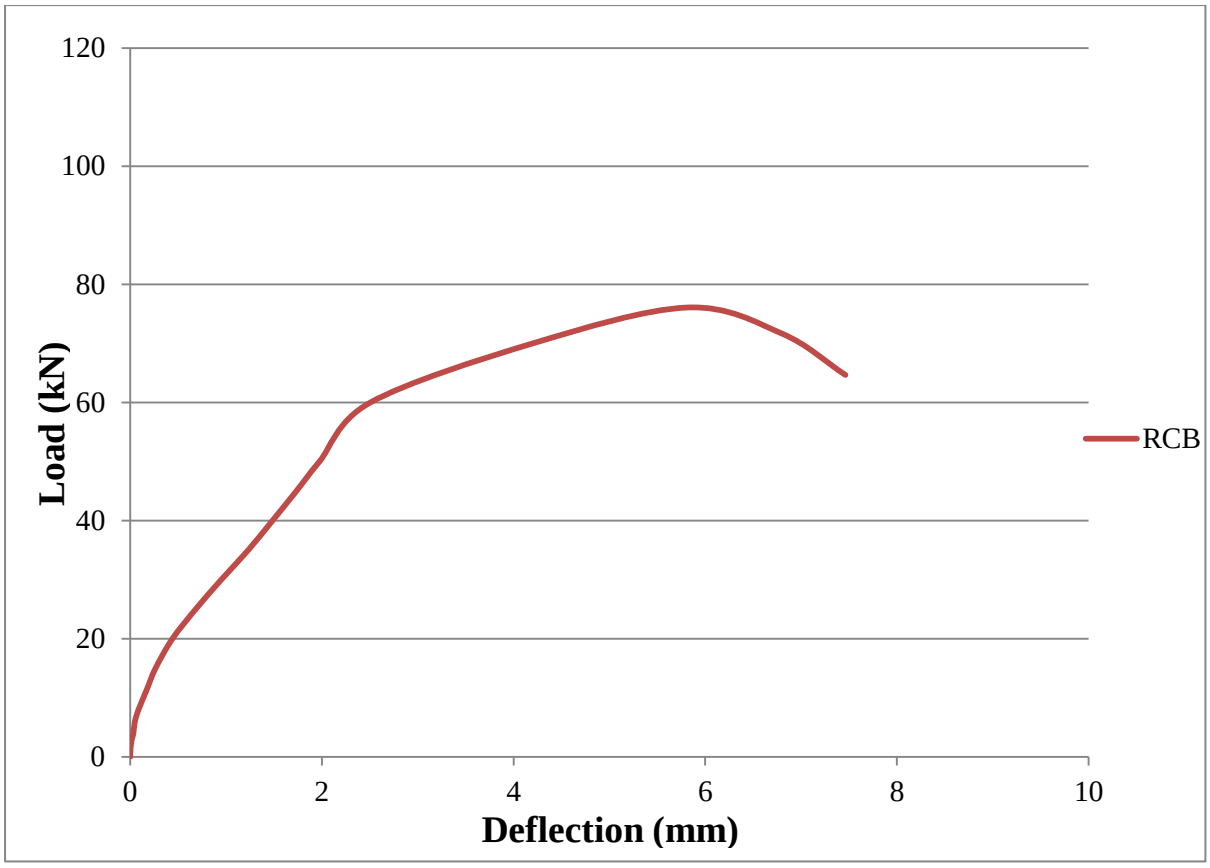

Figure 4.5 - Load v/s Deflection curve of reference control beam (RCB)

The curve shows that up to 60 kN load, the beam is under elastic limit. After that tension steel has started yielding which is seen through gradual increase of deflection up to ultimate load of 76.09 kN. The beam failed due to crushing of concrete in compression zone with large deformations. The maximum displacement measured at the time tension steel started to yield was 2.504 mm and at the ultimate load was 5.81 mm. The stiffness is also checked from the elastic limit of the curve and is calculated to be 23.95 kN/mm.

In the first phase of the test, reference control beam's stiffness is maintained. Later in the second phase the stiffness drops significantly (the beam is cracking), while in the last stage the mid-span deflection grows from 2.5 mm to 5.8 mm with an increase of just 15 kN of load.

4.2.4 Result of Beam Strengthened with Scheme I (SB-01)

The beam is strengthened with single layer of 150 mm wide CFRP sheet at the bottom face and no external shear reinforcement was provided. The load-deflection data is given in Table 4.3 and corresponding to it the load-deflection curve is shown in Fig 4.6.

The first appearance of crack was noted at 21 kN. As the load enhanced, more flexural cracks developed in the region between the two point loads. After 70 kN load, the diagonal cracks appeared in the shear spans of the beam. The load at the time steel reinforcement started to yield was about 80 kN and at that point, the deflection at centre was 2.139 mm. With further increase in load, the shear crack formed at the end of the laminate (on both sides) became wide and the beam stopped taking load at 96.95 kN. At the maximum load, the deflection at centre was 3.460 mm.

Table 4.3 - Load v/s Deflection data of beam SB-01

Load (KN)	Deflection at L/2 (mm)	Load (KN)	Deflection at L/2 (mm)
2	0.032	56	1.352
4	0.073	60	1.478
6	0.111	64	1.600
8	0.157	68	1.712
10	0.202	72	1.814
12	0.246	76	1.980
16	0.350	80	2.139
20	0.464	84	2.341
24	0.560	88	2.664
28	0.661	92	2.935
32	0.762	96	3.262
36	0.864	96.95	3.460
40	0.970	95.4875	3.662
44	1.074	94.025	3.890
48	1.166	92.835	4.010
52	1.264	82.4075	4.340

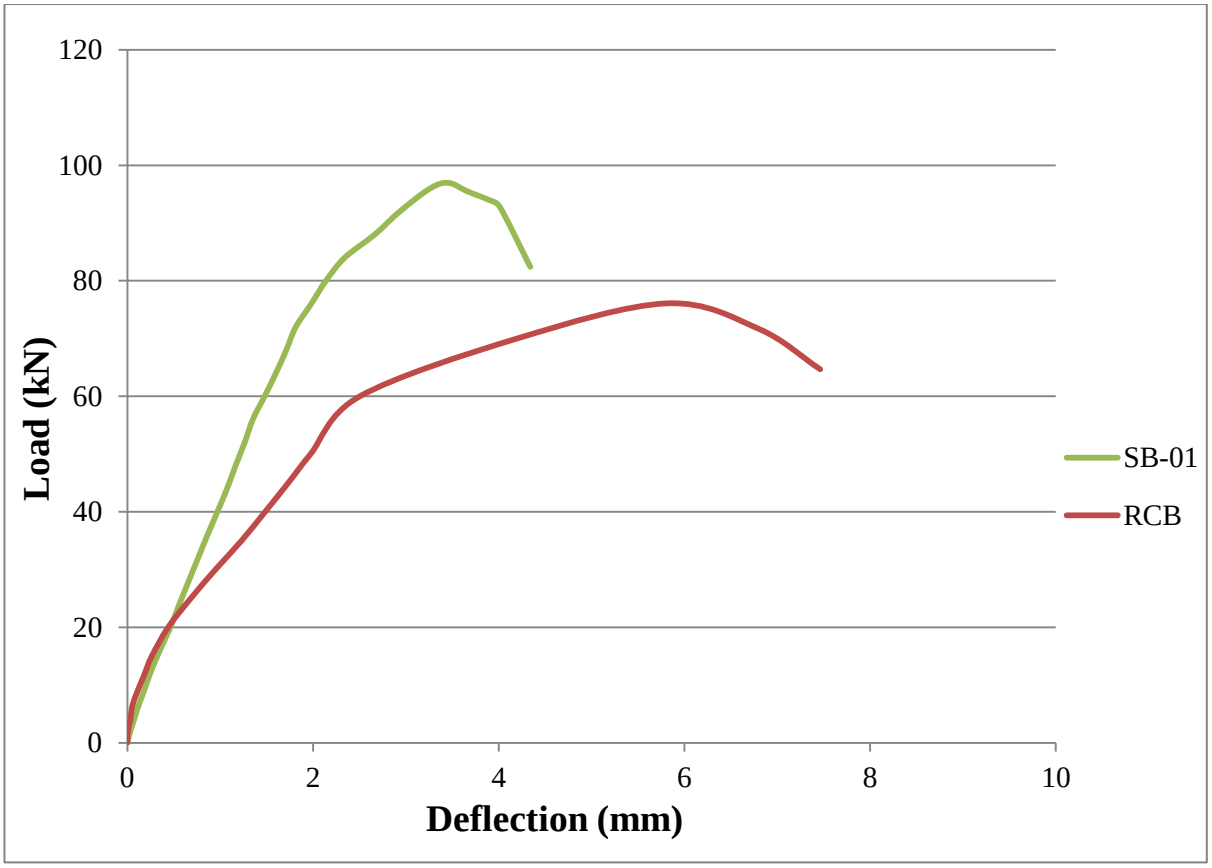

Figure 4.6 - Load v/s Deflection curve of beam SB-01

From the test results, it is observed that the stiffness of the beam increases which in turn results in higher load carrying capacity as compared to reference control beam (RCB) but the beam failed in a sudden manner (shear failure) with less deformations as compared to ductile failure mode of controlled beams.

In the Figure 4.7 we can see the cracks marked as 6 and 9 formed in the shear spans of the beam in SB-01. These cracks became the critical cracks for the ultimate failure of the beam.

Figure 4.7 – Crack patterns in strengthened beam SB-01

4.2.5 Result of Beam Strengthened with Scheme I (SB-02)

Another specimen (SB-02) was tested on the same grounds as SB-01 was tested, to compare the results. The load-deflection data is given in Table 4.4 and corresponding to it the load-deflection curve is shown in Fig 4.8. The cracks pattern in the beams is shown in Figure 4.9.

The same deformation behaviour was noticed as in case of SB-01. The first appearance of crack was noted at 21.5 kN. After 70 kN load, the diagonal cracks appeared in the shear spans of the beam. After 80 kN load, more diagonal shear cracks formed and widened as the load increased. The load at the time steel reinforcement started to yield was about 80 kN and at that point, the deflection at centre was 2.111 mm. With further increase in load, the shear crack formed at the end of the laminate (on both sides) became wide and the beam stopped taking load at 97.47 kN. At the maximum load, the deflection at centre was 3.49 mm.

Table 4.4 - Load v/s Deflection data of beam SB-02

Load (KN)	Deflection at L/2 (mm)	Load (KN)	Deflection at L/2 (mm)
2	0.029	56	1.396
4	0.069	60	1.515
6	0.108	64	1.644
8	0.154	68	1.757
10	0.2	72	1.866
12	0.244	76	2.009
16	0.339	80	2.111
20	0.449	84	2.292
24	0.55	88	2.549
28	0.649	92	2.897
32	0.752	96	3.256
36	0.861	97.47	3.49
40	0.969	96.43	3.786
44	1.1	92.51	4.01
48	1.212	88.53	4.19
52	1.307	82.85	4.41

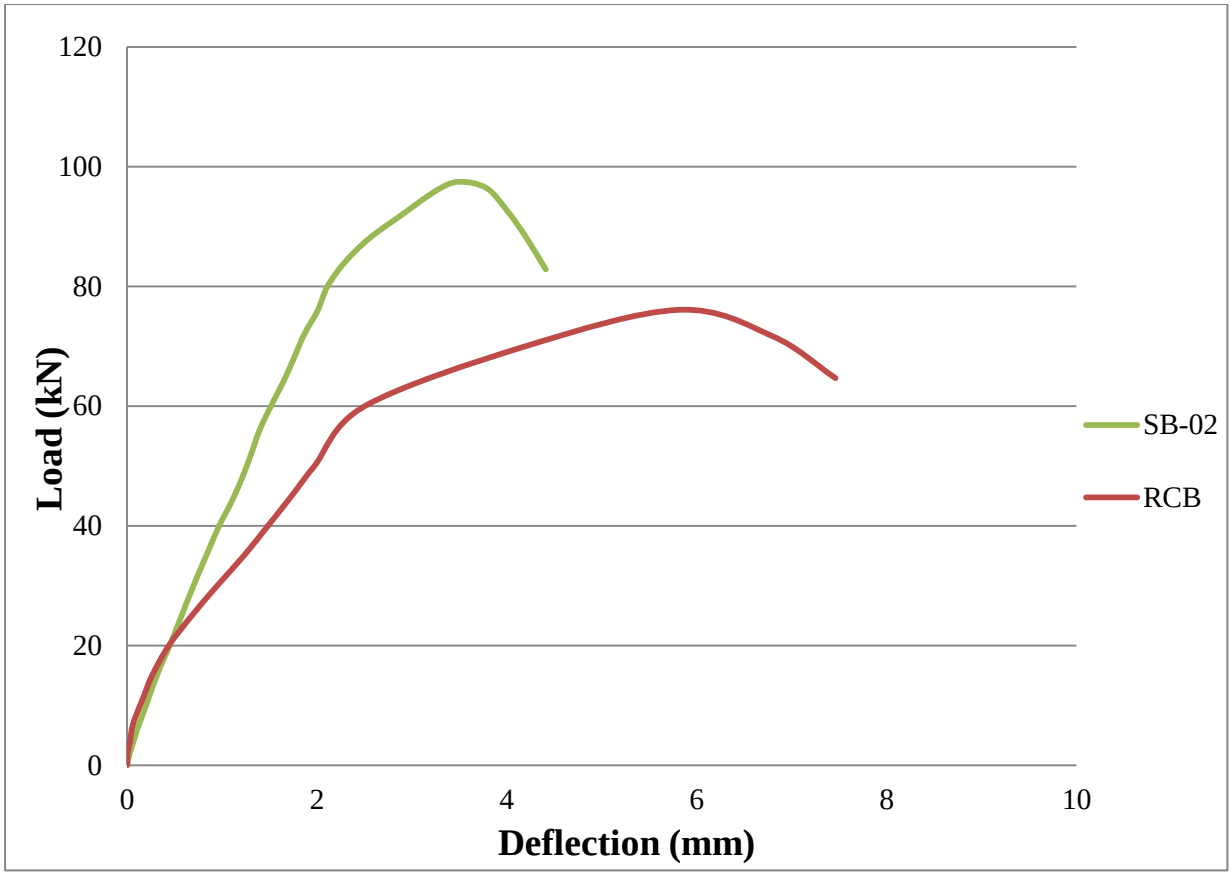

Figure 4.8 - Load v/s Deflection curve of beam SB-02

Figure 4.9 –Crack patterns in strengthened beam SB-02

The strengthened beams SB-01 and SB-02 failed in shear because of high interfacial shear and normal stresses at the end of the laminate and also the internal shear reinforcement was unable to resist the enhanced shear stress (due to increase in load).

In strengthened beams SB-01 and SB-02, the use of a single CFRP laminate allowed for a strength increase up to 28% greater than that of the control beams.

4.2.6 Result of Beam Strengthened with Scheme II (SB-03)

The beam is strengthened with single layer of 150 mm wide CFRP sheet at the bottom face. In addition, the U-strips of 50 mm width and 450 mm length are provided in shear spans of the beam. The load-deflection data is given in Table 4.5 and corresponding to it the load-deflection curve is shown in Fig 4.10. The cracks pattern in the beam is shown in Fig. 4.11.

The first appearance of crack was noted at 24 kN. As the load enhanced, more flexural cracks developed in the region between the two point loads. At the load of 70 kN, the first flexural-shear crack appeared in the shear span adjacent to the U-strips near to the loads. The critical diagonal shear crack was observed on both sides of the beam in the load range between 84-90 kN. The failure occurred due to debonding of CFRP strips over the main diagonal shear crack, in the area between the centre of shear crack and its upper end with a cracking sound.

Table 4.5 - Load v/s Deflection data of beam SB-03

Load (KN)	Deflection at L/2 (mm)	Load (KN)	Deflection at L/2 (mm)
2	0.024	56	1.086
4	0.048	60	1.190
6	0.072	64	1.295
8	0.096	68	1.386
12	0.144	72	1.492
16	0.192	76	1.594
20	0.258	80	1.765
24	0.329	84	1.894
28	0.403	88	2.110
32	0.488	92	2.301
36	0.579	96	2.760
40	0.672	100	3.118
44	0.781	105.215	3.890
48	0.902	100	4.360
52	0.982	89.43	4.740

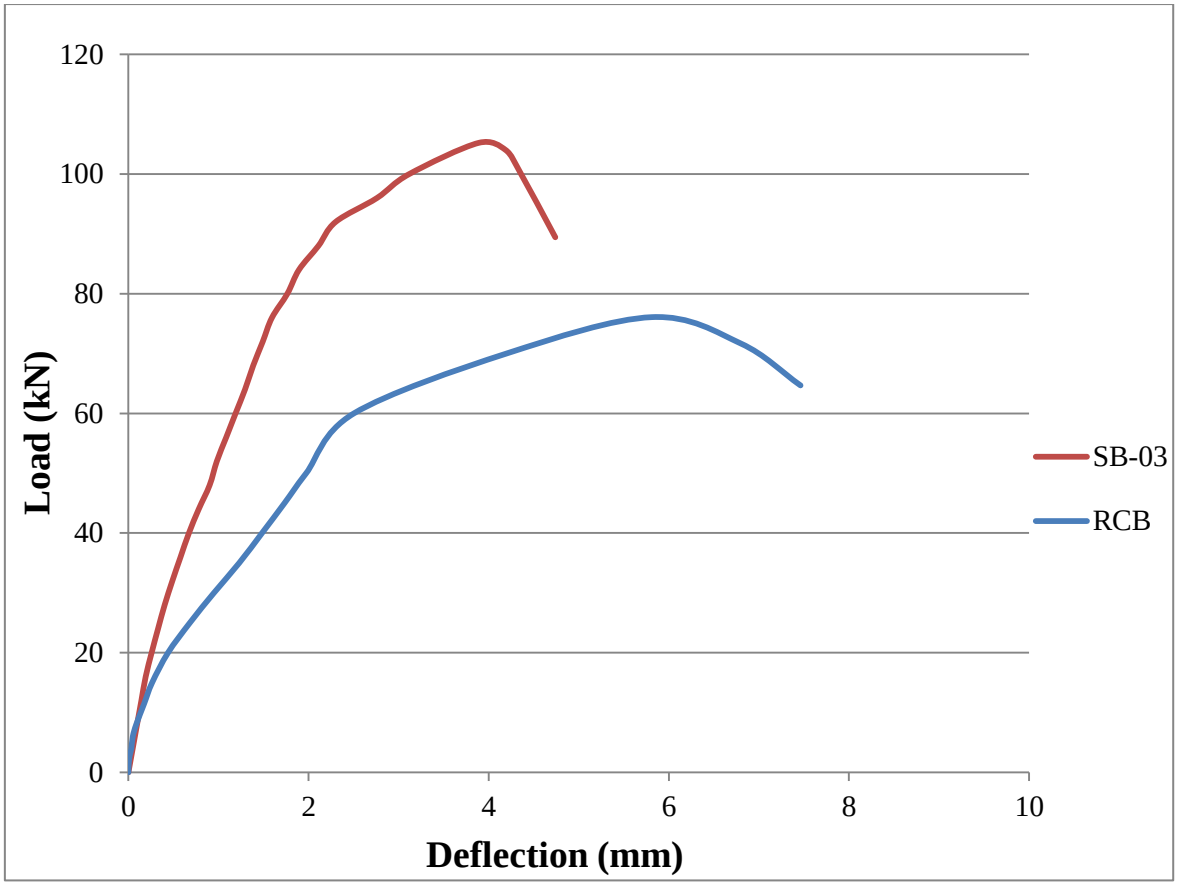

Figure 4.10 - Load v/s Deflection curve of beam SB-03

As seen from the curve the beam stays in elastic domain until 76 kN of load and then changing slope until failure (shear cracks start to appear and develop). The maximum load carrying capacity of the beam was 105.215 kN with 3.890 mm displacement at centre. The shear capacity of beam is calculated using the model proposed by Chen and Teng (2003) based on debonding failure mode and the value works out to be 45.41 kN as compared to experimental value of 45.875 kN.

Figure 4.11 – Crack patterns in strengthened beam SB-03

4.2.7 Result of Beam Strengthened with Scheme II (SB-04)

Another specimen (SB-04) was tested on the same grounds as SB-03 was tested, to compare the results. The load-deflection data is given in Table 4.6 and corresponding to it the load-deflection curve is shown in Fig 4.12. The failure mode of the beam is shown in Figure 4.13.

The same deformation behaviour was noticed as in case of SB-03. The first appearance of crack was noted at 25 kN. After 70 kN load, the flexural-shear cracks appeared in the shear span adjacent to the U-strips near to the loads. After this the critical diagonal shear crack was observed on both sides of the beam in the load range between 84-90 kN. The failure occurred due to debonding of CFRP strips over the main diagonal shear crack, in the area between the centre of shear crack and its upper end with a cracking sound. The ultimate load carrying capacity of the beam was 107.9 kN with maximum displacement of 3.884mm at centre.

Table 4.6 - Load v/s Deflection data of beam SB-04

Load (KN)	Deflection at L/2 (mm)	Load (KN)	Deflection at L/2 (mm)
2	0.019	60	1.152
4	0.041	64	1.259
6	0.066	68	1.366
8	0.088	72	1.455
12	0.134	76	1.578
16	0.188	80	1.722
20	0.244	84	1.856
24	0.312	88	2.014
28	0.379	92	2.159
32	0.454	96	2.499
36	0.541	100	2.712
40	0.633	104	3.138
44	0.742	107.9	3.884
48	0.854	105.46	4.190
52	0.952	99.5	4.41
56	1.044	91.715	4.696

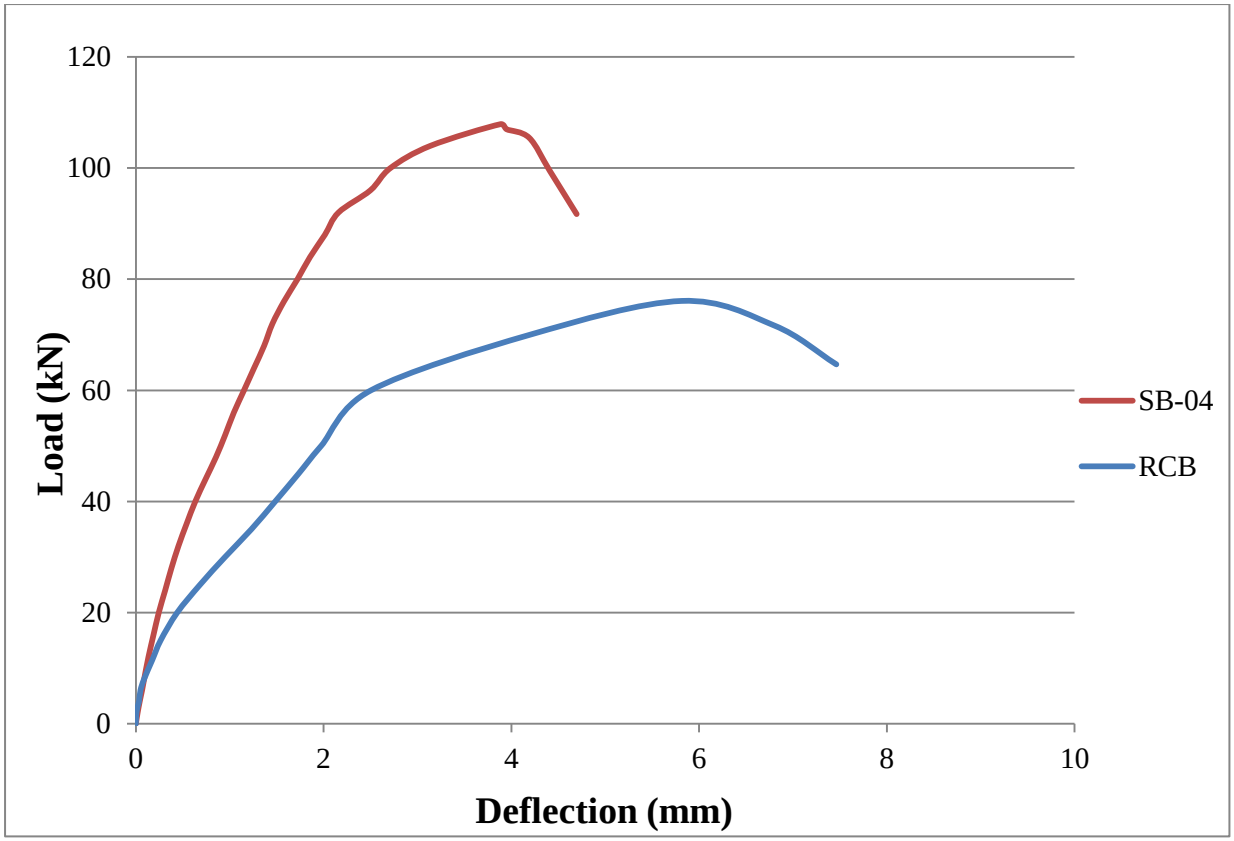

Figure 4.12 - Load v/s Deflection curve of beam SB-04

Figure 4.13 – Debonding of CFRP U-strip in strengthened beam SB-04

In strengthened beams SB-03 and SB-04, the use of CFRP U-strips as external shear reinforcement impeded the propagation and growth of critical diagonal shear crack up to some extent and allowed for a strength increase up to 40% greater than that of control beams.

4.2.8 Result of Beam Strengthened with Scheme III (SB-05)

In contrast to beams strengthened with U-strips, the beam SB-05 is strengthened with 150 mm full U-wrap provided in shear spans of the beam. The load-deflection data is given in Table 4.7 and corresponding to it the load-deflection curve is shown in Fig 4.14.

The first appearance of crack was noted at 25 kN. The initial diagonal crack in shear span as appeared in case of Type II strengthened beams could not be traced out because the shear spans were almost full wrapped with CFRP sheets (150 mm wide). The crack patterns became visible after debonding of CFRP sheets at the load of 97.5 kN. The debonding of CFRP sheets occurred over the main diagonal shear crack in the same location as observed in Type II strengthened beams. As the load enhanced, the debonding failure was followed by the shear failure at an ultimate load of 110.46 kN with displacement of 4.17 mm at centre. The failure mode of the beam is shown in Figure 4.15.

Table 4.7 - Load v/s Deflection data of beam SB-05

Load (KN)	Deflection at L/2 (mm)	Load (KN)	Deflection at L/2 (mm)
2	0.012	64	1.337
4	0.043	68	1.441
6	0.079	72	1.545
8	0.112	76	1.673
12	0.164	80	1.792
16	0.221	84	1.895
20	0.279	88	2.076
24	0.341	92	2.224
28	0.424	96	2.395
32	0.533	100	2.641
36	0.622	104	3.029
40	0.73	106	3.291
44	0.819	108	3.633
48	0.929	110.46	4.17
56	1.117	93.891	4.99

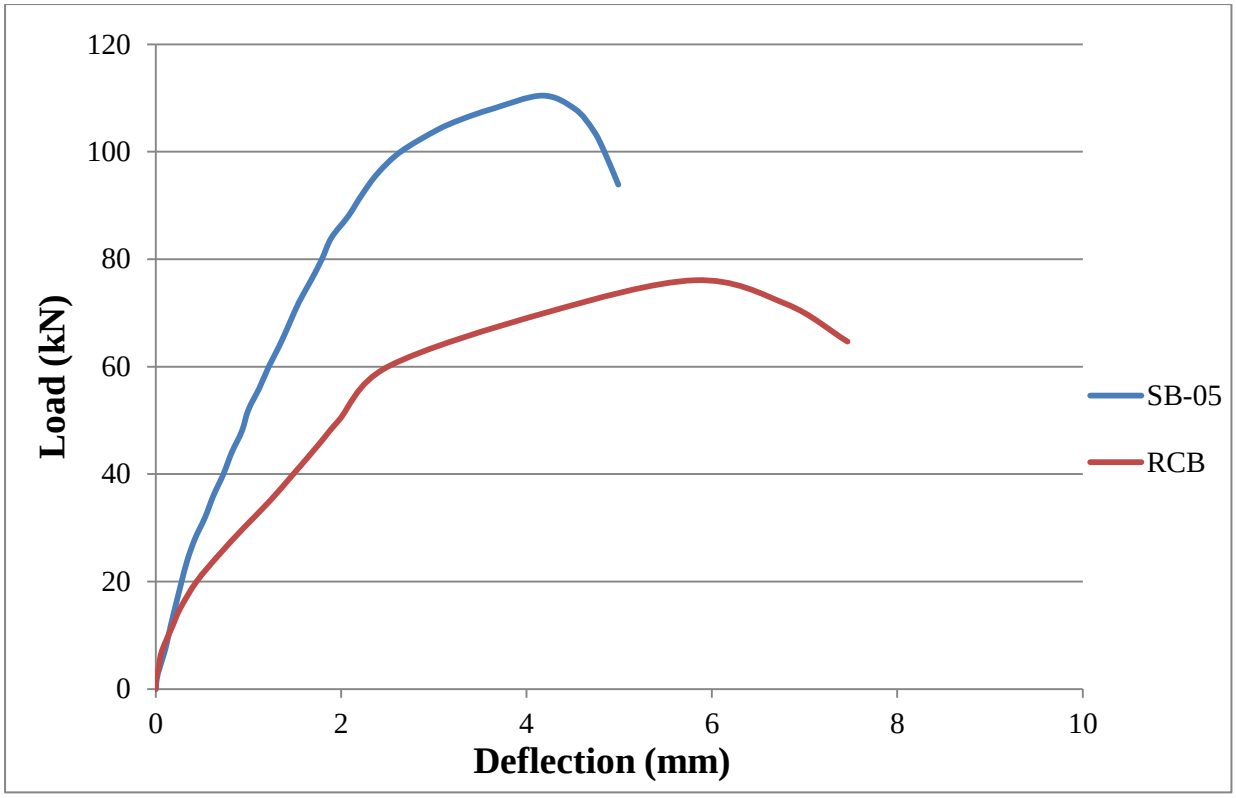

Figure 4.14 - Load v/s Deflection curve of beam SB-05

Figure 4.15 – Debonding of CFRP U-wrap in strengthened beam SB-05

4.2.9 Result of Beam Strengthened with Scheme III (SB-06)

Another specimen (SB-06) was tested on the same grounds as SB-01 was tested, to compare the results. The load-deflection data is given in Table 4.8 and corresponding to it the load-deflection curve is shown in Fig 4.16.

The same deformation behaviour was noticed as in case of SB-05. The first appearance of crack was noted at 26 kN. The initial diagonal crack in shear span as appeared in case of Type II strengthened beams could not be traced out because the shear spans were almost full wrapped with CFRP sheets (150 mm wide). The failure was initiated by the debonding of CFRP sheets over the main diagonal shear crack in the same location as observed in Type II strengthened beams. As the load enhanced, the debonding failure was followed by the shear failure at an ultimate load of 110.70 kN with displacement of 4.246 mm at centre. The failure mode of the beam is shown in Figure 4.17.

Table 4.8 - Load v/s Deflection data of beam SB-06

Load (KN)	Deflection at L/2 (mm)	Load (KN)	Deflection at L/2 (mm)
2	0.011	64	1.341
4	0.042	68	1.447
6	0.076	72	1.551
8	0.11	76	1.679
12	0.161	80	1.8
16	0.219	84	1.92
20	0.276	88	2.093
24	0.338	92	2.249
28	0.42	96	2.433
32	0.528	100	2.694
36	0.618	104	3.088
40	0.724	106	3.331
44	0.814	108	3.695
48	0.922	110.70	4.246
56	1.119	94.095	5.01

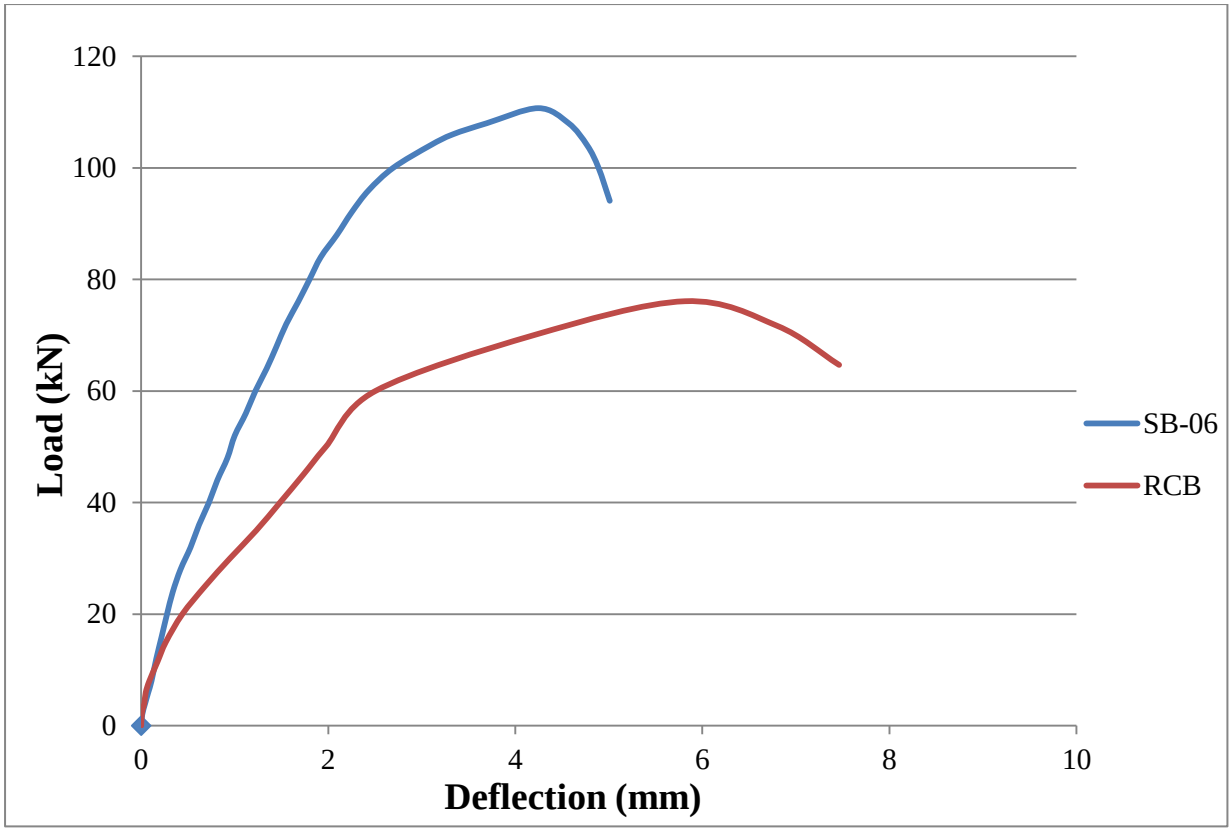

Figure 4.16 - Load v/s Deflection curve of beam SB-06

The shear capacity of beam is calculated using the model proposed by Chen and Teng (2003) based on debonding failure mode and the value works out to be 48.66 kN as compared to experimental value of 48.75 kN.

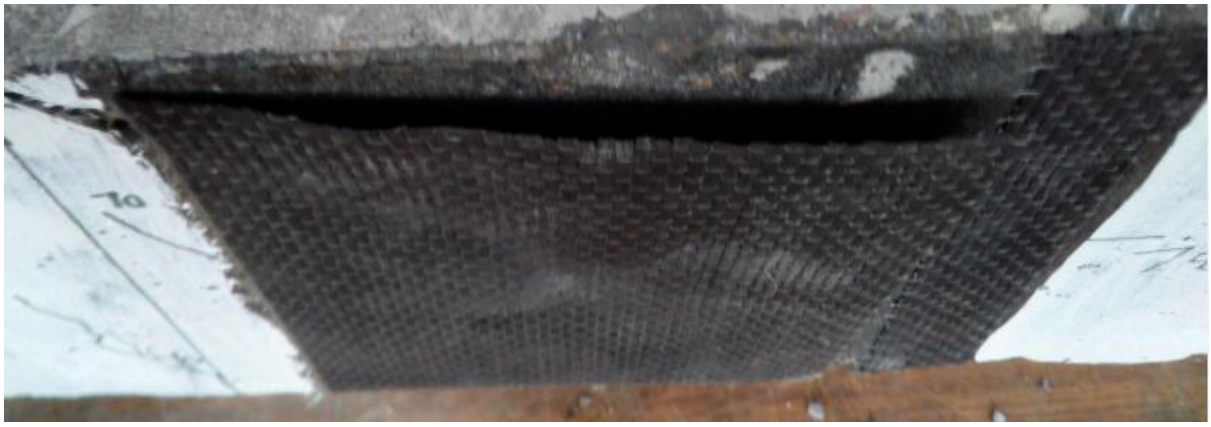

Figure 4.17 – Debonding of CFRP U-wrap in strengthened beam SB-06

In strengthened beams SB-05 and SB-06, the use of CFRP U-strips as external shear reinforcement impeded the propagation and growth of critical diagonal shear crack and allowed for a strength increase up to 45% greater than that of control beams.

4.2.10 Result of Beam Strengthened with Scheme IV (SB-07)

The beam is strengthened with single layer of 150 mm wide CFRP sheet at the bottom face. In shear span, two-strips of 40 mm width, with an inclination of 45° to the longitudinal axis of the beam, are provided. The load-deflection data is given in Table 4.9 and corresponding to it the load-deflection curve is shown in Fig 4.18.

The first appearance of crack was noted at 31 kN. With further increase in load, more flexural cracks formed in the central region of the beam. The initial diagonal shear crack formed after load of 100 kN in the shear span adjacent to the side strips. At this point, the displacement at centre was 2.304 mm. The cracking pattern in the beam is shown in Fig 4.19.

Table 4.9 - Load v/s Deflection data of beam SB-07

Load (KN)	Deflection at L/2 (mm)	Load (KN)	Deflection at L/2 (mm)
2	0.014	64	1.177
4	0.043	68	1.267
6	0.072	72	1.409
8	0.103	76	1.512
12	0.156	80	1.627
16	0.213	84	1.729
20	0.269	88	1.911
24	0.332	92	2.048
28	0.385	96	2.168
32	0.449	100	2.304
36	0.52	104	2.434
40	0.611	108	2.643
44	0.703	112.8	2.944
48	0.801	117.295	3.519
52	0.903	110.695	4.19
56	1.009	101.795	4.54
60	1.088	99.7	4.64

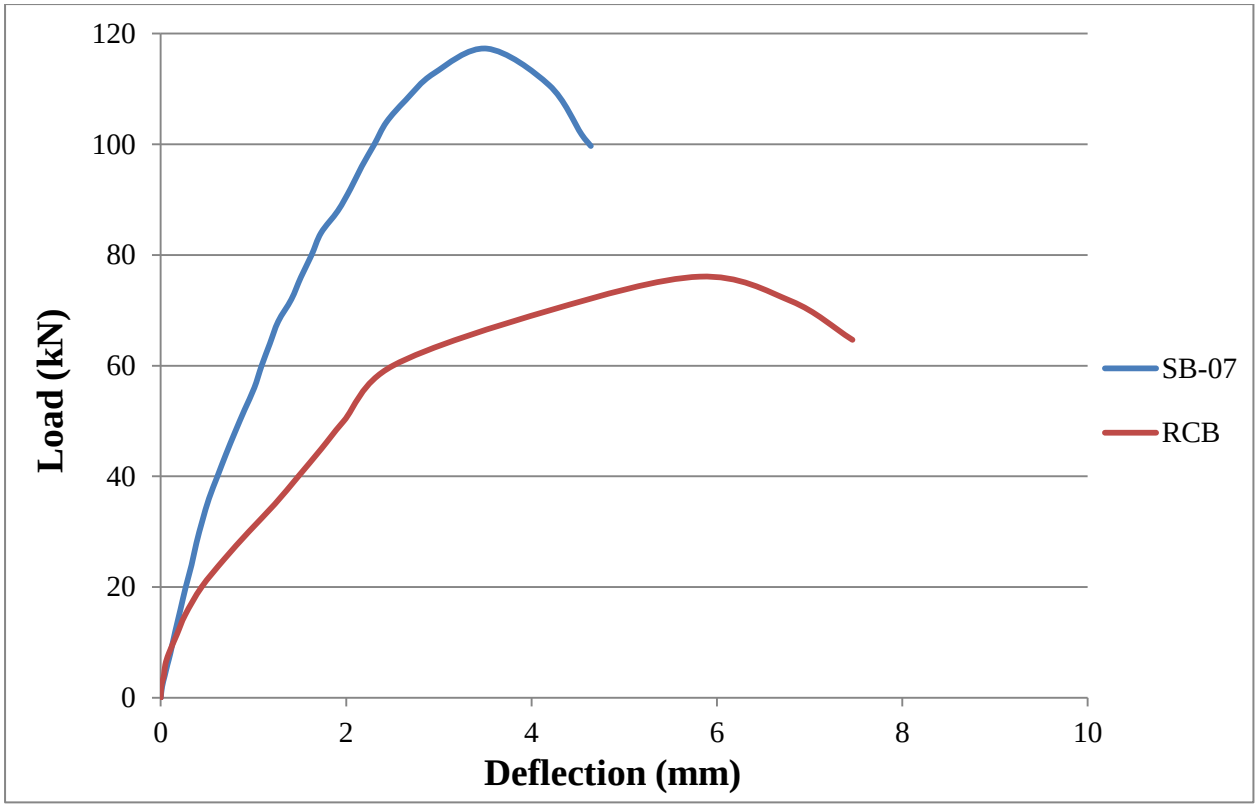

Figure 4.18 - Load v/s Deflection curve of beam SB-07

The brittle failure occurred at the load of 112.8 kN due to debonding of longitudinal CFRP sheet at the one end. The maximum load carrying capacity of the beam was 117.295 kN and at this load, the deflection at centre was 3.519 mm.

It is observed that the beam failed in a brittle manner shows less deflection and maximum load at failure. The beam strengthened with 45° strips was able to mitigate the critical diagonal shear crack which was principal cause of failure in strengthened beams SB-01 to 04.

Figure 4.19 – Crack patterns in strengthened beam SB-07

4.2.11 Result of Beam Strengthened with Scheme IV (SB-08)

Another specimen (SB-08) was tested on the same grounds as SB-01 was tested, to compare the results. The load-deflection data is given in Table 4.10 and corresponding to it the load-deflection curve is shown in Fig 4.20. The failure mode of beams is shown in Figure 4.21.

The same deformation behaviour was noticed as in case of SB-07. Initially, flexural cracks were formed in the central region of the beam with increased loading. The first appearance of crack was noted at 33 kN. The yielding of tension steel occurred after 100 kN load which was highest among all the strengthened beams After 104 kN load, the diagonal shear cracks were formed adjacent to the inclined strips and the deflection increases rapidly.

Table 4.10 – Load v/s Deflection data of beam SB-08

Load (KN)	Deflection at L/2 (mm)	Load (KN)	Deflection at L/2 (mm)
2	0.016	68	1.247
4	0.045	72	1.391
6	0.074	76	1.5
8	0.105	80	1.6
12	0.159	84	1.709
16	0.214	88	1.853
20	0.271	92	1.997
24	0.334	96	2.1
28	0.386	100	2.254
32	0.451	104	2.383
36	0.529	108	2.59
40	0.621	112	2.796
44	0.713	116	3.314
48	0.799	118.35	3.66
52	0.894	115.95	3.98
56	0.991	112.32	4.22
64	1.152	100.5975	4.78

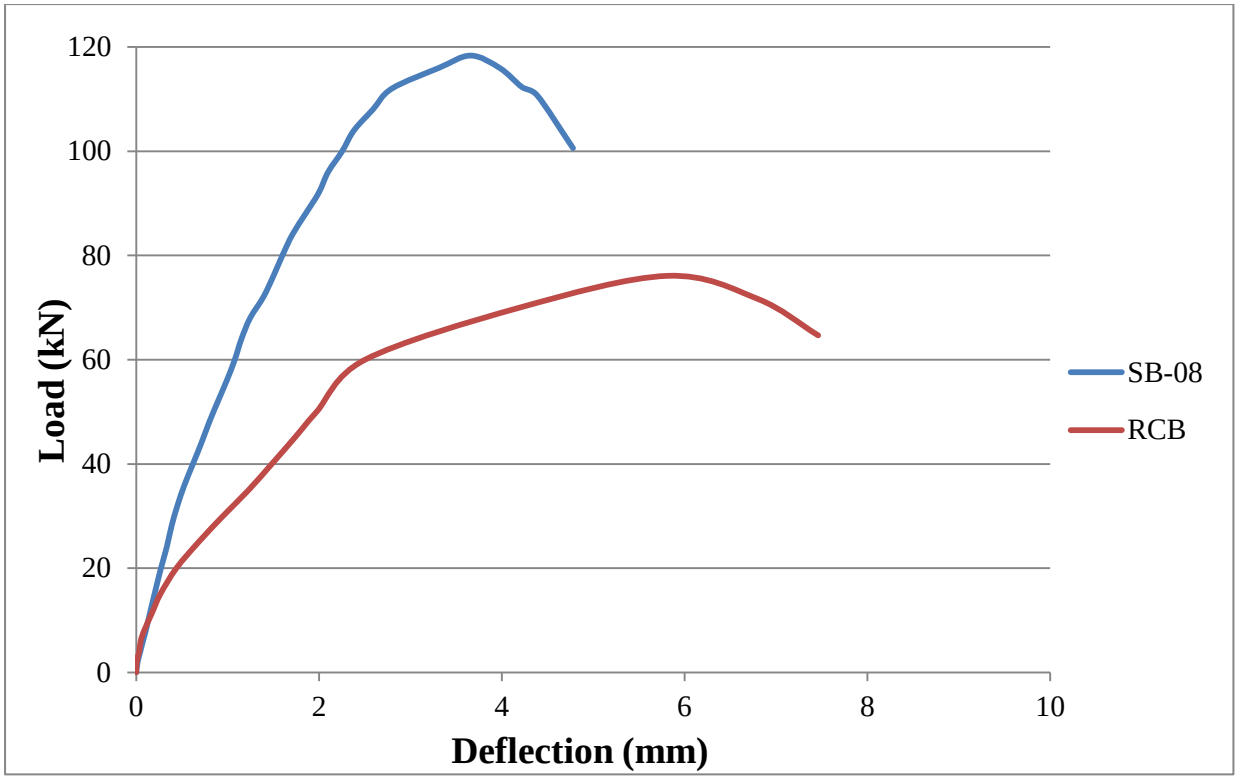

Figure 4.20 – Load v/s Deflection curve of beam SB-08

The brittle failure occurred at the load of 115 kN due to debonding of longitudinal CFRP sheet at the one end (Fig 4.21). The maximum load carrying capacity of the beam was 118.35 kN and at this load, the deflection at centre was 3.66 mm.

Figure 4.21 – Plate End Debonding in strengthened beam SB-08

In beams SB-07 and SB-08, the strengthening of beams with CFRP inclined strips on the beam sides resulted in higher stiffness as compared to 90° strips/wraps and limited the propagation of shear cracks thereby increasing the load carrying capacity of the beam. The load carrying capacity of the beams increases up to 55% greater than that of control beams.

4.2.12 Result of Beam Strengthened with Scheme V (SB-09)

The beam is strengthened in the same manner as SB-07 and SB-08 were done but in addition the grooves of 6 mm width and 10 mm depth are also cut, at the location where strips are to be bonded, and then filled with epoxy to increase the interface area. The load-deflection data is given in Table 4.11 and corresponding to it the load-deflection curve is shown in Fig 4.21.

The same deformation behaviour was noticed as in case of SB-07 and SB-08. The first appearance of crack was noted at 31 kN. The initial diagonal shear crack formed at the load of 95 kN in the shear span adjacent to the side strips. At that time, the deflection at centre was 2.483 mm. After this the beam enters in the post-yielding region. More diagonal cracks were formed as the load enhanced. The brittle failure occurred at the load of 110kN due to end debonding of longitudinal CFRP sheet at the one end. The maximum load carrying capacity of the beam was 112.315 kN and at that load, the deflection at centre was 5.03mm.

Table 4.11 – Load v/s Deflection data of beam SB-09.

Load (KN)	Deflection at L/2 (mm)	Load (KN)	Deflection at L/2 (mm)
2	0.006	60	1.375
4	0.038	64	1.487
6	0.08	68	1.593
8	0.12	72	1.707
12	0.181	76	1.824
16	0.264	80	1.943
20	0.341	84	2.09
24	0.427	88	2.221
28	0.506	92	2.375
32	0.614	96	2.519
36	0.722	100	2.731
40	0.817	104	3.04
44	0.915	108.1575	3.595
48	1.01	112.315	5.03
52	1.143	95.46775	5.633

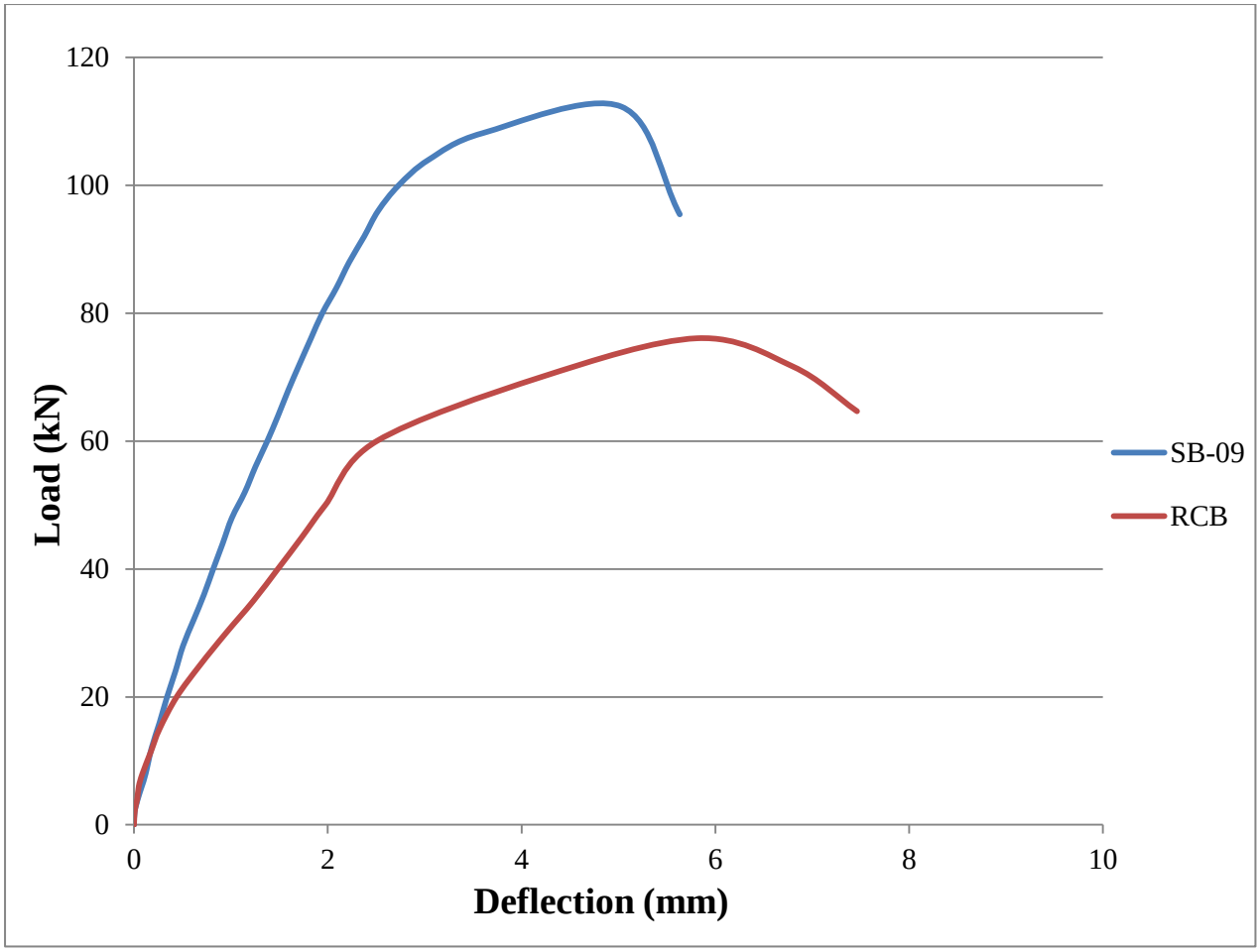

Figure 4.22 – Load v/s Deflection curve of control beam SB-09

Figure 4.23 – Crack patterns in strengthened beam SB-09

4.2.13 Result of Beam Strengthened with Scheme V (SB-10)

Another specimen (SB-10) was tested on the same grounds as SB-09 was tested, to compare the results. The load-deflection data is given in Table 4.12 and corresponding to it the load-deflection curve is shown in Fig 4.24. The failure mode of beams is shown in Figure 4.25.

The same deformation behaviour was noticed as in case of SB-09. The first appearance of crack was noted at 32 kN. The initial diagonal shear crack formed at the load of 92 kN in the shear span adjacent to the side strips. At that time, the deflection at centre was 2.411mm. After this the beam enters in the post-yielding region. More diagonal cracks were formed as the load enhanced. The brittle failure occurred at the load of 108 kN due to end debonding of longitudinal CFRP sheet at the one end. The maximum load carrying capacity of the beam was 113.95 kN and at that load, the deflection at centre was 4.75 mm.

Table 4.12 - Load v/s Deflection data of beam SB-10

Load (KN)	Deflection at L/2 (mm)	Load (KN)	Deflection at L/2 (mm)
2	0.006	64	1.503
4	0.036	68	1.619
6	0.079	72	1.732
8	0.121	76	1.844
12	0.183	80	1.973
16	0.27	84	2.129
20	0.344	88	2.254
24	0.432	92	2.411
28	0.513	96	2.579
32	0.624	100	2.762
36	0.736	104	3.11
40	0.827	108	3.66
44	0.931	112	4.215
48	1.026	113.95	4.75
52	1.16	110.62	5.05
56	1.274	96.85	5.39

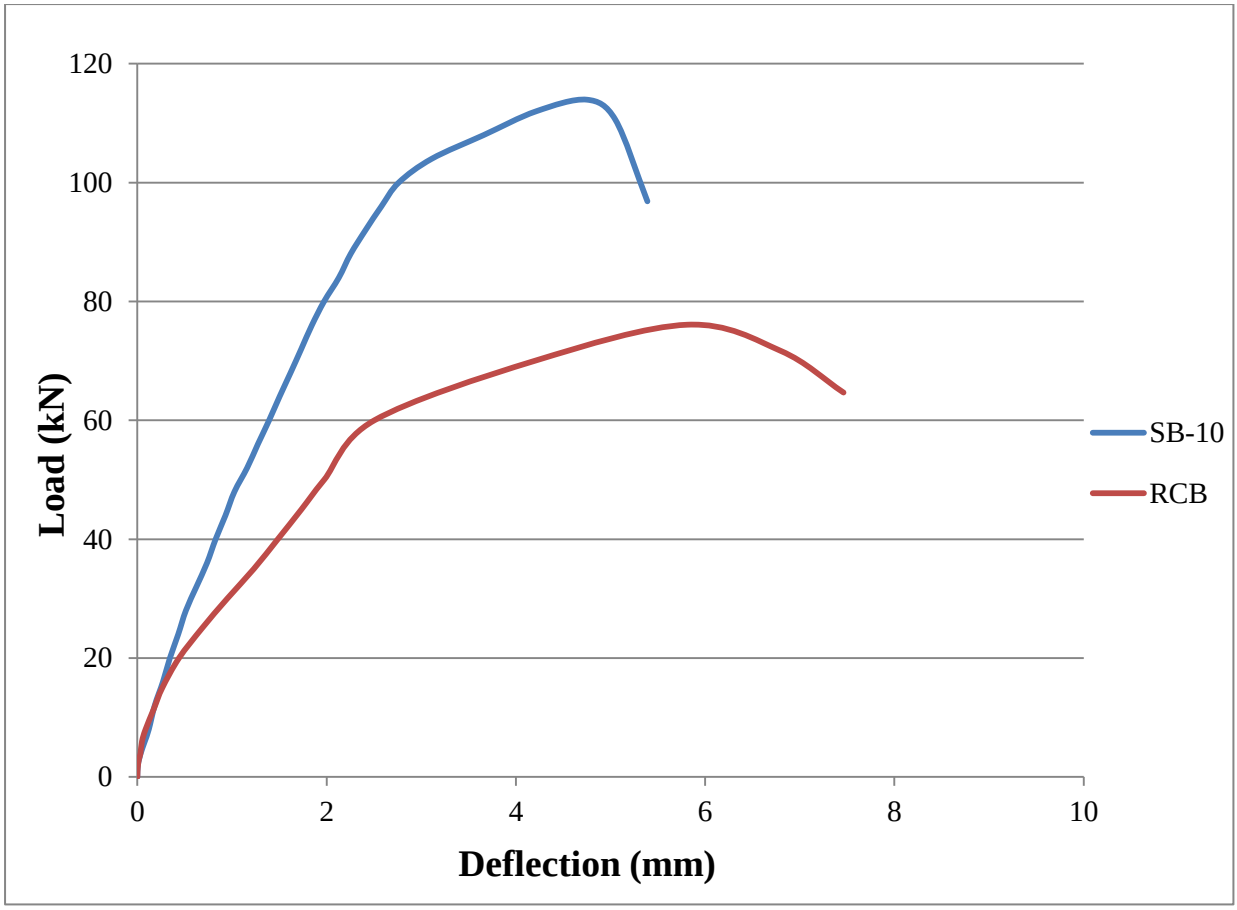

Figure 4.24 - Load v/s Deflection curve of control beam SB-10

Figure 4.25 – Plate End Debonding in strengthened beam SB-10

The advantage of surface preparation (grooving method) was not fully utilized because of plate end debonding of the longitudinal CFRP sheet. From the test results, it is observed that the strengthened beams SB-09 and SB-10 failed with higher deformations as compared to SB-07 and SB-08 whereas the difference in load carrying capacity was not much significant.

4.2.14 Result of Beam Strengthened with Scheme VI (SB-11)

The beams named SB-11 is strengthened with single layer of CFRP sheet at the bottom face. In shear spans 125mm wide side strips are provided to enhance the shear capacity. The grooves of 6 mm width and 10 mm depth are cut, at the location where strips are to be bonded, and then filled with epoxy to increase the interface area. The load-deflection data is given in Table 4.13 and corresponding to it the load-deflection curve is shown in Fig 4.26.

The first appearance of crack was noted at 26 kN. At the load of 92 kN, the initial diagonal shear crack was observed near the support and at that time the displacement at centre was 2.278 mm. The second and third shear crack were formed at the load of 107 kN and 110 kN respectively and at that time the displacement was almost double as compared to displacement at the time of first diagonal crack appeared.

Table 4.13 - Load v/s Deflection data of beam SB-11

Load (KN)	Deflection at L/2 (mm)	Load (KN)	Deflection at L/2 (mm)
2	0.014	64	1.342
4	0.047	68	1.452
6	0.084	72	1.575
8	0.118	76	1.684
12	0.178	80	1.816
16	0.235	84	1.944
20	0.29	88	2.122
24	0.355	92	2.278
28	0.436	96	2.452
32	0.547	100	2.745
36	0.641	104	3.388
40	0.737	108	3.956
44	0.825	110	4.678
48	0.938	112	5.714
52	1.023	112.7	6.029
56	1.129	95.795	6.63

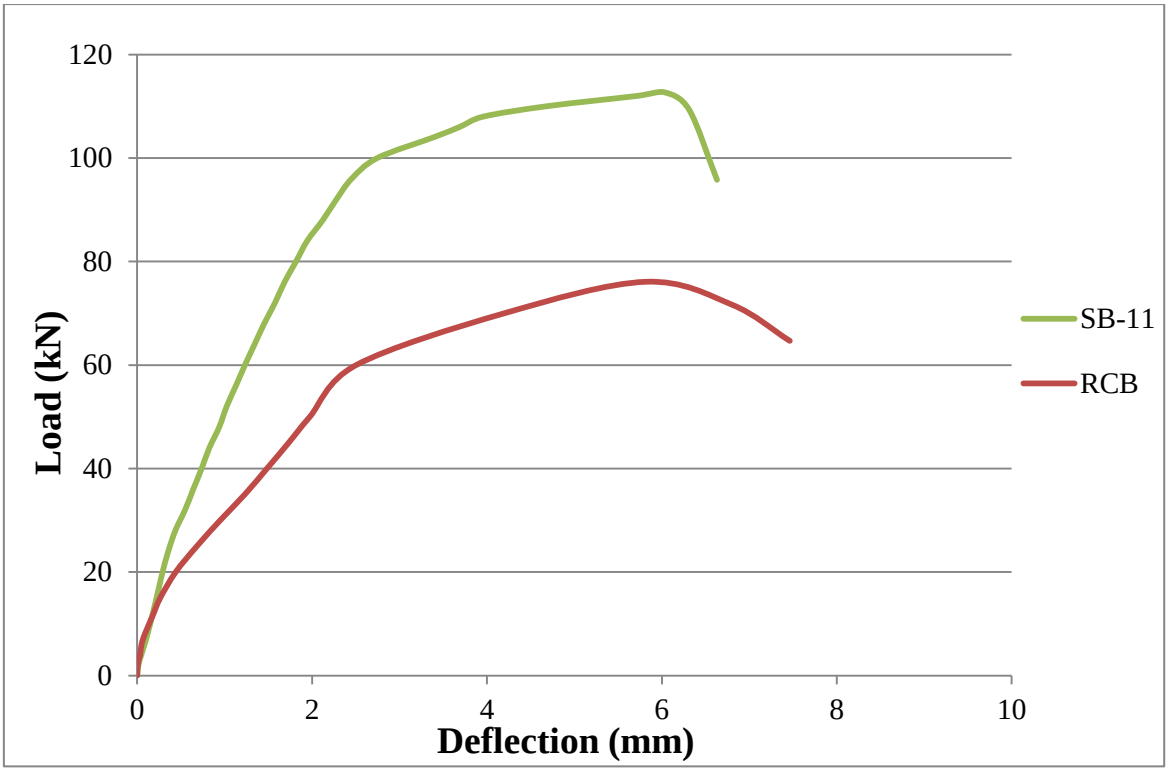

Figure 4.26 - Load v/s Deflection curve of beam SB-11

The failure was initiated by the plate end debonding of the longitudinal CFRP sheet at the load of 112 kN. The maximum load carrying capacity of the beam was 112.7 kN and at that point, the displacement at centre was 6.029 mm.

As compared to SB-05 in which the 150 mm wide full U-wrap was used, the failure occurred due to debonding of U-wraps at the load of 97.5 kN. In this strengthened beam, the grooving method helped to eliminate the debonding of side strips which in turn impeded the growth and propagation of critical diagonal shear crack and allowed the beam to carry higher loads.

Figure 4.27 – Crack patterns in strengthened beam SB-11

4.2.15 Result of Beam Strengthened with Scheme VI (SB-12)

Another specimen (SB-12) was tested on the same grounds as SB-01 was tested, to compare the results. The load-deflection data is given in Table 4.14 and corresponding to it the load-deflection curve is shown in Fig 4.28.

The same deformation behaviour was noticed as in the case of SB-11. The first appearance of crack was noted at 27 kN. After 100 kN load, the flexural-shear cracks start to form and the deflection of the beam increases rapidly. The failure occurred due to end debonding of the longitudinal CFRP sheet at the load of about 112 kN (shown in Fig. 4.29). After debonding, the flexural cracks start to grow in length and propagated towards the top compression face.

Table 4.14 - Load v/s Deflection data of beam SB-12

Load (KN)	Deflection at L/2 (mm)	Load (KN)	Deflection at L/2 (mm)
2	0.015	64	1.355
4	0.049	68	1.466
6	0.086	72	1.592
8	0.12	76	1.7
12	0.184	80	1.838
16	0.238	84	1.977
20	0.295	88	2.149
24	0.361	92	2.306
28	0.441	96	2.478
32	0.552	100	2.756
36	0.646	104	3.189
40	0.746	106	3.446
44	0.838	108	3.792
48	0.949	112	4.96
52	1.038	113.95	5.72
56	1.139	108.75	6.36
60	1.245	96.85	6.57

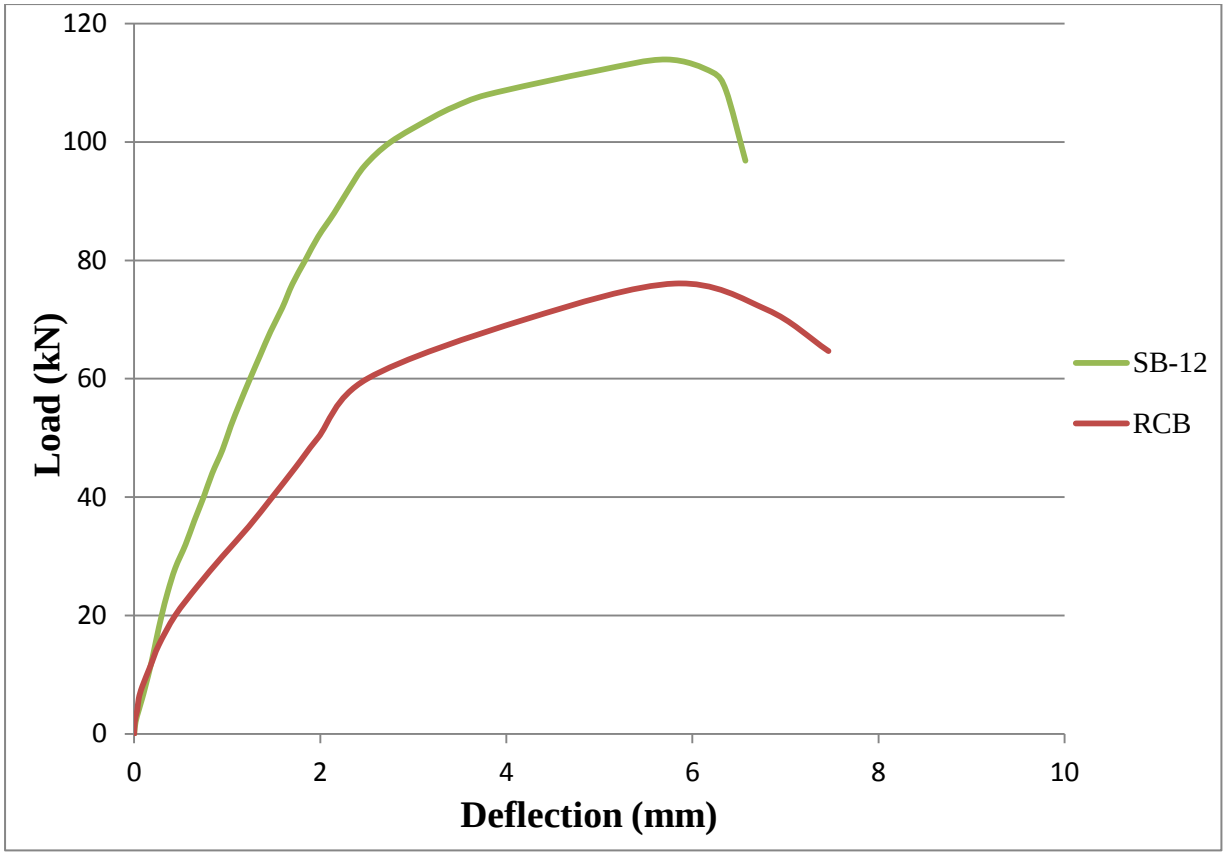

Figure 4.28 - Load v/s Deflection curve of beam SB-12

The maximum load carrying capacity of the beam was 113.95 kN and at that point the displacement at centre was 5.72 mm. In strengthened beams SB-11 and SB-12, the grooving method helped to eliminate the debonding of side strips and allowed them to carry higher loads. But the advantage of surface preparation (grooving method) was not fully utilized because of plate end debonding of the longitudinal CFRP sheet.

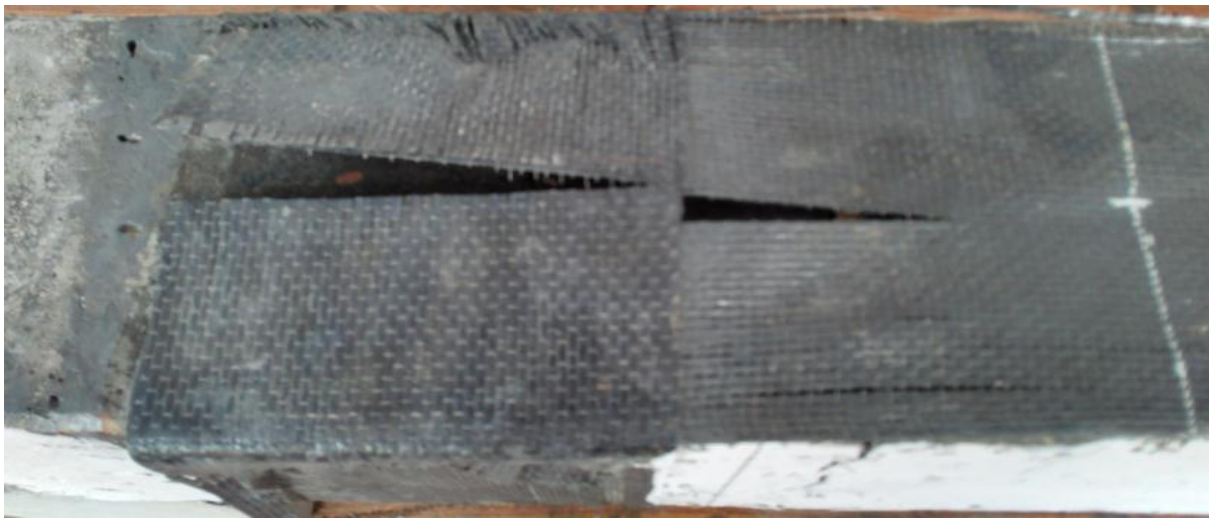

Figure 4.29 – Plate End Debonding in strengthened beam SB-12

4.2.16 Result of Beam Strengthened with Scheme VII (SB-13)

The beam named SB-13 is provided with a single layer of 100 mm wide CFRP sheet at the bottom face. In shear span, 65 mm wide U-strip is provided. The load-deflection data is given in Table 4.15 and corresponding to it the load-deflection curve is shown in Fig 4.30.

The deformation behaviour of SB-13 was quite different from all the strengthened beams i.e. from SB-01 to SB-12. It was very much similar to the controlled beams i.e. CB-01 and CB-02 up to the yielding of tension steel. The first crack was visible at the load of 19 kN (shown in Figure 4.31). At the load of 56 kN the yielding of tension steel was started and at that point, the deflection at centre was 1.903 mm. The diagonal shear cracks were formed after 60 kN load and the deflection in the beam increased gradually.

Table 4.15 - Load v/s Deflection data of control beam SB-13

Load (KN)	Deflection at L/2 (mm)	Load (KN)	Deflection at L/2 (mm)
2	0.037	60	2.347
4	0.063	64	2.624
6	0.097	68	2.974
8	0.134	72	3.382
12	0.238	76	3.786
16	0.357	80	4.474
20	0.481	84	5.201
24	0.611	89	6.145
28	0.733	89.93	6.360
32	0.871	91.56	6.845
36	0.995	92.42	7.155
40	1.078	93.185	7.610
44	1.282	94.14	8.110
48	1.493	92.23	8.375
52	1.699	90.795	8.640
56	1.903	80.019	8.942

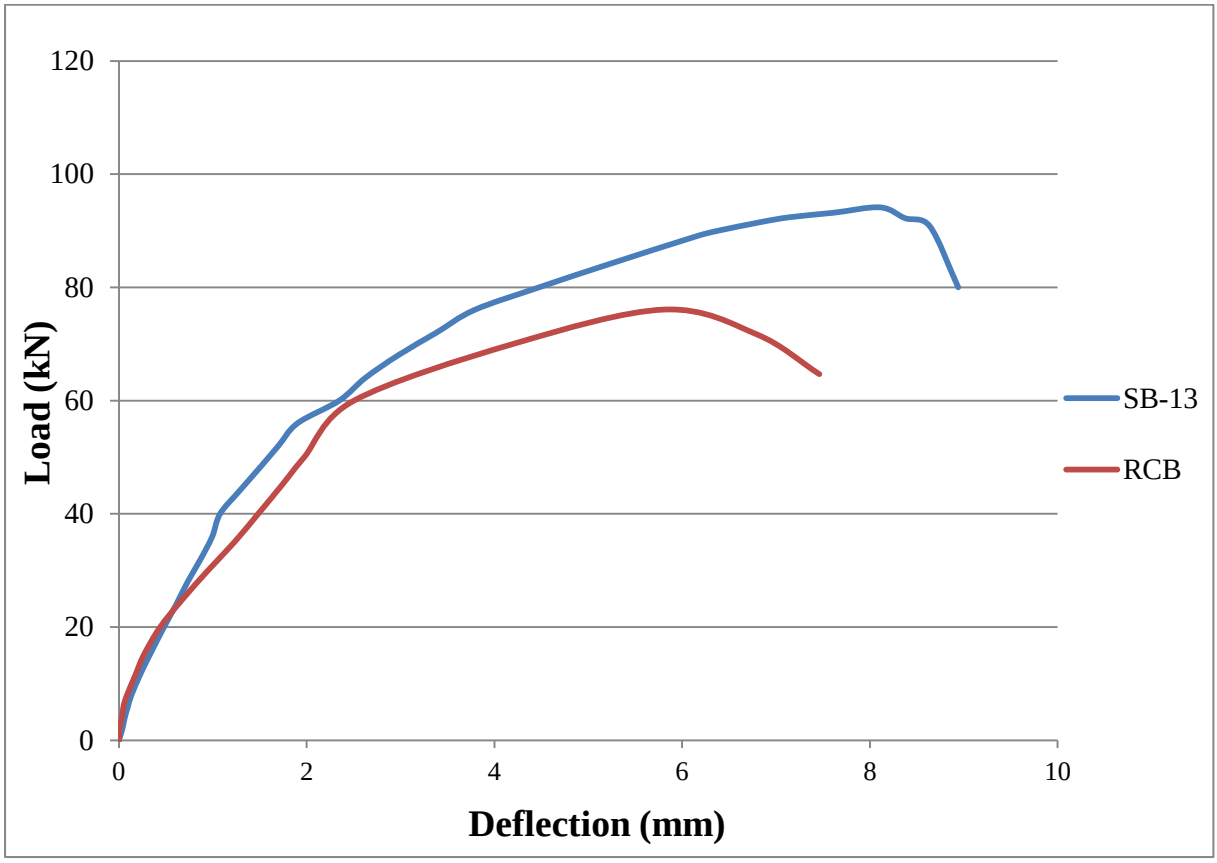

Figure 4.30 - Load v/s Deflection curve of control beam SB-13

At the load of 90 KN, the failure was initiated by the debonding of CFRP U-wraps provided at the ends. As the load was enhanced, the debonding failure was followed by the rupture of U-wrap at the one end. This was due to high interfacial shear and normal stresses at the end of the laminate, which also results in debonding of the longitudinal CFRP laminate at the same end (shown in Figure 4.32). At the maximum load of 94.14 kN, the deflection at centre was 8.110 mm, which was highest among all the cases.

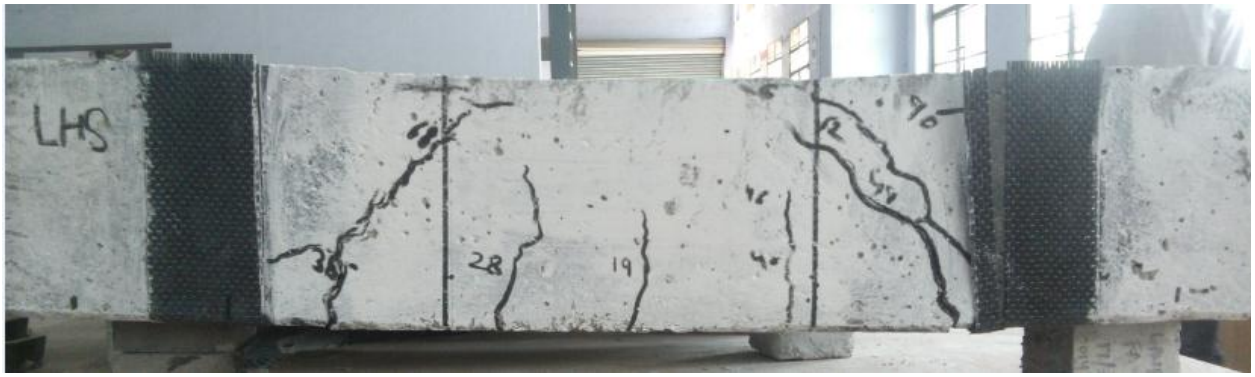

Figure 4.31 – Crack patterns in strengthened beam SB-13

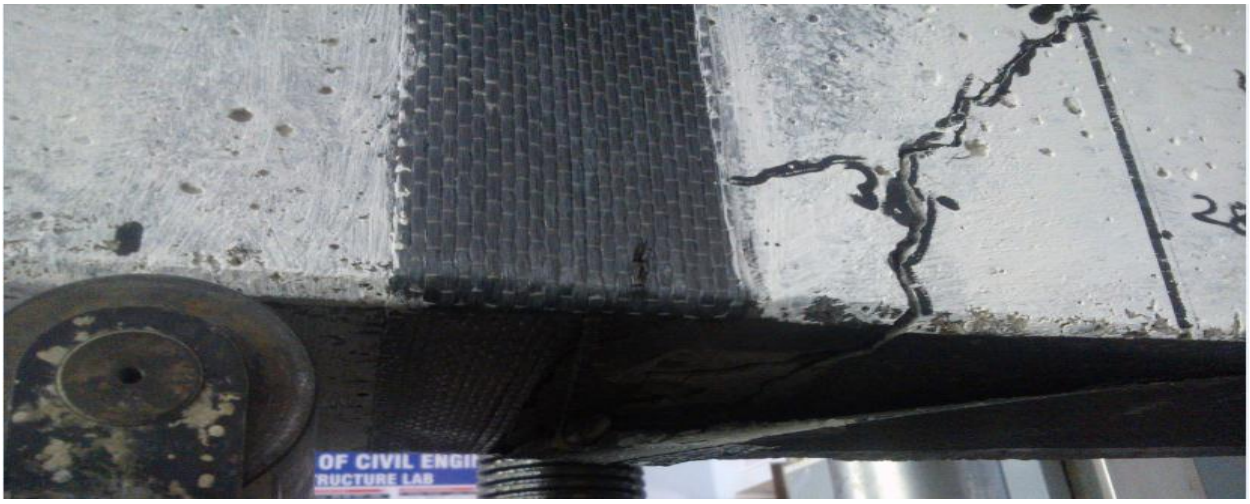

Figure 4.32 –Plate End Debonding in strengthened beam SB-13

4.3 EFFECT OF STRENGTHENING ON LOAD CAPACITY OF BEAMS

In this section the effect of strengthening beams with externally bonded CFRPs in various schemes is presented in terms of: First crack load and Ultimate load carrying capacity. The results are compared with reference control beam (RCB) and beams having no external shear reinforcement or strengthened with scheme I (SB-01 and SB-02).

4.3.1 First Crack Load

The first crack load of reference control beam (RCB) and beams strengthened with scheme I (SB-01 and SB-02) are presented in Figure 4.33. It is observed that the first crack load of beams SB-01 and SB-02 is increased by **28.79%** (avrg.) as compared to reference control specimen (RCB).

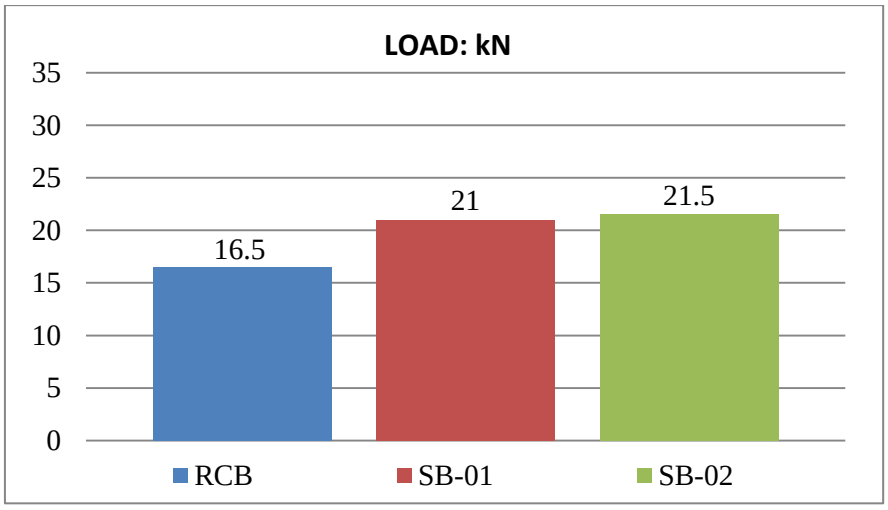

Figure 4.33 - First Crack Load of RCB, SB-01 and SB-02

The first crack load of reference control beam (RCB) and beams SB-01, SB-02 and beams strengthened with scheme II (SB-03 and SB-04) having 50 mm wide CFRP U-strips in shear spans are presented in Figure 4.34. It is observed that the first crack load of beams SB-03 and SB-04 is increased by **48.48%** (avrg.) as compared to reference control specimen (RCB) and **15.29%** (avrg.) as compared to beams SB-01 and SB-02.

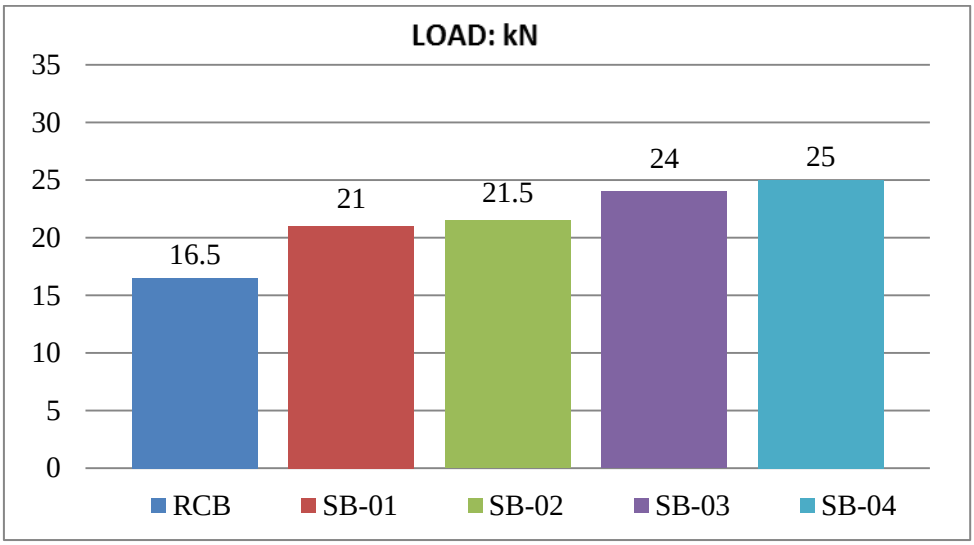

Figure 4.34 - First Crack Load of RCB, SB-01, SB-02, SB-03 and SB-04

The first crack load of reference control beam (RCB) and beams SB-01,SB-02 and beams strengthened with scheme III (SB-05 and SB-06) having 150 mm wide CFRP full U-wrap in shear spans are presented in Figure 4.35. It is observed that the first crack load of beams SB-05 and SB-06 is increased by **54.54%** (avrg.) as compared to reference control specimen (RCB) and **20%** (avrg.) as compared to beams SB-01 and SB-02.

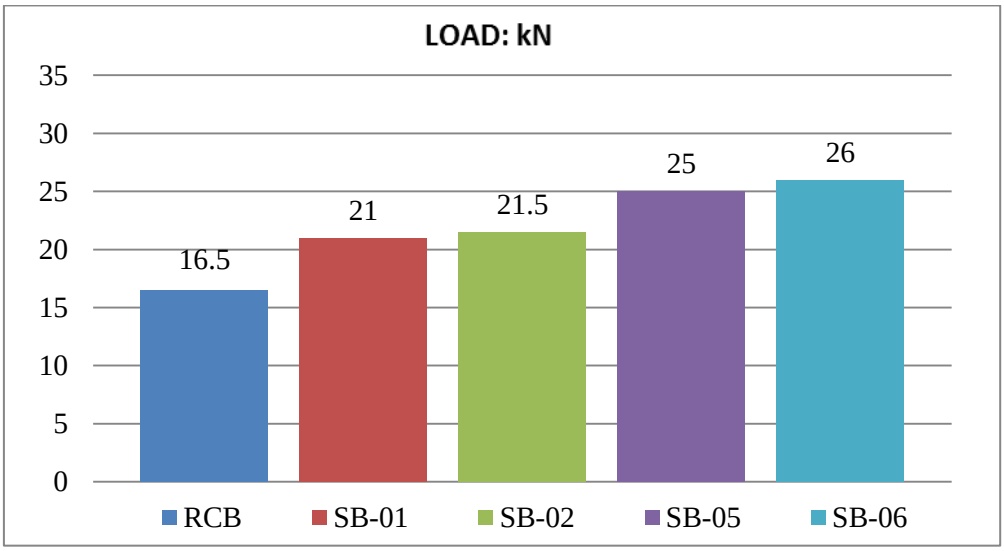

Figure 4.35 - First Crack Load of RCB, SB-01, SB-02, SB-05 and SB-06

The first crack load of reference control beam (RCB) and beams SB-01,SB-02 and beams strengthened with scheme IV (SB-07 and SB-08) having 40 mm wide inclined (45°) CFRP strips in shear spans are presented in Figure 4.36. It is observed that the first crack load of SB-07 and SB-08 is increased by **93.94%** (avrg.) as compared to reference control specimen (RCB) and **50.59%** (avrg.) as compared to beams SB-01 and SB- 02.

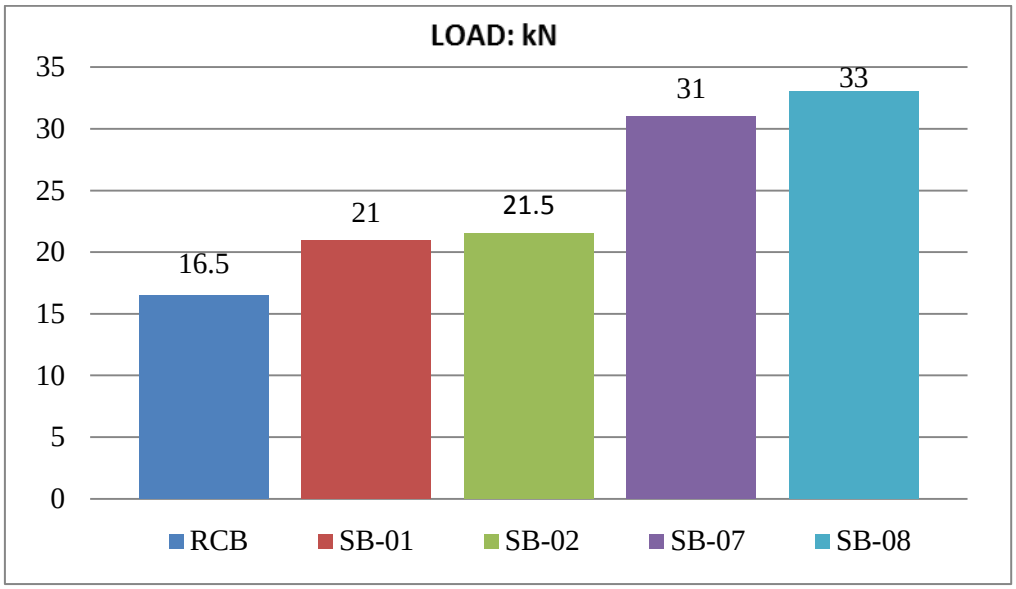

Figure 4.36 - First Crack Load of RCB, SB-01, SB-02, SB-07 and SB-08

The first crack load of reference control beam (RCB) and beams SB-01, SB-02 and beams strengthened with scheme V (SB-09 and SB-10) having 40 mm wide inclined (45°) CFRP strips (grooving method) are presented in Figure 4.37. It is observed that first crack load of beams SB-09 and SB-10 is increased by **90.91%** (avrg.) as compared to reference control specimen (RCB) and **48.23%** (avrg.) as compared to beams SB-01 and SB-02.

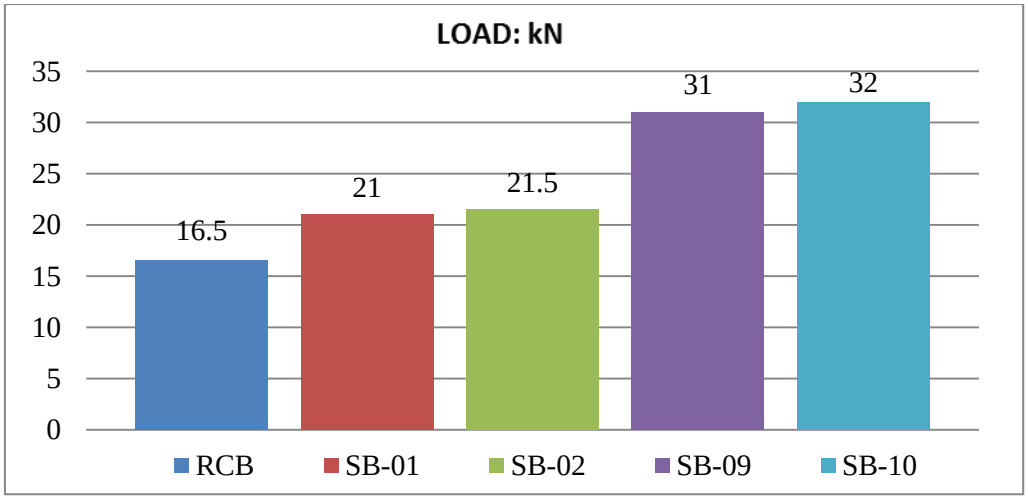

Figure 4.37 - First Crack Load of RCB, SB-01, SB-02, SB-09 and SB-10

The first crack load of reference control beam (RCB) and beams SB-01,SB-02 and beams strengthened with scheme VI (SB-11 and SB-12) having 125 mm wide side wrap in shear spans (grooving method) are presented in Figure 4.38. It is observed that the first crack load of beams SB-07 and SB-08 is increased by **60.61%** (avrg.) as compared to reference control specimen (RCB) and **24.71%** (avrg.) as compared to beams SB-01 and SB-02.

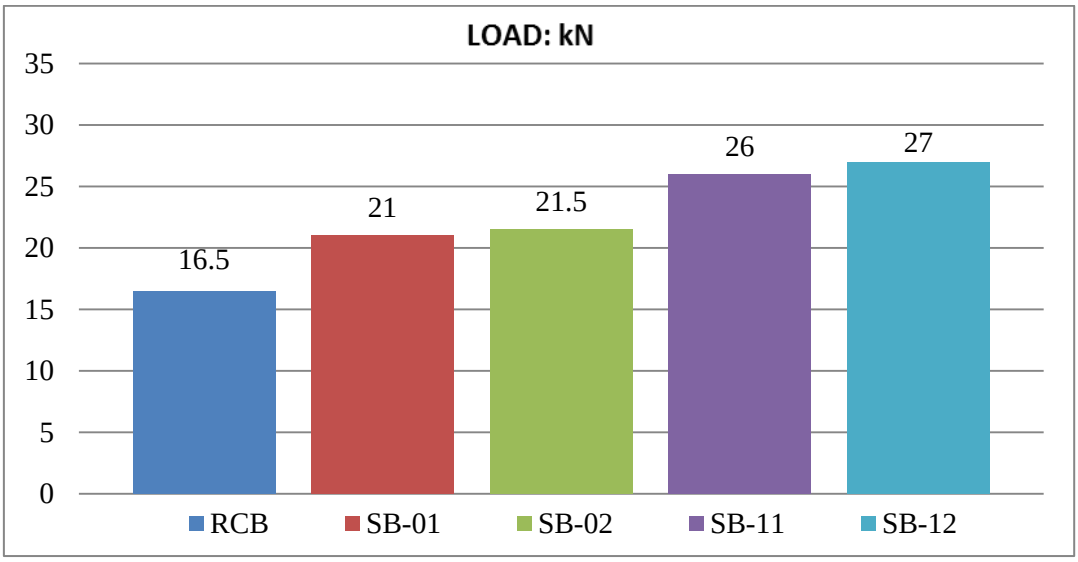

Figure 4.38 - First Crack Load of RCB, SB-01, SB-02, SB-11 and SB-12

The first crack load of reference control beam (RCB) and beam strengthened with scheme VII (SB-13) having 100 mm wide laminate at bottom face and 60 mm wide U-strip at ends of the beam are presented in Figure 4.39. It is observed that the first crack load of beam SB-13 is increased by **15.15%** (avrg.) as compared to reference control specimen (RCB).

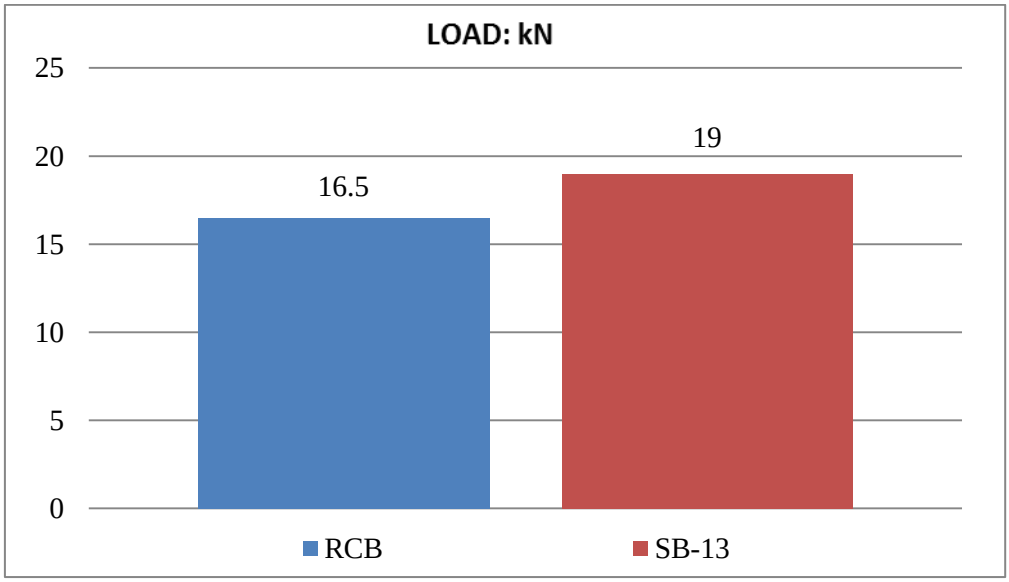

Figure 4.39 - First Crack Load of RCB and SB-13

4.3.2 Ultimate Load Carrying Capacity

The ultimate load carrying capacities of reference control beam (RCB) and strengthened with scheme I (SB-01 and SB-02) are presented in Fig. 4.40. It is observed that the ultimate load carrying capacity of beams SB-01 and SB-02 is increased by **27.75%** (avrg.) as compared to reference control specimen (RCB).

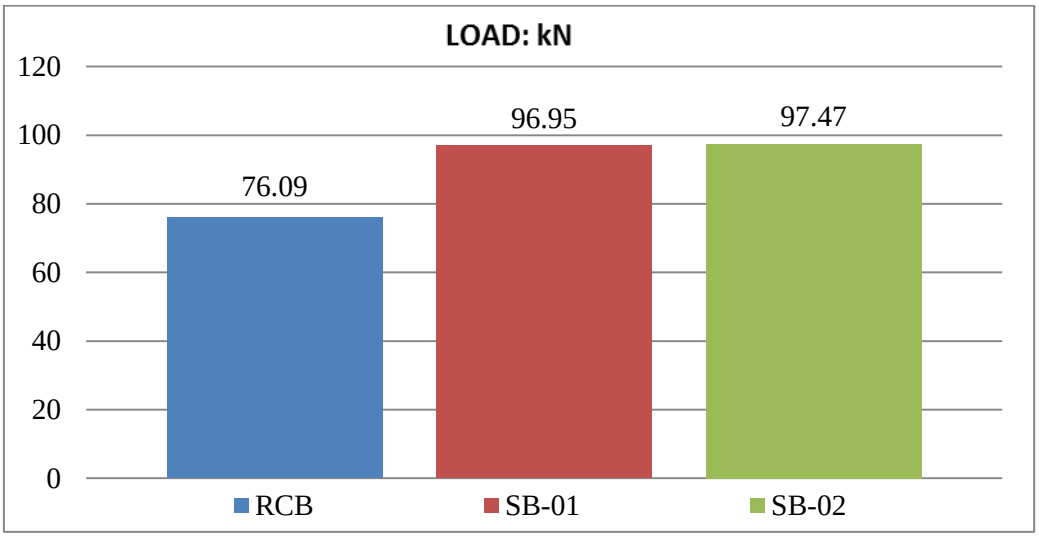

Figure 4.40 – Ultimate Load Capacities of RCB, SB-01 and SB-02

The ultimate load carrying capacities of reference control beam (RCB) and beams SB-01, SB-02 and beams strengthened with scheme II (SB-03 and SB-04) having 50 mm wide CFRP U-strips in shear spans are presented in Fig 4.41. It is observed that the ultimate load carrying capacity of beams SB-03 and SB-04 is increased by **40.04%** (avrg.) as compared to reference control specimen (RCB) and **9.61%** (avrg.) as compared to beams SB-01 and SB-02.

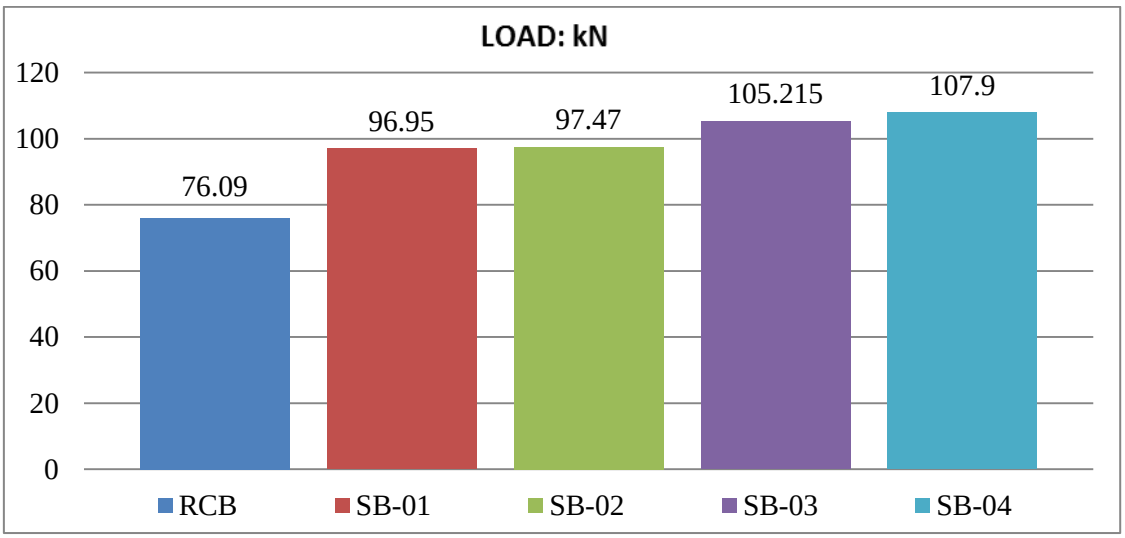

Figure 4.41 – Ultimate Load Capacities of RCB, SB-01, SB-02, SB-03 and SB-04

The ultimate load carrying capacities of reference control beam (RCB) and beams SB-01, SB-02 and beams strengthened with scheme III (SB-05 and SB-06) having 150 mm wide CFRP full U-wrap in shear spans are presented in Fig 4.42. It is observed that ultimate load carrying capacity of beams SB-05 and SB-06 is increased by **45.33%** (avrg.) as compared to reference control specimen (RCB) and **13.75%** (avrg.) as compared to SB-01 and SB-02.

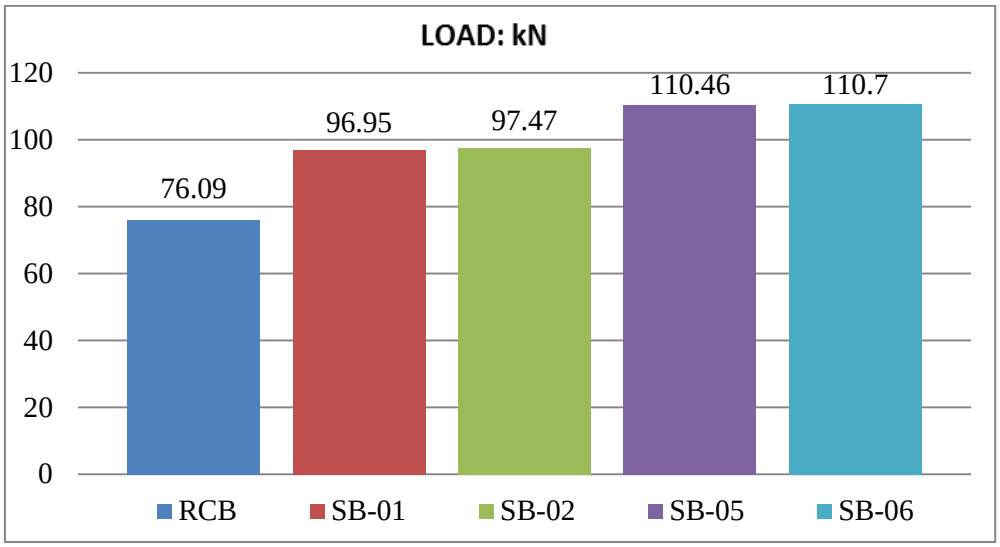

Figure 4.42 – Ultimate Load Capacities of RCB, SB-01, SB-02, SB-05 and SB-06

The ultimate load carrying capacities of reference control beam (RCB) and beams SB-01, SB-02 and beams strengthened with scheme IV (SB-07 and SB-08) having 40 mm wide inclined (45°) CFRP strips in shear spans are presented in Figure 4.43. It is observed that the ultimate load carrying capacity of beams SB-07 and SB-08 is increased by **54.84%** (avrg.) as compared to reference control specimen (RCB) and **21.12%** (avrg.) as compared to beams SB-01 and SB-02.

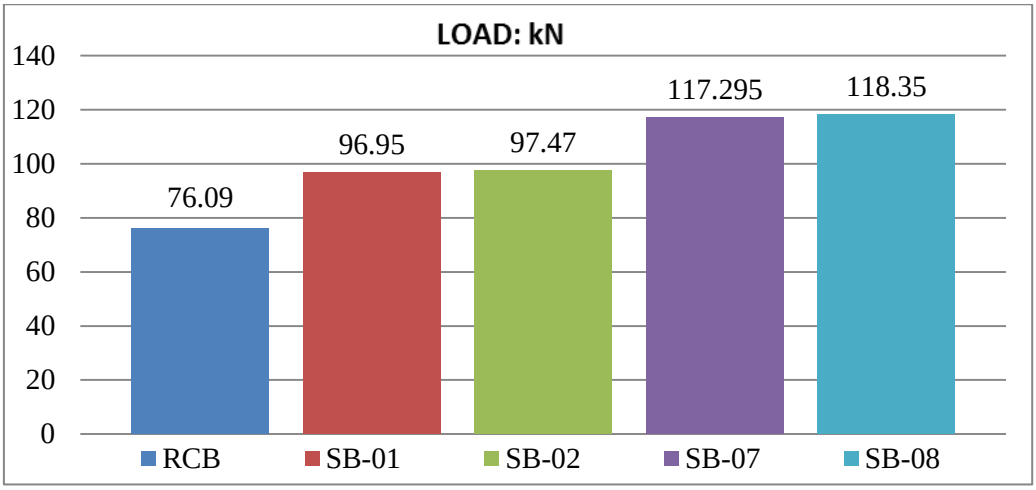

Figure 4.43 – Ultimate Load Capacities of RCB, SB-01, SB-02, SB-07 and SB-08

The ultimate load carrying capacities of reference control beam (RCB) and beams SB-01, SB-02 and beams strengthened with scheme V (SB-09 and SB-10) having 40 mm wide inclined (45°) CFRP strips in shear spans (grooving method) are presented in Figure 4.44. It is observed that the ultimate load carrying capacity of beams SB-07 and SB-08 is increased by **48.68%** (avrg.) as compared to reference control specimen (RCB) and **16.38%** (avrg.) as compared to beams SB-01 and SB-02.

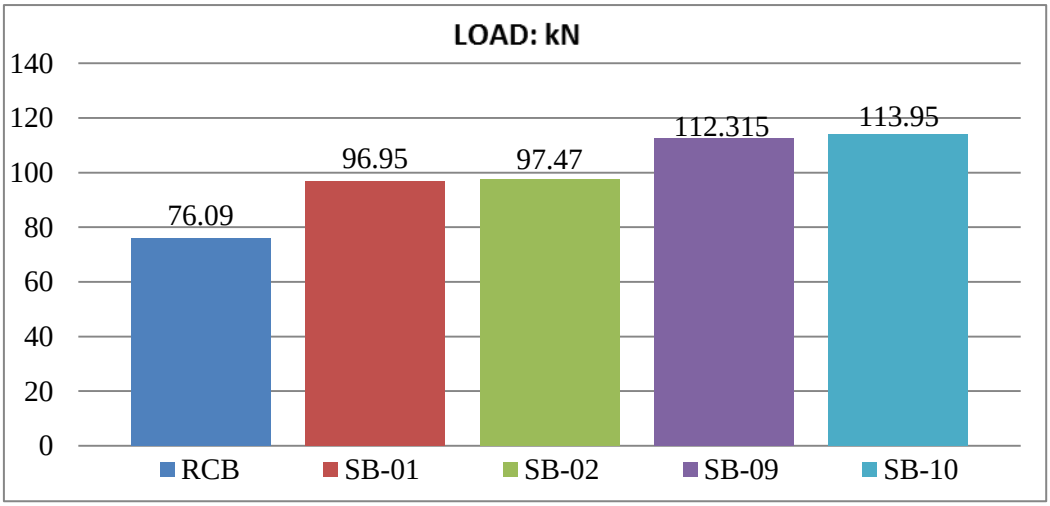

Figure 4.44 – Ultimate Load Capacities of RCB, SB-01, SB-02, SB-09 and SB-10

The ultimate load carrying capacities of reference control beam (RCB) and beams SB-01, SB-02 and beam strengthened with scheme VI (SB-11 and SB-12) having 125 mm wide side wrap in shear spans (grooving method) are presented in Figure 4.45. It is observed that the ultimate load carrying capacity of beams SB-07 and SB-08 is increased by **48.93%** (avrg.) as compared to reference control specimen (RCB) and **16.58%** (avrg.) as compared to beams SB-01 and SB-02.

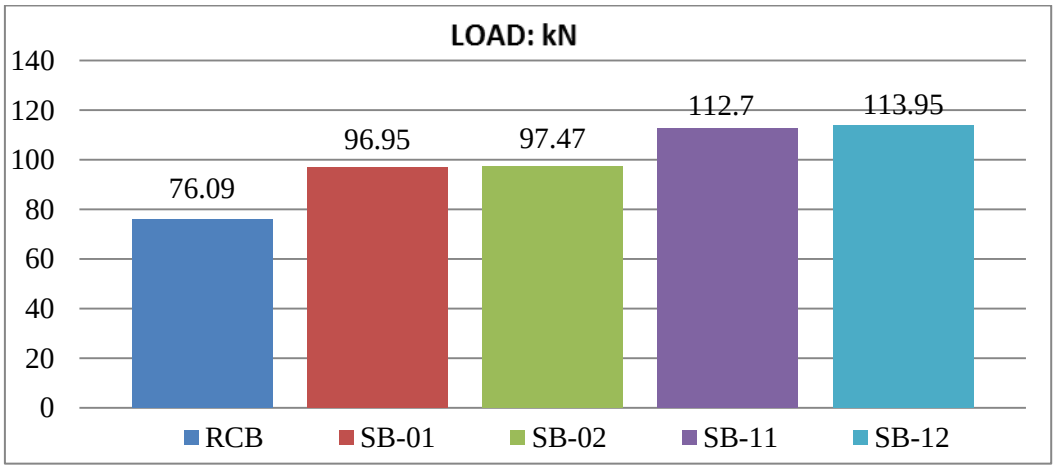

Figure 4.45 – Ultimate Load Capacities of RCB, SB-01, SB-02, SB-11 and SB-12

The ultimate load carrying capacities of reference control beam (RCB) and beam strengthened with scheme VII (SB-13) having 100 mm wide laminate at bottom face and 60 mm wide U-strip at ends of the beam are presented in Figure 4.46. It is observed that the ultimate load carrying capacity of beam SB-13 is increased by **23.72%** (avrg.) as compared to reference control specimen (RCB).

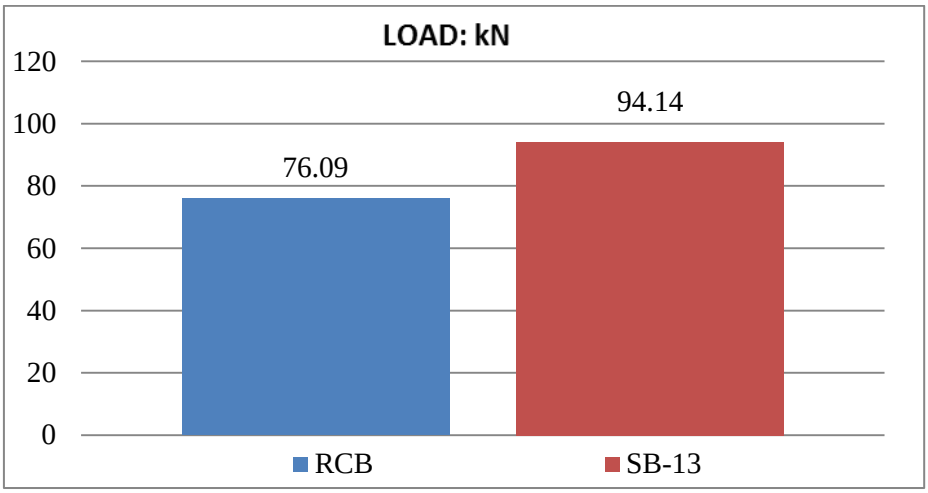

Figure 4.46 – Ultimate Load Capacities of RCB and SB-13

4.4 EFFECT OF STRENGTHENING ON STIFFNESS OF BEAMS

The stiffness (up to elastic limit) of reference control beam (RCB) and beams strengthened with scheme I (SB-01 and SB-02) are presented in Figure 4.47. It is observed that the stiffness (up to elastic limit) of beams SB-01 and SB-02 is increased by **57.18%** (avrg.) as compared to reference control specimen (RCB).

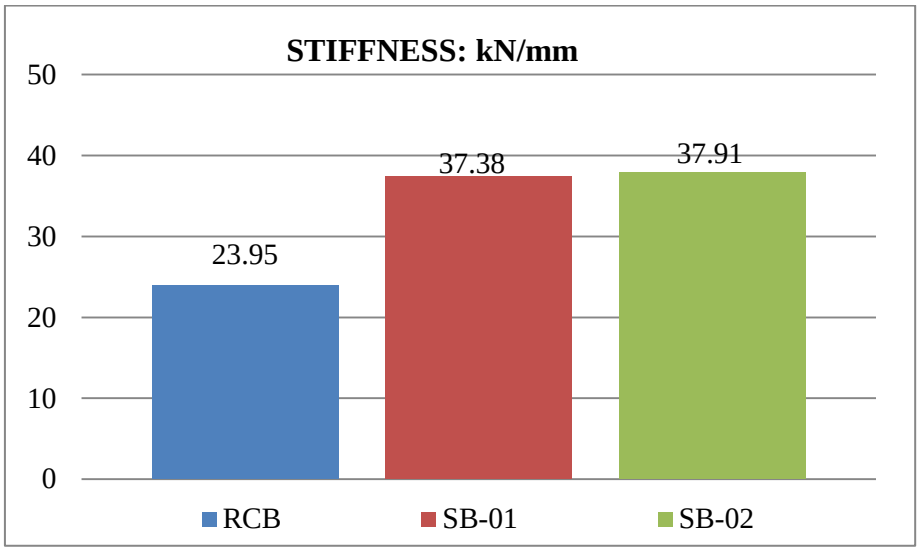

Figure 4.47 – Stiffness variation of RCB, SB-01 and SB-02

The stiffness (up to elastic limit) of reference control beam (RCB) and beams SB-01, SB-02 and beams strengthened with scheme II (SB-03 and SB-04) having 50 mm wide CFRP U-strips in shear spans are presented in Figure 4.48. It is observed that the stiffness (up to elastic limit) of beams SB-03 and SB-04 is increased by **64.15%** (avrg.) as compared to reference control specimen (RCB) and **4.44%** (avrg.) as compared to beams SB-01 and SB-02.

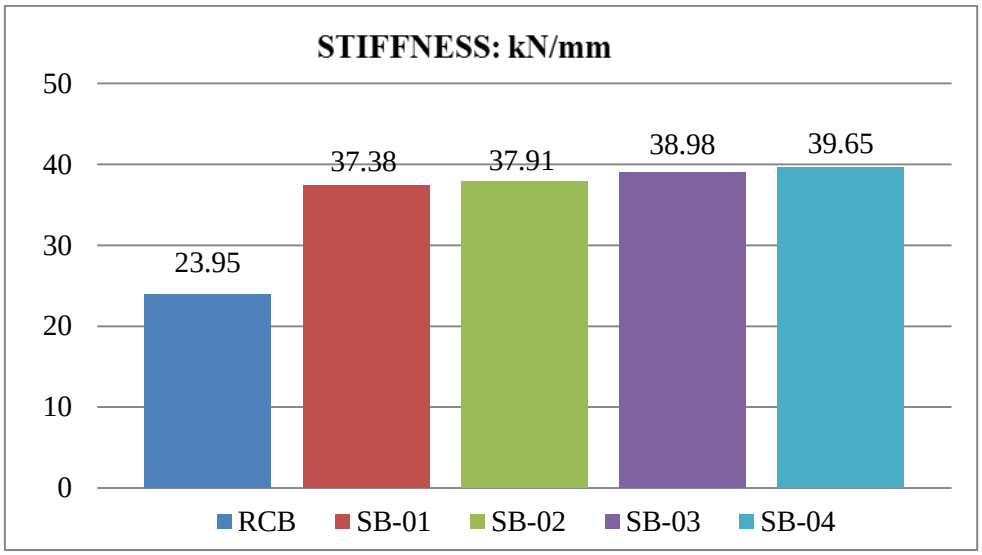

Figure 4.48 – Stiffness variation of RCB, SB-01, SB-02, SB-03 and SB-04

The stiffness (up to elastic limit) of reference control beam (RCB) and beams SB-01, SB-02 and beams strengthened with scheme III (SB-05 and SB-06) having 150 mm wide CFRP full U-wrap in shear spans are presented in Fig. 4.49. It is observed that the stiffness (up to elastic limit) of beams SB-05 and SB-06 is increased by **66.34%** (avrg.) as compared to reference control specimen (RCB) and **5.83%** (avrg.) as compared to beams SB-01 and SB-02.

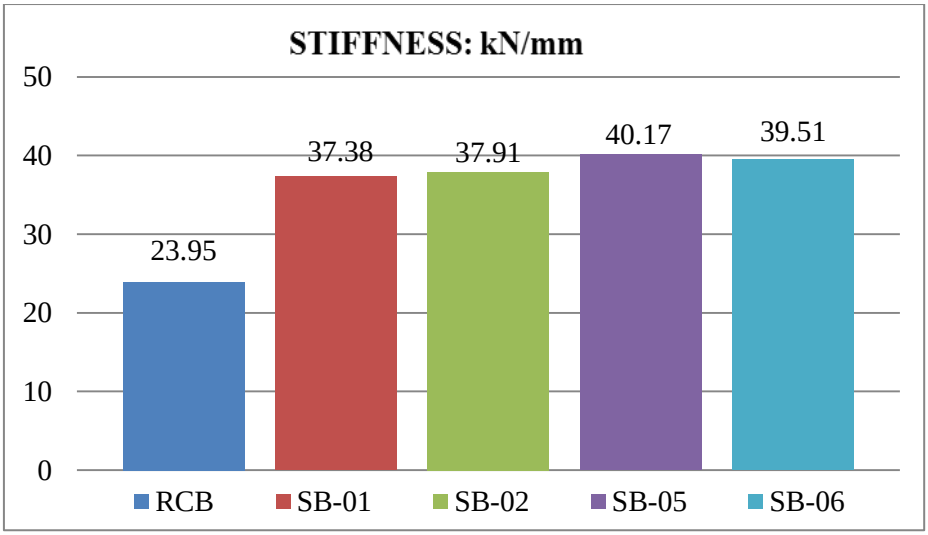

Figure 4.49 – Stiffness variation of RCB, SB-01, SB-02, SB-05 and SB-06

The stiffness (up to elastic limit) of reference control beam (RCB) and beams SB-01,SB-02 and beams strengthened with scheme IV (SB-07 and SB-08) having 40 mm wide inclined (45°) CFRP strips are presented in Figure 4.50. It is observed that the stiffness (up to elastic limit) SB-07 and SB-08 is increased by **80.58%** (avrg.) as compared to reference control specimen (RCB) and **14.89%** (avrg.) as compared to beams SB-01 and SB-02.

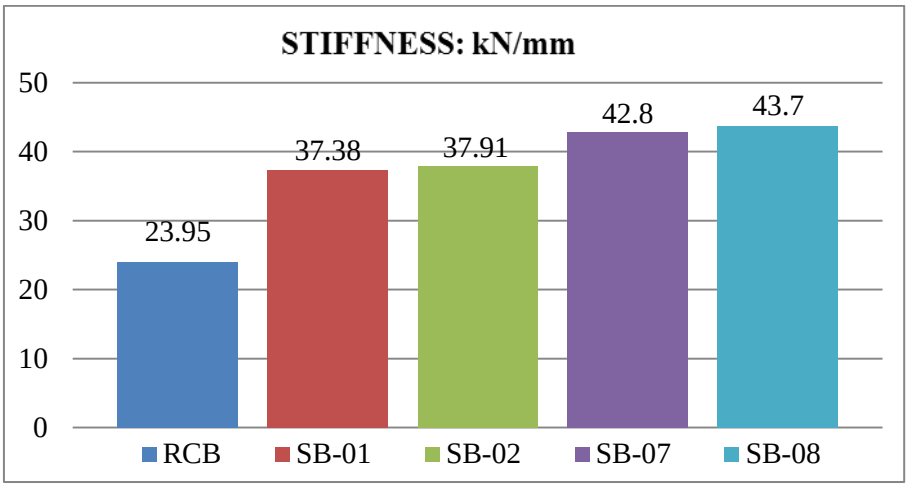

Figure 4.50 – Stiffness variation of RCB, SB-01, SB-02, SB-07 and SB-08

The stiffness (up to elastic limit) of reference control beam (RCB) and beams SB-01, SB-02 and beams strengthened with scheme V (SB-09 and SB-10) having 40 mm wide inclined (45°) CFRP strips (grooving method) are presented in Figure 4.51. It is observed that the stiffness (up to elastic limit) of beams SB-09 and SB-10 is increased by **73%** (avrg.) as compared to reference control specimen (RCB) and **10.05%** (avrg.) as compared to beams SB-01 and SB-02.

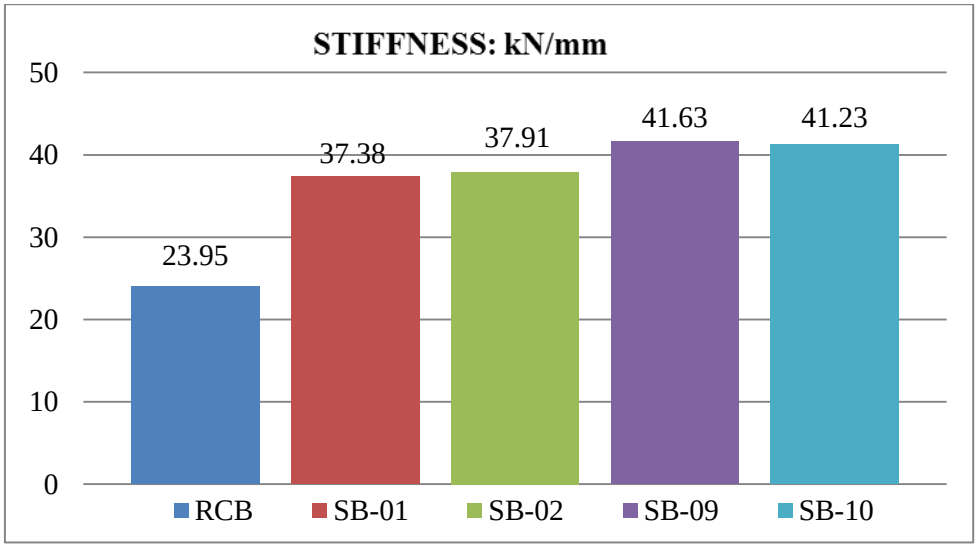

Figure 4.51 – Stiffness variation of RCB, SB-01, SB-02, SB-09 and SB-10

The stiffness (up to elastic limit) of reference control beam (RCB) and beams SB-01, SB-02 and beams strengthened with scheme VI (SB-11 and SB-12) having 125 mm wide side wrap in shear spans (grooving method) are presented in Figure 4.52. It is observed that the stiffness (up to elastic limit) of beams SB-11 and SB-12 is increased by **62.61%** (avrg.) as compared to reference control specimen (RCB) and **3.45%** (avrg.) as compared to beams SB-01 and SB-02.

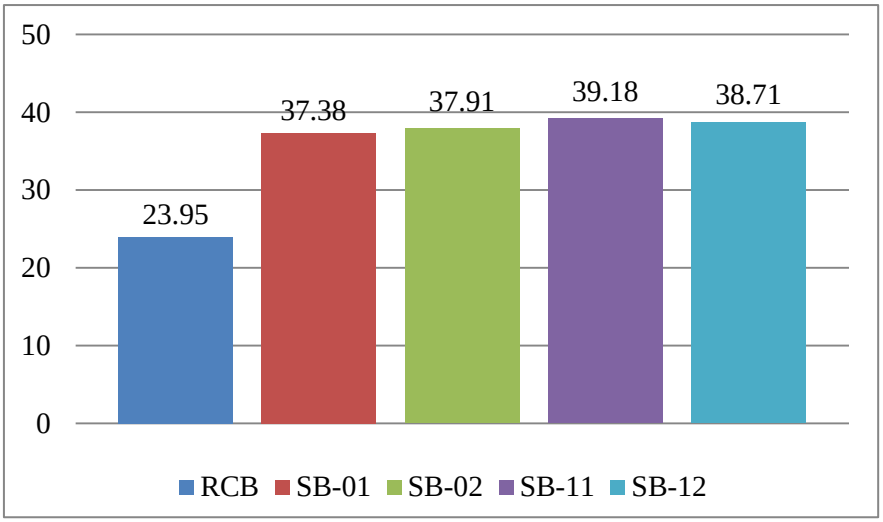

Figure 4.52 – Stiffness variation of RCB, SB-01, SB-02, SB-11 and SB-12

The stiffness (up to elastic limit) of reference control beam (RCB) and beam strengthened with scheme VII (SB-13) having 100 mm wide laminate at bottom face and 60 mm wide U-strip at ends of the beam are presented in Figure 4.53. It is observed that the stiffness (up to elastic limit) of beam SB-13 is increased by **23.05%** (avrg.) as compared to reference control specimen (RCB).

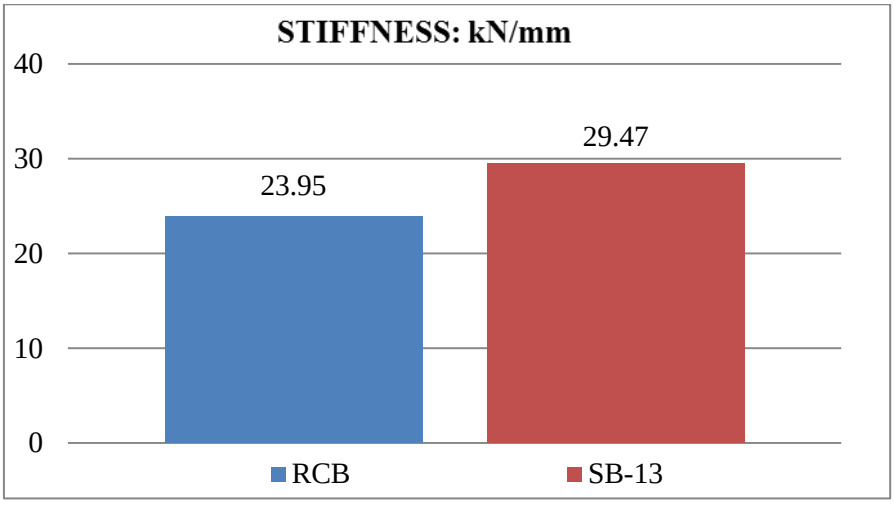

Figure 4.53 – Stiffness variation of RCB and SB-13

4.5 EFFECT OF STRENGTHENING ON DUCTILITY OF BEAMS

Ductility is the capacity of a material, section, structural element, or structural system to tolerate large inelastic deformations prior to total collapse. The load–deflection curves of all the strengthened beams from SB-01 to SB-13 shows that the strengthening by externally bonded CFRPs could affect the overall structural ductility of the beam.

Measures of ductility are best related to structural parameters which engineers can easily understand, such as mid-span deflection and area under the load–deflection diagram (as a measure of energy absorption). These quantities are expressed as indices or factors, through relationship at two different stages, namely, at yielding of the tension steel and at ultimate load capacity. Thus, the more common ductility indices, the implications of which can be easily appreciated, can be expressed as:

i. $\mu_{\Delta} = \Delta_{\mu}/\Delta_{y}$
ii. $\mu_{E} = E_{TOT}/E_{0.75Fu}$

where:
μ_{Δ} = Deflection ductility;
μ_{E} = Energy ductility;
Δ_{μ} = mid-span deflection at point where load drops about 0.85 of ultimate load;
Δ_{y} = mid-span deflection at tension steel yielding;
E_{μ} = area under the load-deflection diagram up to, load drops about 0.85 of ultimate load;
E_{y} = area under the load-deflection diagram up to, yielding of tension steel.

The ductility indices calculated as above are shown in the Table 4.16 and 4.17. For the sake of clarity and for a synthetic comparison, these data are also given in isograms of Figure 4.54 and 4.55.

These data definitely show that strengthening with externally bonded FRP systems results in significant losses in structural ductility of the strengthened beams from SB-01 to SB-10. The ductility of these beams is about two-third of that of the original control beams. The beams SB-11 and SB-12 show higher ductility indices as compared to beams SB-01 to SB-10 but about 10% less as compared to that of the controlled/ unstrengthened beams.

Table 4.16 – Deflection ductility index of beams

Beam label	Δ_{μ} (mm)	Δ_{y} (mm)	μ_{Δ}
CB-01	7.43	2.54	2.93
CB-02	7.5	2.47	3.03
SB-01	4.34	2.14	2.03
SB-02	4.41	2.11	2.09
SB-03	4.74	2.36	2.00
SB-04	4.70	2.16	2.17
SB-05	4.99	2.39	2.08
SB-06	5.01	2.43	2.06
SB-07	4.64	2.43	1.91
SB-08	4.78	2.38	2.00
SB-09	5.63	2.73	2.06
SB-10	5.39	2.76	1.95
SB-11	6.63	2.45	2.70
SB-12	6.57	2.48	2.65
SB-13	8.94	1.90	4.70

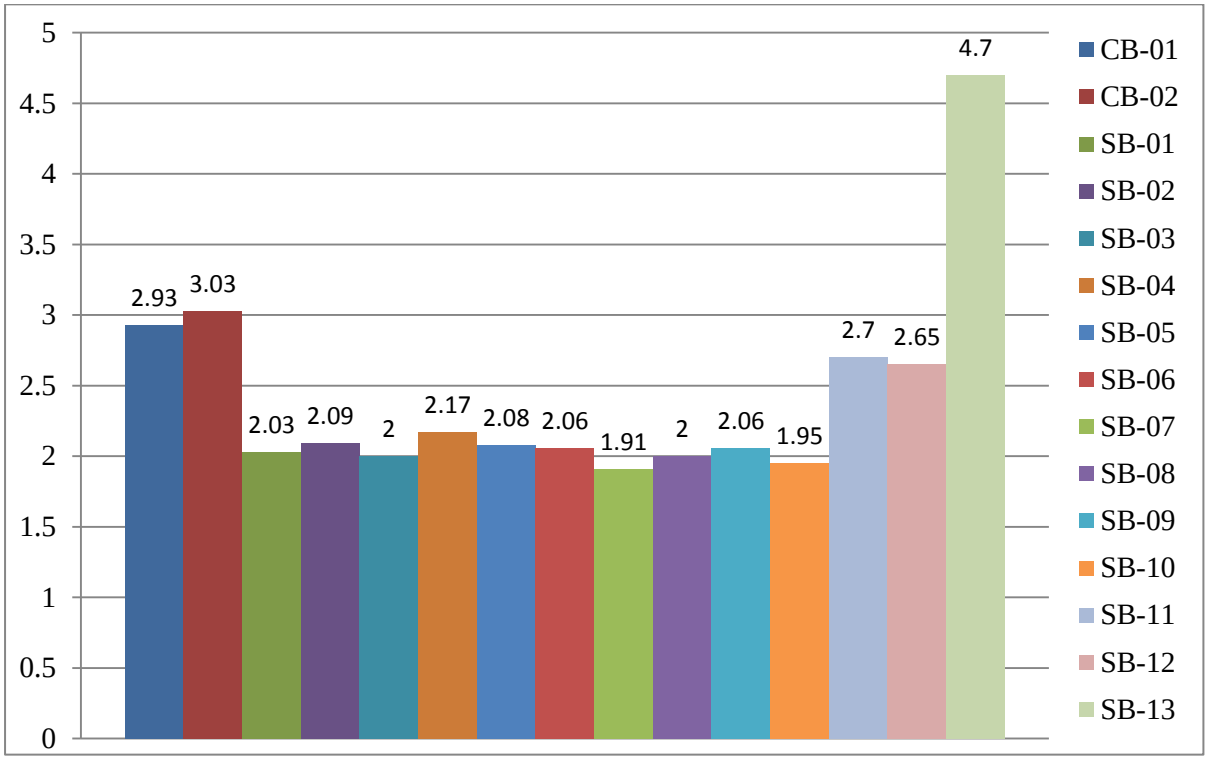

Figure 4.54 - Deflection ductility index of beams

Table 4.17 – Energy ductility index of beams

Beam label	E_μ (KN-mm)	E_y (KN-mm)	μ_E
CB-01	428.14	89.29	4.79
CB-02	440.64	87.05	5.06
SB-01	292.41	92.67	3.15
SB-02	298.96	89.31	3.35
SB-03	370.50	128.35	2.89
SB-04	376.07	118.28	3.18
SB-05	407.66	135.00	3.02
SB-06	409.35	138.35	2.96
SB-07	394.62	149.34	2.64
SB-08	414.74	145.50	2.85
SB-09	468.94	157.72	2.97
SB-10	443.29	159.05	2.79
SB-11	586.32	138.73	4.23
SB-12	583.26	140.05	4.16
SB-13	637.58	62.61	10.18

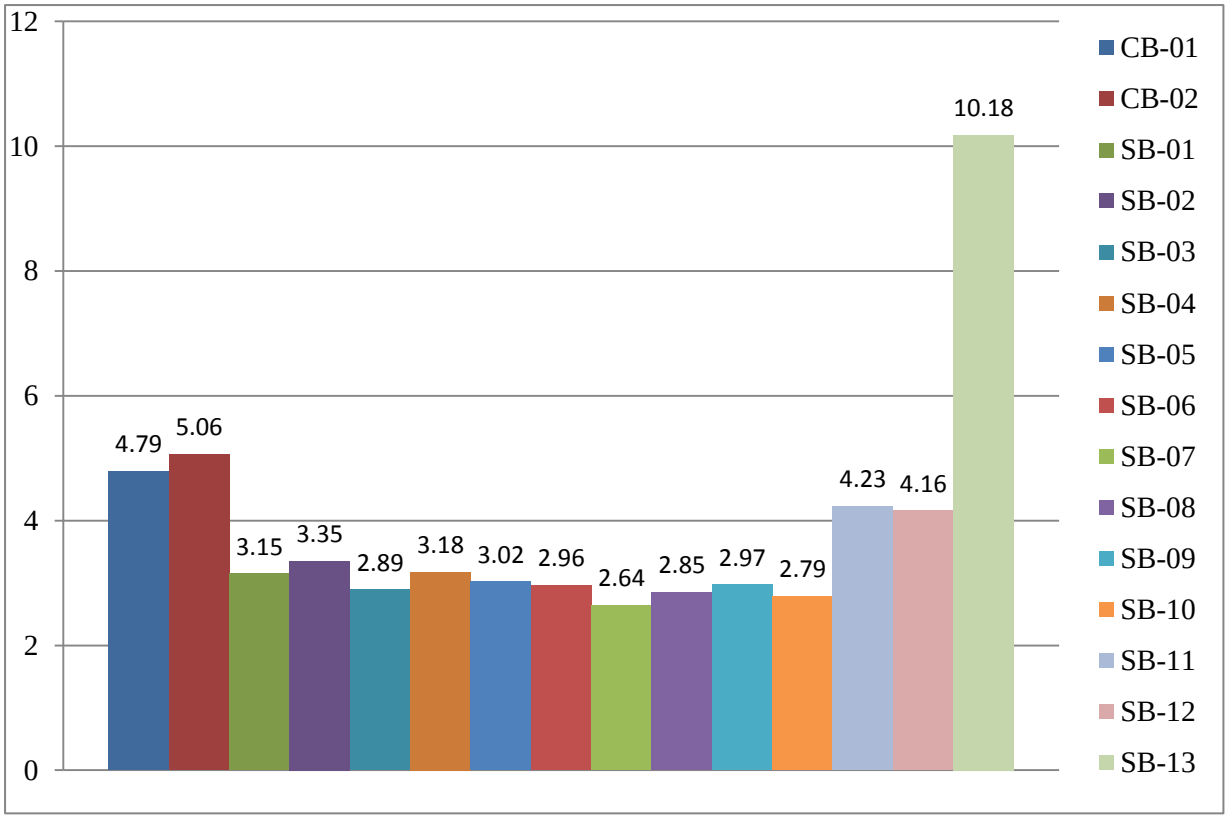

Figure 4.55 – Energy ductility index of beams

4.6 OVER ALL COMPARATIVE VIEW OF THE TESTED BEAMS

Table 4.18 summarizes the outcomes of the experiments corresponding to the beam label: the maximum load (F_u), the increase of load capacity due to laminate application, the mid span deflection corresponding to F_u and the failure mode.

Table 4.18 – Comparison between failure loads and deflections

Beam label	Maximum load F_u (KN)	Increase in load capacity (%)	Mid span deflection (mm)	Failure Mode
CB-01	75.10	-	5.782	Concrete crushing
CB-02	77.08	-	5.49	Concrete crushing
SB-01	96.95	27.41	3.460	Shear failure
SB-02	97.47	28.10	3.49	Shear failure
SB-03	105.215	38.28	3.890	Debonding + Shear
SB-04	107.9	41.81	3.884	Debonding + Shear
SB-05	110.46	45.17	4.17	Debonding + Shear
SB-06	110.7	45.49	4.246	Debonding + Shear
SB-07	117.295	54.15	3.519	Plate end debonding
SB-08	118.35	55.54	3.66	Plate end debonding
SB-09	112.315	47.61	5.03	Plate end debonding
SB-10	113.95	49.76	4.75	Plate end debonding
SB-11	112.7	48.11	6.029	Plate end debonding
SB-12	113.95	49.76	5.72	Plate end debonding
SB-13	94.14	23.72	8.110	Plate end debonding

It can be seen from the Table 4.16 that all beams with bonded external reinforcement performed significantly better than the control beams, in terms of strength and stiffness. Cleary the strength is influenced and by the type and amount of external reinforcement.

The experimental increase in ultimate strength is very significant: about 55% for beams strengthened with scheme IV i.e. SB-07 and SB-08 they both utilize the capacity of diagonal side strips (L-shape), and only about 28% for beams strengthened with scheme I i.e. SB-01 and SB-02 in which no external shear reinforcement was provided.

General variation of the values of the maximum displacement during failure of the strengthened beams is about 3.5 to 6 mm except for strengthened beam SB-13 in which the displacement at failure load was 8.110 mm.

One conclusion that can be made regarding the response behaviour of beams in same category is that for the same causes and in the same testing conditions, similar results are obtained which imply similar behaviour.

The experimental results showed that the main failure mode was debonding which reduces the efficiency of strengthening.

In figure 4.56 we will illustrate, by overlapping the previous load-deflection graphics, the different aspects that arise from comparing the results of the strengthened beams between them and against the control beams.

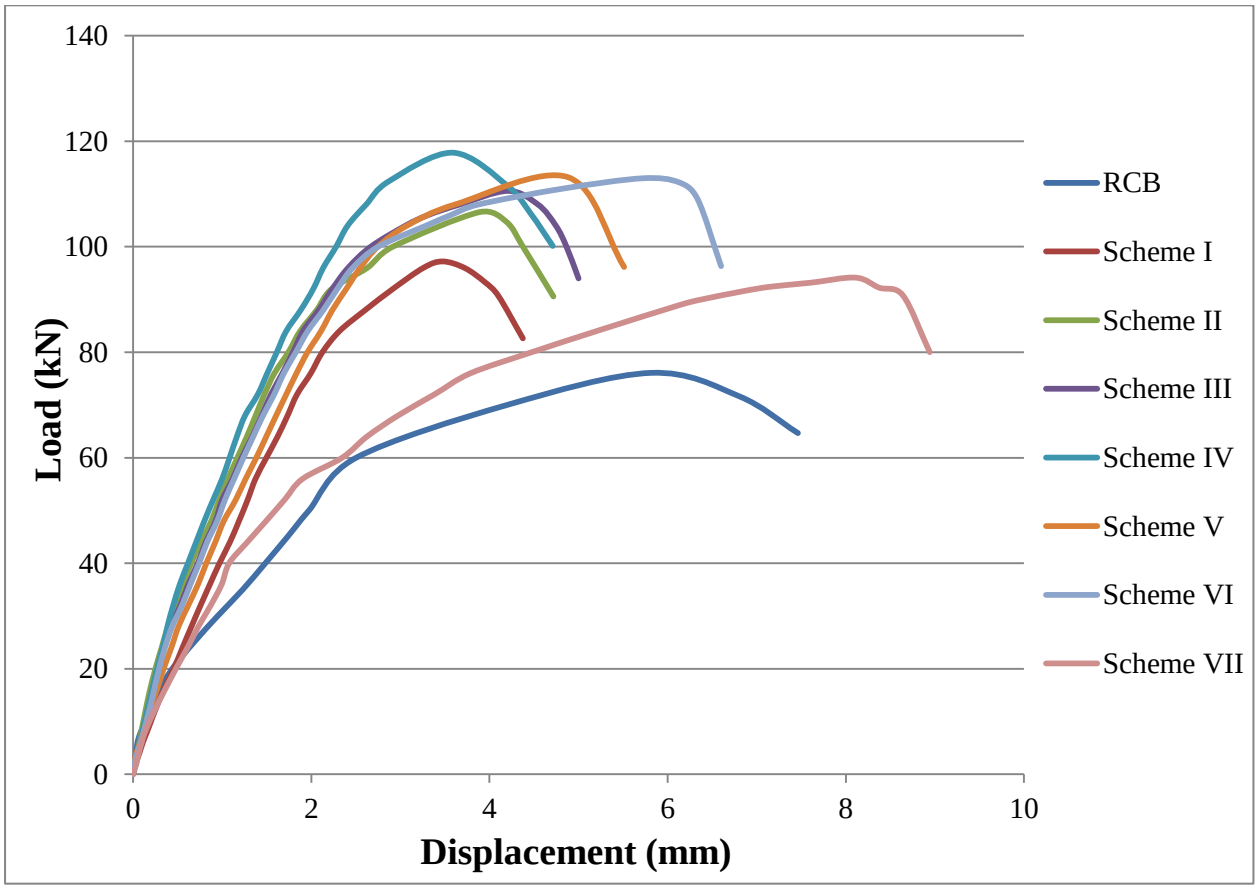

Figure 4.56 –Comparative view of the response behaviour of all the tested beams

Note: The average load-deflection curve is plotted for beams in same scheme of strengthening.

It can be noticed that, before concrete cracks, all the strengthened beams have a similar behaviour to the control beams. After cracking, strengthened beams show themselves to be stiffer than the control beams.

The beams strengthened with 150 mm wide full U-wrap in shear spans of the beam (Scheme-III) performed better than the beams strengthened with 50 mm wide U-strips in shear spans of the beam (Scheme II), in enhancing both stiffness and strength.

It can be seen that beams strengthened with scheme IV (SB-07 and SB-08) shows the minimum deflection as compared to other strengthened beams having external shear reinforcement. These beams also have the maximum load carrying capacity, as compared to other strengthened beams.

In beams strengthened with scheme III (SB-05 and SB-06), the main failure was due to debonding of U-wraps, whereas in beams strengthened with scheme VI (SB-11 and SB-12) the grooving method helped to eliminate the debonding of side wraps which in turn impeded the growth and propagation of critical diagonal shear crack and allowed the beam to carry more load with higher deformations.

The beam strengthened with scheme VII (SB-13) has the maximum post yielding region with minimum brittleness as compared with other strengthened beams. This is because the beam is reinforced externally with less width of CFRP laminate (100 mm) as compared to width of the beam (150 mm). As a result, the beam deform plastically under the tensile stress regime hence absorb more internal strain energy, contrarily to most of the strengthened beams having 150 mm wide CFRP laminate in tension face.

All strengthened beams experienced a brittle failure mechanism due to debonding of CFRP laminate attached either on beam sides or in tension face. The failure was due to high stress occurring at the interface with the CFRP plates. The properties of the adhesive are probably important in relation to the debonding failure. A lower stiffness and high fracture energy will probably weaken the tendency of debonding.

CHAPTER -5 CONCLUSIONS

Starting from the results obtained in various research papers, we tried to study the efficiency of FRP systems in strengthening RC members. The main subject of this thesis is to study the response behaviour of reinforced concrete beams strengthened with externally bonded CFRP laminates under combined flexure and shear. The analysis focused mainly on the ultimate behaviour and allowed assessing the strength gains provided by FRP system. Based on the specific findings of this research the following conclusions can be drawn:

1. The Externally bonded CFRPs have increased the stiffness (the extent to which it resists the deformation in response to an applied force) of all the strengthened beams.

2. The Externally bonded CFRPs have increased the load carrying capacity of all the strengthened beams. The increase in capacity varies from 23.72 to 55.54% with different configurations.

3. The increase in strength, however, is at a sacrifice of ductility. The strengthening with externally bonded FRP systems results in significant losses in structural ductility of the strengthened beams SB-01 to SB-10. The ductility of these beams is about two-third of that of the original control beams.

4. Cutting longitudinal grooves and filling them with an appropriate epoxy is an effective substrate for surface preparation, it prevents the debonding of CFRP side strips as in case of SB-11 and SB-12 which also shows slightly higher ductility indices as compared to that of the control beams.

5. For every type of plate-bonded beam, there is a limiting point beyond which no further increase in beam strength can be obtained. The ultimate load-carrying capacities of strengthened beams depend largely on the type of external reinforcement provided.

6. Among all the CFRP strip configurations (i.e. vertical strips, strips inclined at 45°, U-wraps), the strips inclined at 45° is more effective than the others.

7. The control beams failed in a gradual manner whereas the strengthened beams failed in an abrupt manner with a significant drop in load almost after reaching the peak load.

8. The crack-width and the deflection have decreased for the strengthened beams.

9. The main failure mode was debonding which reduces the efficiency of strengthening. The full capacity of the composite system was not utilized.

10. The experimental results match closely the theoretical calculation on shear capacity of strengthened beams based on debonding failure mode.

Although the Carbon Fibre Reinforced Polymers (CFRP) reinforcement is very effective in enhancing both, stiffness and strength, sudden failure occurs when the beams approach their load carrying capacity. The high local interface shear and peeling stresses at the ends of the FRP laminates results in debonding, which reduces the efficiency of strengthening.

Some researchers have pointed out that the use of additional anchorage system delay premature failures by peeling off (debonding) and might increase the load capacity and ductility of beam, because they provide better anchorage and hinder the development of inclined cracks in shear spans of the beam. The future research should be focused on the development of anchorage systems to eliminate premature debonding failure modes.

REFERENCES

1. ACI Committee 440 (2008), Guide for the Design and Construction of Externally Bonded FRP systems for Strengthening Concrete Structures (ACI 440.2R-08), American Concrete Institute, Farmington Hills, MI, USA.

2. Adhikary, B.H. and Mutsuyoshi (2004), "Behaviour of concrete beams strengthening in shear with carbon-fibre sheets", Composites for Construction, 8, 158-169.

3. Al-Amery R., and Al-Mahaidi R. (2006), "Coupled flexural-shear retrofitting of RC Beams using CFRP straps", *Construction and Building Materials*, 21, 1997-2006.

4. Bukhari I. A., Vollum R. L., Ahmad S., and Sagaseta J. (2010), "Shear strengthening of reinforced concrete beams with CFRP", Magazine of Concrete Research, 62, No. 1, 65–77.

5. Chaallal O., Nollet M. J., and Perraton D. (1998), "Strengthening of reinforced concrete beams with externally bonded fibre-reinforced-plastic plates: design guidelines for shear and flexure", Canadian Journal of Civil Engineering, Vol. 25, No. 4, 692-704.

6. Chen J. F., and Teng J. G. (2003), "Shear capacity of FRP-strengthened RC beams: FRP debonding", Construction and Building Materials, 17, 27-41.

7. D. Duthinh, and M. Starnes (2004), "Strength and ductility of concrete beams reinforced with carbon fiber-reinforced polymer plates and steel", Composites for Construction, 8 (1), 59–69.

8. Esfahani M. R., Kianoush M. R., and Tajari A. R. (2007), "Flexural behaviour of reinforced concrete beams strengthened by CFRP sheets", *Engineering Structures*, 29, 2428–2444.

9. Habibur Rahman Sobuz. (2011), “Use of carbon fiber laminates for strengthening reinforced concrete beams in bending” International journal of civil and structural engineering Vol. 2, No. 1, 67-84.

10. Islam M. R., Mansur M. A., and Maalej M. (2005), “Shear strengthening of RC deep beams using externally bonded FRP systems”, Cement & Concrete Composites, 27, 413–420.

11. Kaushal Parikh and C.D. Modhera (2012), “Application of GFRP on preloaded retrofitted beam for enhancement in flexural strength”, International Journal of Civil and Structural Engineering, 1070-1080.

12. Khalifa A, Gold WJ, Nanni A and Aziz A. (1998), “Contribution of externally bonded FRP to shear capacity of RC flexural members”, *Journal of Composites for Construction*, 2, 195–201.

13. Khalifa A., and Nanni A. (2000), “Improving shear capacity of existing RC T-section beams using CFRP composites”, Cement & Concrete Composites, 22, 165-174.
14. Mosallam A. S., and Banerjee S. (2007), “Shear enhancement of reinforced concrete beams strengthened with FRP composite laminates”, Composites Part B Eng., 38, 781-793.
15. Mostofinejad D., and Shameli S.M. (2013), “Externally bonded reinforcement in grooves (EBRIG) technique to postpone debonding of FRP sheets in strengthened concrete beams”, Construction and Building Materials, 38, 751–758.

16. Mostofinejad D., and Tabatabaei Kashani A. (2013), “Experimental study on effect of EBR and EBROG methods on debonding of FRP sheets used for shear strengthening of RC beams”, Composites Part B Eng., 45 (1) ,1704–1713.

17. Nadeem A. Siddiqui.(2009), “Experimental investigation of RC beams strengthened with externally bonded FRP composites”, Latin American journal of solids and structures 6, 343-362.

18. Obaidat Y. T., Heyden S., Dahlblom O., Farsakh G. A. and Jawad Y. A. (2011), "Retrofitting of reinforced concrete beams using composite laminates", *Construction and Building Materials*, 25, 591–597.

19. Pannirselvam N., Nagaradjane V., and Chandramouli K. (2009), "Strength behaviour of fiber reinforced polymer strengthened beam", *ARPN Journal of Engineering and Applied Sciences*, Vol. 4, NO. 9, ISSN 1819-6608.

20. Rita S.Y.W., and Vecchio F.J. (2003), "Towards modeling of reinforced concrete members with externally bonded fiber-reinforced polymer composites", ACI Struct. J. 100, 47–55.

21. Saafan M. A. A. (2006), "Shear strengthening of Reinforced Concrete beams using GFRP wraps", Czech Technical University in Prague Acta Polytechnica, Vol. 46 No. 1, 24–32.

22. Sherif H. Al-Tersawy. (2013), "Effect of fiber parameters and concrete strength on shear behaviour of strengthened RC beams", Construction and Building Materials, 44, 15–24.

23. Sundarraja M. C., and Rajamohan S. (2009), "Strengthening of RC beams in shear using GFRP inclined strips – an experimental study", Construction and Building Materials, 23, 856–864.

24. Taljsten B. (2003), "Strengthening concrete beams for shear with CFRP sheets", Construction and Building Materials, 17, 15-26.

25. Toutanji H., and Ortiz G., (2001), "The effect of surface preparation on the bond interface between FRP sheets and concrete members", Composites Structures, 53 (4) 457–462.

26. V.P.V. Ramana., T. Kanta, and S.E. Morton.(2000), "Behaviour of CFRP strengthened reinforced concrete beams with varying degrees of strengthening", Composites Part B Eng., 31, 461–470.

APPENDIX - A

(a) INTRODUCTION

The design approach for computing the shear capacity of RC beams strengthened with externally bonded CFRP sheets based on debonding failure mode is presented in this section. Firstly the shear capacity of the beam section without considering the effect of external reinforcement is presented. Secondly the contribution of externally bonded FRP composites to the shear strength is calculated by Chen and Teng model (2003). In the end, shear strength of beams strengthened with CFRP sheets obtained from the experimental study is compared to the theoretical design shear strength of the beams.

(b) SHEAR CAPACITY OF BEAM (without external reinforcement)

In this section, the shear capacity of the beam without considering the effect of external reinforcement with respect to critical diagonal shear crack is calculated. The calculations are based on American Concrete Institute (ACI) guidelines to compute shear capacity in case of deep beams. In the present case, the beam has shear span to effective depth ratio of 1.6 and effective span to total depth ratio of 4.0 which falls in the category of deep beam.

As per ACI code :- $V_u = V_c + V_s$

where,

V_c = shear carried by the concrete,

V_s = shear carried by the steel.

$V_c = C_1 (1 – 0.35\ a_v/d)*f_1*t*D$……..... (1)

where,

C_1 = constant; 0.72 for normal grade concrete,

a_v = shear span (200 mm),

d = effective depth (125 mm),

f_1 = tensile strength of concrete (2.236 N/mm^2),

t = width of beam (150mm),

D = total depth (150 mm)

$V_s = C_2 [A_1*(y_1/D) \sin^2\alpha] + C_2 [A_2*(y_2/D) \sin^2\alpha]$ ……..... (2)

where,

$C_2 = 270$ N/mm^2 (Fe-500 grade steel)

A_i = Area of shear reinforcement,

y_i = distance from top of the beam to the point where the bar intersects critical diagonal crack,

α = Angle between the bar considered and critical diagonal shear crack (45°).

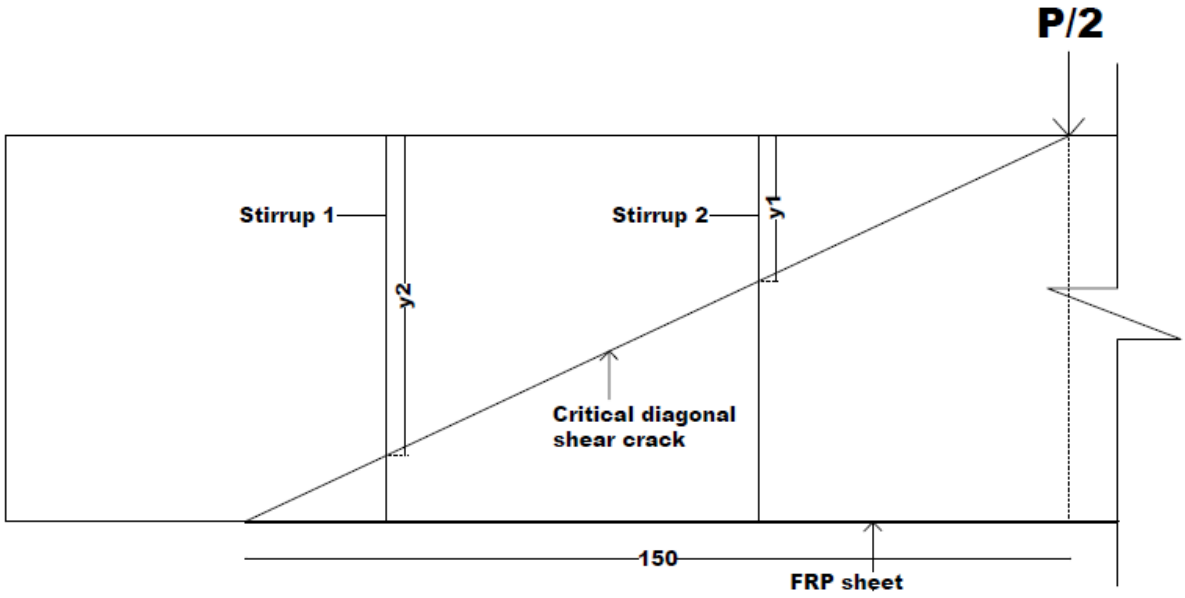

Figure A.1 – Representation of critical diagonal shear crack in beam

Calculations:

$V_c = C_1 (1 – 0.35\ a_v/d)*f_1*t*D$

$V_c = 0.72 (1 – 0.35 (200/125))*2.236*150*150$

$V_c = 15938.208$ N

$V_s = C_2 [A_1*(y_1/D) \sin^2\alpha] + C_2 [A_2*(y_2/D) \sin^2\alpha]$

$V_s = 270 [113.04*(50/150) \sin^2 45°] + 270 [113.04*(125/150) \sin^2 45°]$

$V_s = 17803.8$ N

$V_c + V_s = 15938.208 + 17803.8 =$ **33742.008 N**

(c) FRP CONTRIBUTION TO SHEAR STRENGTH

Chen and Teng (2003) presented method to computing the contributions of FRP to shear strength in reinforced concrete beam. For a general strengthening scheme with FRP strips bonded on both sides of the beam and an assumed critical shear crack inclined to the longitudinal axis of the beam by an angle of 45^o (Figure A.1), the contribution of the FRP to the shear strength of the RC beam is given by:

$$V_{frp} = 2*f_{frp,e}*t_{frp}*w_{frp}* [h_{frp,e}(\sin\beta + \cos\beta)/ s_{frp}] \quad \ldots\ldots (3)$$

where,

$f_{frp,e}$ = average stress of FRP interested by the shear crack at the ultimate limit state,

t_{frp} = thickness of the FRP,

w_{frp} = width of each individual FRP strip (perpendicular to the fibre orientation),

$h_{frp,e}$ = effective height of the FRP bonded on the web (0.9d),

β = angle of the inclination of fibres in the FRP to the longitudinal axis of the beam,

s_{frp} = horizontal spacing of FRP strips (i.e. the centre-to-centre distance of FRP strips).

The strain distribution in FRP strips intersected by the critical shear crack is closely related to the variation of the crack width at FRP rupture failure and, in general, the crack width is significantly non-uniform. Similarly, the FRP stress distribution at debonding failure is also non-uniform, chiefly because the bond lengths of the FRP strips vary along the critical shear crack. Therefore, the stress distribution in the FRP along the critical shear crack is non-uniform at the ultimate limit state for both modes of FRP rupture and FRP debonding failure. At the ultimate limit state, the average (or effective) stress in the FRP along the critical crack $f_{frp,e}$ is thus:

$$f_{frp,e} = D_{frp} * \sigma_{frp,max}$$

in which $\sigma_{frp,max}$ is the maximum stress that can be reached in the FRP intersected by the critical shear crack and D_{frp} is the stress distribution factor defined by: $D_{frp} = f_{frp,e}/ \sigma_{frp,max}$

The values of D_{frp} and $\sigma_{frp,max}$ depend on whether the shear failure is controlled by FRP rupture or debonding.

Debonding failure

For debonding failure of FRP strips intersected by the critical shear crack, the maximum stress in the FRP occurs at the location where the FRP has the longest bond length. The maximum stress in the FRP is limited by either the bond strength or the tensile strength of the FRP. This maximum can be found from (min. of the two equations):

$\sigma_{frp,max} = 0.8*(f_{frp}/\gamma_{frp})$

$\sigma_{frp,max} = \alpha/\gamma_b * \beta_w*\beta_l * [(E_{frp}/t_{frp})*(f_c)^{1/2}]^{1/2}$

Where the coefficient α has the 95 percentile characteristic value of 0.315 for design based on Chen and Teng's (2001) bond strength model, γ_b is the partial safety factor for debonding failures, β_L, reflects the effect of bond length and β_W the effect of the FRP-to-concrete width ratio. The expression for β_L and β_W are:

$\beta_L = 1$ if $\lambda \geq 1$

$\beta_L = \sin(\pi\lambda/2)$ if $\lambda < 1$

$\beta_w = [2- (w_{frp}/ s_{frp} \sin\beta) / 1+ (w_{frp}/ s_{frp} \sin\beta) \geq \sqrt{2}/2$

Note that $w_{frp}/(s_{frp} \sin\beta)$ is less than 1 for FRP strips with gaps. It becomes 1 when no gap exists between FRP strips and for continuous sheets or plates, yielding the lower limit value of $\sqrt{2}/2$ for β_w. The normalized maximum bond length λ, the maximum bond length L_{max} and the effective bond length L_e of the FRP strips are given by:

$\lambda = L_{max} /L_e$

$L_{max} = h_{frp,e}/ \sin\beta$ for U-jackets

$L_{max} = h_{frp,e}/ 2\sin\beta$ for side plates

$L_e = [E_{frp}*t_{frp} / (f_c)^{1/2}]^{1/2}$

The number 2 appears in the denominator for side plates because the FRP strip with the maximum bond length appears at the lower end of the critical shear crack for U-jacketing but at the middle for side plates.

Assuming that all the FRP strips intersected by the critical shear crack are able to develop their bond strength fully, the stress distribution factor for debonding failure D_{frp} can be derived as:

$D_{frp} = 2/\pi\lambda*[1-\cos \pi\lambda/2 / \sin \pi\lambda/2]$ if $\lambda \leq 1$

$D_{frp} = [1- (\pi-2/ \pi\lambda)]$ if $\lambda > 1$

The above equation is applicable to both U-jackets and side strips. The actual calculated values are different for these two cases even if the configuration of the bonded FRP is the same on the beam sides because the maximum bond length L_{max} for U-jackets is twice that for side strips.

Calculations:

(1) For beams which are strengthened with 50 mm wide CFRP U-strips i.e. SB-03 and SB-04.

$L_{max} = h_{frp,e}/ \sin\beta$

$L_{max} = 112.5/ \sin 90°$

$L_{max} = 112.5$

$L_e = [E_{frp}*t_{frp} / (f_c)^{1/2}]^{1/2}$

$L_e = [(2.52*10^5)*0.167 / (20)^{1/2}]^{1/2}$

$L_e = 97$

$\lambda = L_{max}/ L_e$

$\lambda = 112.5/ 97$

$\lambda = 1.16$

$D_{frp} = [1- (\pi-2/ \pi\lambda)]$

$D_{frp} = [1- (\pi-2/ \pi*1.16)]$

$D_{frp} = 0.69$

$\beta_L = 1$ for $\lambda \geq 1$

β_w = [2- (w_{frp}/ s_{frp} sinβ) / 1+ (w_{frp}/ s_{frp} sinβ)

β_w = [2- (50/ 85 sin90°) / 1+ (50/ 85 sin90°)

β_w = 0.94

$\sigma_{frp,max}$ = $\alpha/\gamma_b * \beta_w * \beta_L * [(E_{frp}/t_{frp})*(f_c)^{1/2}]^{1/2}$

$\sigma_{frp,max}$ = $0.315 * 0.94*1 * [(2.52*10^5/ 0.167)*(20)^{1/2}]^{1/2}$

$\sigma_{frp,max}$ = 765.30 N/mm^2

$f_{frp,e}$ = $D_{frp} * \sigma_{frp,max}$

$f_{frp,e}$ = 0.69*765.30

$f_{frp,e}$ = 528.05 N/mm^2

V_{frp} = $2*f_{frp,e}*t_{frp}*w_{frp}* [h_{frp,e}(\sin\beta + \cos\beta)/ s_{frp}]$

V_{frp} = 2*528.05*0.167*50*[112.5/85]

V_{frp} = 11671 N

(2) For beams which are strengthened with 150 mm wide full U-wrap i.e. SB-05 and SB-06.

L_{max} = 112.5

L_e = 97

λ = 1.16

D_{frp} = 0.69

β_L = 1

β_w = 0.707 (as $w_{frp} = s_{frp}$ = 150 mm)

$\sigma_{frp,max}$ = $\alpha/\gamma_b * \beta_w * \beta_L * [(E_{frp}/t_{frp})*(f_c)^{1/2}]^{1/2}$

$\sigma_{frp,max}$ = $0.315 * 0.707*1 * [(2.52*10^5/ 0.167)*(20)^{1/2}]^{1/2}$

$\sigma_{frp,max}$ = 575.60 N/mm^2

$f_{frp,e}$ = $D_{frp} * \sigma_{frp,max}$

$f_{frp,e}$ = 0.69*575.60

$f_{frp,e}$ = 397.164 N/mm^2

V_{frp} = $2*f_{frp,e}*t_{frp}*w_{frp}* [h_{frp,e}(\sin\beta + \cos\beta)/ s_{frp}]$

V_{frp} = 2*397.164*0.167*150* [112.5/ 150]

V_{frp} = 14923.4373 N

(d) TOTAL SHEAR CAPACITY OF BEAM (w.r.t. critical diagonal shear crack)

(1) For beams which are strengthened with 50 mm wide CFRP U-strips i.e. SB-05 and SB-06.

V_{Total} = $V_c + V_s + V_{frp}$

V_{Total} = 15938.208 + 17803.8 + 11671

V_{Total} = 45413.008 N

(2) For beams which are strengthened with 150 mm wide full U-wrap i.e. SB-05 and SB-06.

V_{Total} = $V_c + V_s + V_{frp}$

V_{Total} = 15938.268 + 17803.8 + 14923.4373

V_{Total} = 48665 .443 N

(e) COMPARISON OF THEORETICAL AND EXPERIMENTAL RESULTS

The shear strength of beams strengthened with CFRP sheets obtained from the experimental study is compared to the theoretical design shear strength by combining the contribution of concrete, steel and externally bonded FRP sheet. Different nomenclatures used in Table A.1 are explained below for clarity.

V_u (exp.) = Shear force in the beam at which debonding occurs, obtained from test.

V_u (th.) = Theoretical Shear force at which debonding occurs.

V_u (max.) = Ultimate Shear capacity of the beam, obtained from test.

Table A.1 – Comparison of Experimental and Theoretical shear strength results

Beam Label	V_u (exp.) KN	V_u (th.) KN	V_u (max.) KN	V_u (exp.) / V_u (th.)	Failure Mode
SB-03	45.875	45.41	52.61	1.010	Debonding + Shear
SB-04	46.10	45.41	53.95	1.015	Debonding + Shear
SB-05	48.75	48.66	55.23	1.002	Debonding + Shear
SB-06	48.90	48.66	55.35	1.005	Debonding + Shear

It is observed from the table that experimental results correlate very well with the theoretical calculations of shear capacity based on debonding failure mode with an average ratio of 1.008.